

## ABSTRACT

Title of Document: NUCLEIC ACID EXTRACTION AND  
DETECTION ACROSS TWO-DIMENSIONAL  
TISSUE SAMPLES

Michael Daniel Armani, Doctor of Philosophy,  
2010

Directed By (co-advisors): Professor Benjamin Shapiro,  
Fischell Department of Bioengineering,

&

Professor Elisabeth Smela,  
Department of Mechanical Engineering.

Visualizing genetic changes throughout tissues can explain basic biological functions and molecular pathways in disease. However, over 90% of mammalian messenger RNA (mRNA) is in low abundance (<15 copies per cell) making them hard to see with existing techniques, such as in-situ hybridization (ISH). In the example of diagnosing cancer, a disease caused by genetic mutations, only a few cancer-

associated mRNAs can be visualized in the clinic due to the poor sensitivity of ISH. To improve the detection of low-abundance mRNA, many researchers combine the cells across a tissue sample by taking a scrape. Mixing cells provides only one data point and masks the inherent heterogeneity of tissues. To address these challenges, we invented a sensitive method for mapping nucleic acids across tissues called 2D-PCR. 2D-PCR transfers a tissue section into an array of wells, confining and separating the tissue into subregions. Chemical steps are then used to free nucleic acids from the tissues subregions. If the freed genetic material is mRNA, a purification step is also performed. One or more nucleic acids are then amplified using PCR and detected across the tissue to produce a map. As an initial proof of concept, a DNA map was made from a frozen tissue section using 2D-PCR at the resolution of 1.6 mm per well. The technique was improved to perform the more challenging task of mapping three mRNA molecules from a frozen tissue section. Because the majority of clinical tissues are stored using formalin fixation and not freezing, 2D-PCR was improved once more to detect up to 24 mRNAs from formalin-fixed tissue microarrays. This last approach was used to validate genetic profiles in human normal and tumor prostate samples faster than with existing techniques. In conclusion, 2D-PCR is a robust method for detecting genetic changes across tissues or from many tissue samples. 2D-PCR can be used today for studying differences in nucleic acids between tumor and normal specimens or differences in subregions of the brain.

NUCLEIC ACID EXTRACTION AND DETECTION ACROSS TWO-  
DIMENSIONAL TISSUE SAMPLES

By

Michael Daniel Armani

Dissertation submitted to the Faculty of the Graduate School of the  
University of Maryland, College Park, in partial fulfillment  
of the requirements for the degree of  
Doctor of Philosophy  
2010

Advisory Committee:  
Professor Benjamin Shapiro, Chair  
Professor Elisabeth Smela  
Professor Yu Chen  
Professor Joonil Seog  
Professor Jason D. Kahn, Dean's Representative  
Dr. Michael W. Phelan, M.D.

© Copyright by  
Michael Daniel Armani  
2010

## Dedication

To my loving parents, for all their hard work and motivation.

## Acknowledgements

I am especially thankful for my wonderful advisors, Dr. Benjamin Shapiro, Dr. Elisabeth Smela, and Dr. Michael Emmert-Buck for guiding me for so many years. They taught me how question the status quo, formulate my own objectives logically, and keep from being biased by my own assumptions. Although I had three advisors at the same time, I am certain this created a unique mindset and proved that too many cooks do not spoil the broth. The skills they taught me branched out into all aspects of my life.

I would like to thank Dr. Steven Hewitt and the TARP lab members Kris Ylaya and Jennifer Martinez for helpful discussions, sharing their time, and providing research support.

A very special thanks also goes to Michael Tangrea, who shared countless hallway conversations and brainstorming sessions with me, resulting in many ideas that I pursued. I would also like to acknowledge the past and present members of Dr. Emmert-Buck's lab (John Gillespie, Skye Kim, Brian Yang, Jaime Rodriguez-Canales, Jeff Hansen, Rodrigo Chuaqui, Heidi Erickson, Liang Zhu, Wusheng Yan, Sumana Mukherjee, Anneley Richardson, Alex Rosenberg), for discussing ideas with me, teaching me how to use the current molecular biology tools, doing experimental work with me, and for kindly sharing reagents or space.

A very special thanks also goes to Belhu Metaferia, who essentially taught me a crash-course in organic chemistry, synthetic chemistry, and hydrogel chemistry even though he was not associated with our project or lab officially.

I also must acknowledge many other colleagues, who helped me develop my ideas and supported my project in many ways including Disha Pant, Jeff Burke, Marc Dandin, Mark Kujawski, Mario Urdaneta, and Bavani Balakrisnan, from Dr. Smela's lab; also Roland Probst, Pramod Mathai, Alek Nacev, Nir Kalush, and Derek Metzger from Dr. Shapiro's lab. A special thanks to Eddie Chen and Maura Manion who were actually the first ones to work on 2D-PCR and who passed their project to me.

I would also like to thank many more people who helped facilitate this project. This includes Tom Loughran and Jonathan Hummel at the UMD FabLab, Howie Grossenbacher at the UMD aerospace machine shop, Connie Newcome at Adhesives Research, who supplied us with specialty adhesive samples that were essential to this project, and Kelley Banfield at SAIC-Frederick who ran our Fluidigm experiments.

I would like to thank people outside of my work who helped me and supported me, especially Sarah, and many others. Lastly, I have to thank the U.S. tax-payers, as their financial support made it to this project one way or another.

# Table of Contents

DEDICATION.....	II
ACKNOWLEDGEMENTS.....	III
TABLE OF CONTENTS.....	V
LIST OF FIGURES.....	IX
LIST OF TABLES.....	XIII
CHAPTER 1 : MOTIVATION AND BACKGROUND.....	1
1.1    Introduction.....	1
1.2    Background.....	4
1.2.1    Nucleic acids.....	4
1.2.2    Changes in nucleic acids.....	6
1.2.3    Detecting genetic changes by the polymerase chain reaction (PCR) ...	7
1.2.4    Typical methods of tissue sample preservation and storage.....	17
1.2.5    Typical methods for recovering nucleic acids.....	22
1.2.6    A common lab workflow to study changes in nucleic acids.....	28
1.2.7    Summary.....	29
1.3    Current methods for localizing nucleic acids in tissue.....	29
1.3.1    In-situ hybridization (ISH).....	29
1.3.2    In-situ PCR (ISP).....	33
1.3.3    Laser microdissection & PCR.....	35
1.3.4    Macrodissection or voxelation & PCR.....	39
1.3.5    Immunohistochemistry (IHC).....	42
1.3.6    Summary.....	43
1.4    Aims.....	44
1.4.1    A robust nucleic acid mapping method.....	44
1.4.2    2D-PCR addresses all of these needs.....	49
1.4.3    Aim 1 – Map DNA using 2D-PCR.....	51
1.4.4    Aim 2 – Map RNA using 2D-PCR.....	52
1.4.5    Aim 3 – Mapping total RNA in FFPE tissue using 2D-PCR.....	52
CHAPTER 2 : DNA MAPS FROM FROZEN TISSUE.....	55
2.1    Abstract.....	56
2.2    Introduction.....	56
2.3    DNA Mapping Methodology.....	59
2.4    Materials and Methods.....	63
2.4.1    Device fabrication.....	63
2.4.2    Tissue sectioning and transfer.....	64
2.4.3    Device heating and sealing.....	65
2.4.4    DNA amplification protocol.....	67
2.4.5    Visualization.....	67
2.5    Results.....	68
2.5.1    Direct DNA extraction and amplification: protocols and validation.	68
2.5.2    2D-PCR mapping.....	71
2.5.3    Preliminary work towards miniaturization.....	74

2.6	Discussion.....	76
2.7	Conclusions.....	82
2.8	Acknowledgements.....	83
2.9	Supplementary Materials .....	83
2.10	Supplementary Information for Mini-Vial Results.....	83
2.10.1	Compression Rig.....	83
2.10.2	Electrophoresis Gels for Validation of 2D-PCR Method .....	84
2.11	Supplementary Information for Further Miniaturization.....	87
2.11.1	Purpose of Further Miniaturization.....	87
2.11.2	Challenges Addressed.....	87
2.11.3	PCR.....	93
2.11.4	Discussion of Miniaturization Results .....	96
CHAPTER 3 : RNA MAPS FROM FROZEN TISSUE .....		98
3.1	Abstract.....	99
3.2	Introduction.....	100
3.3	Materials and Methods.....	102
3.3.1	Quantitative PCR Primers and Probes .....	102
3.3.2	Tissue Sections and Scrapes .....	102
3.3.3	Materials and Equipment .....	103
3.3.4	Buffers and Commercial Purification Kits .....	103
3.3.5	Determination of Nucleic Acid Purification Efficiency .....	104
3.3.6	2D-PCR Method .....	104
3.3.7	Optimal 2D-PCR Protocol for Quantifying mRNA Across Tissue Sections.....	106
3.4	Results.....	108
3.4.1	Validation of Efficient Purification at Small Scales .....	108
3.4.2	Enabling GITC Buffer Use in Magnetic Bead-Based Purifications .	110
3.4.3	Single-Well Lysis and Purification on Tissue Samples.....	112
3.4.4	Proof of Concept for 2D-PCR.....	113
3.4.5	Identification of the Best Lysis Buffer for 2D-PCR .....	115
3.5	Discussion and Conclusions .....	118
3.5.1	Single-Well Lysis and Purification.....	118
3.5.2	2D-RT-PCR .....	118
3.5.3	Conclusions.....	119
3.6	Acknowledgements.....	120
3.7	Electronic Supplementary Information (ESI) .....	120
3.7.1	Primer sequences used in this study.....	120
3.7.2	Specific protocol for duplex mRNA mapping (ChargeSwitch buffer)...	120
3.7.3	Specific protocol for triplex mRNA mapping (ChargeSwitch or custom GITC buffer) .....	121
3.7.4	Determination of Cts.....	122
CHAPTER 4 : RNA AND MICRORNA MAPS FROM FFPE TISSUE.....		124
4.1	Abstract.....	125
4.2	Introduction.....	125
4.3	Results and Discussion .....	127

4.3.1	Speed and sensitivity 2D-PCR vs. a four-step workflow for microRNA detection.....	128
4.3.2	Sensitivity 2D-PCR vs. a four-step workflow for mRNA detection	132
4.3.3	Reproducibility of 2D-PCR for microRNA and mRNA detection...	132
4.3.4	Dynamic range and specificity of 2D-PCR in different tissues.....	132
4.3.5	Validation of microarray data using human prostate cancer and normal samples.....	134
4.4	Discussion.....	136
4.4.1	RNA quality and detection from TMAs .....	136
4.4.2	Challenges in the application of TMAs to RNA expression analysis	137
4.4.3	Potential use for Validation Studies and Clinical Diagnosis and Prognosis.....	137
4.5	Methods.....	139
4.5.1	Crafting of 384-well format TMAs.....	139
4.5.2	Tissue sectioning and transfer to 2D-PCR Plates .....	139
4.5.3	Reverse crosslinking treatment for recovering mRNA.....	140
4.5.4	2D-PCR lysis and purification .....	140
4.5.5	One-step microRNA or mRNA reverse-transcriptase PCR.....	141
4.5.6	Tandem mRNA Pre-amplification (to detect up to 100 targets).....	141
4.6	Electronic Supplemental Information (ESI) .....	142
4.6.1	TMAs tested.....	142
4.6.2	Selection of adhesive films .....	143
4.6.3	Validation of mRNA specificity and dynamic range in mouse tissues in a triplex reaction .....	144
4.6.4	Worst-Case and negative control tests using autopsy and decalcified tissues.....	145
4.6.5	Optimization of reverse-crosslinking strategy .....	146
4.6.6	Pre-amplification linearity and PCR efficiency (Direct PCR – not Fluidigm).....	146
4.6.7	Pre-amplification linearity and PCR efficiency (Fluidigm).....	147
4.6.8	Primer Sets Used.....	149
<b>CHAPTER 5 : DISCUSSION AND POSSIBLE FUTURE WORK.....</b>		<b>150</b>
5.1	Advantages of 2D-PCR.....	150
5.2	Limitations of 2D-PCR.....	152
5.3	Possible future work .....	153
5.3.1	Miniaturization.....	153
5.3.2	Simpler purification surface.....	153
5.3.3	Other downstream methods .....	154
5.3.4	Speculation on the application of 2D-PCR to clinical diagnostics ...	155
5.3.5	Immediate applications of 2D-PCR .....	156
<b>CHAPTER 6 : CONCLUSION AND TECHNICAL DEVELOPMENTS .....</b>		<b>158</b>
<b>CHAPTER 7 : INTELLECTUAL CONTRIBUTIONS .....</b>		<b>161</b>
7.1	Contribution 1 – Cutting tissues into subregions.....	161
7.2	Contribution 2 – Lysis of frozen tissue for DNA recovery .....	161
7.3	Contribution 3 – Visualization of tissue .....	162
7.4	Contribution 4 – Lysis and purification of RNA from frozen samples ....	162

7.5	Contribution 5 – Dewax formalin-fixed tissues on adhesive films.....	163
7.6	Contribution 6 – Lysis of formalin-fixed tissue for RNA recovery.....	163
7.7	Contribution 7 – Studying microRNA without dilution .....	164
7.8	Contribution 8 – Studying nucleic acids in multiplex .....	164
CHAPTER 8 : APPENDICES .....		165
8.1	2D-PCR Publications and presentations .....	165
8.2	Single-well lysis & purification compared to existing methods.....	166
CHAPTER 9 : BIBLIOGRAPHY .....		170

## List of Figures

Figure 1 – PCR and quantitative PCR publications by year. Data generated by performing a Pubmed search by year, in title or abstract, for the quoted phrase “polymerase chain reaction” or the phrase [qPCR or "quantitative PCR" or "real-time PCR"].	8
Figure 2 – The polymerase chain reaction doubles the amount of DNA using the three steps of a PCR cycle. In step 1), the double-stranded DNA is first heated to denature (separate) the two strands. In step 2) primers are hybridized to the target DNA by lowering the reaction temperature. In step 3) the primers are elongated in a 5' to 3' direction by DNA polymerase, copying the template DNA strand.	9
Figure 3 – The quantitative real-time polymerase chain reaction (qPCR) detects the amount of template by monitoring fluorescence, allowing for the quantification of starting template. The qPCR reaction is based on a standard PCR reaction. However, a molecular probe (TaqMan probe) is added to the reaction mix. Upon elongation, the primer hydrolyses and releases fluorescent molecules into the reaction mixture. The fluorescence is measured at the end of each PCR cycle. The fluorescence intensity is presented as a graph that can be used to determine the amount of starting template relative to another qPCR reaction.	13
Figure 4 – <i>In-situ</i> hybridization (ISH) publications by year. Data generated by performing a Pubmed search by year, in title or abstract, for the quoted phrase “in situ hybridization.”	30
Figure 5 – <i>In-situ</i> PCR publications by year. Data generated by performing a Pubmed search by year, in title or abstract, for the phrase [PCR in situ hybridization or "in situ PCR"].	35
Figure 6 – Laser capture microdissection (LCM) publications by year. Data generated by performing a Pubmed search by year, in title or abstract, for the phrase [laser microdissection or "laser capture microdissection].	38
Figure 7 – <i>LCM, PCR, qPCR, and microarray</i> publications by year. Data generated by performing a Pubmed search by year, in title or abstract as described previously for LCM, PCR and qPCR. Microarray history was generated using the phrase [gene expression profiling or microarray not "cell microarray" not "tissue microarray"]. The difference in publications between LCM and these other techniques was 21,743 in year 2009. These studies are presumed to use large tissue scrapes, cell culture, or other methods that do not provide spatially resolved information.	42
Figure 8 – Immunohistochemistry IHC publications by year. Data generated by performing a Pubmed search by year, in title or abstract, for the quoted phrase “immunohistochemistry.”	43
Figure 9 – Schematic view of the 2D-PCR technique for spatial mapping of changes in genes and gene expression. All of the genes from a tissue section are transferred to a grid of wells, a target nucleic acid is amplified by PCR under clean conditions	

within each well, and amplified gene products can be detected by staining within the wells using a fluorescent dye. (Figure courtesy of Dr. Smela)..... 49

Figure 10 – 2D-PCR is achieved by transferring a tissue section vertically into a multiwell array device, isolating tissue subregions. The DNA is extracted and then amplified by the polymerase chain reaction. A detection map is created by imaging the amplified DNA, for example using a DNA-intercalating dye. .... 60

Figure 11 – Experimental protocol used to demonstrate the 2D-PCR concept. Tissue is transferred into wells, isolated, and lysed to extract the genomic DNA (represented by “x”s). PCR is performed to amplify the target DNA, and the targets are visualized with fluorescent dye (indicated by vertical lines “|”)...... 62

Figure 12 – Image of a breast tissue section (stained pink for visualization with Eosin Y) after transfer onto the multi-well device, and the visualization map created by fluorescent DNA detection with SYBR Green I after amplification by 2D-PCR. The tissue position is indicated by the pink outline. .... 72

Figure 13 – A) The wells chosen for electrophoretic validation of the fluorescent signal. B) In wells containing tissue (lanes 1-6) there was a bright fluorescent signal corresponding to detection of a 167 bp GAPDH genomic product, while negative wells (lanes 7-12) had no amplification of the 167 bp target and only weak bands of ~50 bp primer-dimers, an artifact from PCR. .... 74

Figure 14 – Silicon substrate having a 1 cm square area with 100 μm diameter holes spaced 100 μm apart. The surface was pretreated with BSA and spotted with water containing food dye for visualization (dark area in center). The wells filled completely by capillary action. .... 75

Figure 15 – Schematic view of the compression-heating rig used for sealing and thermocycling. .... 84

Figure 16 – Gel electrophoresis from PCR validation experiment. Lanes 1 and 7 show 50 bp molecular weight ladders. Lane 2 had a negative water control, lanes 3-5 had increasing concentrations of purified genomic DNA, and lane 6 had a tissue-derived DNA extract. .... 84

Figure 17 – a) Geometric arrangement of the wells. b) Gel electrophoresis validation of DNA extraction experiment. The lane numbers correspond with the well numbers in Table 8. Lane 13 had a 50 bp ladder. The gel lanes show bands at (1) 167 bp, (2) 489 bp, (3) 167 bp, (4) 582 bp, (5) no bands, (6) no bands, (7) 582 bp, (8) 582 bp, (9) no bands, (10) 582 bp, (11) 582 bp, (12) 582 bp. .... 86

Figure 18 – a) Silicon chip having a 1 cm square area with 100 μm holes spaced 100 μm apart. b) SEM sidewall profile of 50 μm wide holes made by DRIE. c) Silicon chip with 100 μm holes that was pretreated with BSA and spotted in an arbitrary diamond-shaped pattern with water containing food dye. The wells filled completely by capillary action. .... 89

Figure 19 – Compression-thermocycling rig showing PCR machine on a weight scale. .... 93

Figure 20 – PCR results from (lane 2) a standard plastic PCR tube with control DNA added, (3) a micro-well plate with control DNA added, (4 and 5) a plastic tube and another micro-well plate containing only water, and (6) a lane containing unamplified PCR supermix. Lanes 1 and 7 contained 50 bp ladders..... 95

Figure 21 – TaqMan in 100 μm micro-wells, looking at different areas on one plate.  
a) Strong positive control with Ct value of 24. b) Negative control with no Ct value.  
c) Strong positive control with Ct value of 29.69..... 96

Figure 22 – 2D-PCR is achieved by transferring a tissue section vertically into a multiwell array device, thereby isolating tissue sub-regions. RNA is extracted by cell lysis, captured and purified on ChargeSwitch beads by rinsing steps, and quantified by one-step reverse-transcriptase PCR in each well. Visualization of targets is performed within the wells using standard molecular probe chemistry. .... 102

Figure 23 – Cross-sectional schematic illustration of 2D-RT-PCR method. A) Tissue transfer. B) Tissue lysis. C) Addition of magnetic beads. D) Purification by washing, DNase. E) Amplification by qPCR..... 105

Figure 24 – A) Mouse brain, mouse kidney, and chicken thymus on an adhesive film, stained red with Eosin Y and transferred onto a 384-well plate. A) The layout of a 384-well format plate is outlined over the tissue. B) KCNJ1 mRNA detection and C) HPRT1 detection showing quantitative cycles of detection thresholds (Cts) determined by qPCR. .... 115

Figure 25 – Two serial recuts of a tissue sample containing mouse brain, kidney, and heart tissue, stained red with acid Fuchsin and transferred onto the wells of a 384-well plate containing either ChargeSwitch or custom buffer (image of tissue after lysis). A) The layout of a 384-well format plate is outlined over the tissue. B) KCNJ1 mRNA detection, C) HPRT1 mRNA detection, and D) GYS2 mRNA detection showing quantitative cycles of detection thresholds (Cts) determined by qPCR. .... 117

Figure 26 – 2D-PCR can be used to validate up to 100 RNAs in multiplex from each core in a single 10 micron thick tissue microarray. .... 127

Figure 27 – A) Comparison of RecoverAll and 2D-PCR for the recovery of microRNA (mir-191) and B) mRNA (SOD2) and smallRNA (RNU48). Mir-191 is a stable microRNA normalizer<sup>148</sup>. Panels C and D show a plot of the measure Cts versus the calculated Cts as predicted by  $\log_2(\text{core size})$ . .... 131

Figure 28 – Significant differential expression (percent changes determined from Cts,  $p < .025$ ) of 14 genes, each normalized to the average of 4 housekeeping genes in 24 prostate tumor cases versus 18 normal prostates. .... 135

Figure 29 – Overhead view of TMA blocks embedded in paraffin wax with tissue core sizes ranging from 0.6 mm to 3 mm. .... 143

Figure 30 – Demonstration of tissue specific amplification in high-quality mouse FFPE samples using a triplex qPCR reaction from the purified template. Delta Cts are shown. KCNJ1 (FAM) was shown to be highest in Kidney and GYS2 was shown

to be highest in Liver as expected. There is also a large dynamic range demonstrated which is owed to the high quality of these samples..... 145

Figure 31 – Failure to amplify RNU48 in negative tissue controls (decalcified bone). ..... 145

Figure 32 – Pre-amplification and Fluidigm qPCR vs. direct one-step RT-qPCR assay on 0.5 mm distant serial recuts of the prostate TMA..... 148

Figure 33 – Comparison between Invitrogen Trizol, based on the Chomzinski method, and 2D-PCR’s single-well lysis and purification method..... 166

Figure 34 – Comparison between Qiagen RNeasy, based on the GITC lysis and silica column purification methods, and 2D-PCR’s single-well lysis and purification method..... 167

Figure 35 – Comparison between Picopure RNA extraction kit, based on the GITC lysis and silica column purification methods, and 2D-PCR’s single-well lysis and purification method..... 168

Figure 36 – Comparison between Invitrogen Dynabeads magnetic bead purification kit, based on the lithium chloride based lysis and oligo-dT magnetic bead purification methods, and 2D-PCR’s single-well lysis and purification method. .... 169

## List of Tables

Table 1 – The essential components, their functions, and typically ranges for a basic PCR reaction. Abbreviations: picogram (pg), microgram (µg), nanomolar (nM), micromolar (µM), nanomoles (nmol). .....	11
Table 2 – Benefits and limitations of <i>in-situ</i> hybridization (ISH). .....	33
Table 3 – Benefits and limitations of <i>in-situ</i> PCR (ISP). .....	34
Table 4 – Benefits and limitations of laser capture microdissection + PCR (LCM). .	38
Table 5 – Benefits and limitations of microdissection + PCR. ....	41
Table 6 – Benefits and limitations of four methods for localizing nucleic acids in tissues. ....	44
Table 7 – Benefits and limitations of 2D-PCR and four methods for localizing nucleic acids in tissues. ....	51
Table 8 – Well contents for validating DNA amplification. ....	85
Table 9 – Testing evaporation and spreading for different micro-well sealing films.	93
Table 10 – <u>Rows 1-4:</u> Comparison of sheared herring sperm DNA recovery efficiency with two commercially available kits: CS – ChargeSwitch Total RNA Cell Kit, PP – PicoPure. <u>Rows 5-6:</u> Recovery efficiency of 20x scaled-down ChargeSwitch protocol. <u>Rows 7-9:</u> The same protocol with the addition of acetic acid (AA). ....	109
Table 11 – Recovery efficiencies of GITC-based buffers with sheared herring sperm DNA. ....	111
Table 12 – Relative effectiveness of single-well lysis and purification using different lysis buffers determined by quantitative reverse-transcriptase PCR. ....	113
Table 13 – Primer sequences .....	120
Table 14 – Example calculation of Cts from raw data. ....	123
Table 15 – Cts of mouse-specific amplification of a low-abundance gene (HPRT1) in well-controlled FFPE mouse samples that are 4-months old. Three triplicate samples of human breast tissues from the cooperative human tissue network were also used and two showed amplification of human-specific small RNA (RNU48). ....	134
Table 16 – Selection of adhesive film for TMA sectioning, dewaxing, and transfer to 384-well plates .....	144
Table 17 – PCR efficiency of single-plex amplification after pre-amplification .....	147
Table 18 – PCR efficiency of B2M as a multiplex endogenous control .....	147
Table 19 – Custom and Taqman probe sets used. ....	149
Table 20 – Successful application of 2D-PCR to different tissues, fixation methods, and nucleic acid targets. ....	151

# Chapter 1: Motivation and Background

In molecular biology research and clinical diagnosis, there is a need for a robust method that can detect and quantify nucleic acids across tissue samples. A robust technique is one that works sensitively, quickly, consistently, and in a way that is compatible with a wide range of specimens and molecular targets. Current techniques do not address this need. This dissertation establishes a new technique, 2D-PCR, for mapping nucleic acids across tissue samples robustly.

## 1.1 Introduction

There is a vast potential resource of biological information in human tissue samples, including about 20,500 genes<sup>1</sup> and about 1000 known microRNAs<sup>2</sup>. Identifying how genes (nucleic acids) change in space and time can explain normal biological processes or the development of disease. Genetic patterns can also provide novel starting points for medical therapy<sup>3,4</sup>.

However, it is not yet known how the 3D structure of a normal or diseased tissue is formed and influenced by the one-dimensional sequence of nucleic acids<sup>5,6</sup>. The following examples demonstrate the need to detect and learn more about how nucleic acids function with respect to location in tissues.

- *Where are the genes expressed in the brain that are responsible for Alzheimer's disease<sup>7</sup>?*
- *Are there DNA mutations within a subregion of a prostate tumor<sup>8</sup>?*
- *How does microRNA expression vary across embryos<sup>9</sup>?*
- *How does gene expression change as stem cells differentiate<sup>10</sup>?*

The answers to these and similar questions are elusive because it is difficult to detect nucleic acids as a function of position in biological tissues with current techniques. Current techniques for mapping or visualizing nucleic acids across tissues are constrained by issues with assay sensitivity, reproducibility, cost, or complexity. Part of the problem is that the majority of mammalian mRNAs (about 95%) are in low abundance (less than 15 copies per cell)<sup>11, 12</sup>. It is difficult to measure low copy number mRNAs with cellular-resolution techniques, such as *in-situ* hybridization (ISH)<sup>13-17</sup>. Alternatively, the polymerase chain reaction (PCR) is used to amplify rare mRNAs to improve detection<sup>13, 17</sup>, but laborious techniques<sup>6, 18</sup> are required to preserve spatial resolution at the scale of even a few millimeters.

Therefore, the focus of this thesis is on the development of a new method for detecting nucleic acids across tissue samples by dividing a tissue into subregions, purifying nucleic acids from each tissue subregion, amplifying target nucleic acids within the tissue subregions using PCR, and detecting the targets using fluorescent labels. This new method for mapping nucleic acids across tissue samples is therefore called 2D-PCR. The hope was that this approach would be more robust (sensitive,

consistent, widely-applicable, and not prohibitively expensive or time-consuming) compared to existing techniques. A more detailed description of existing techniques, their advantages, their limitations, and comparisons among them are provided in section 1.3.

The aims are described in section 1.4. Initially, 2D-PCR was developed and tested at the resolution of a few millimeters for detecting DNA across a frozen tissue section as a proof of concept, as presented in Chapter 2. Next, the method was improved to perform the more challenging task of detecting and quantifying messenger RNA from frozen tissue sections, as presented in Chapter 3. Finally, the method was developed further to quantify up to 24 messenger RNAs in archival formalin-fixed tissue samples, as presented in Chapter 4. Many intellectual contributions were made to develop this method, as described in Chapter 6 and Chapter 7,

2D-PCR will serve two purposes, as discussed in Chapter 5. First, it will allow for biological research to identify the function of nucleic acids with respect to their locations in tissue. Second, it can translate from a research setting to a clinical setting for analysis of solid tissues. In the long-term, 2D-PCR could be used to inform medical diagnosis, prognosis, and treatment decisions, provided that spatial nucleic acid profiles are validated through extensive clinical testing.

## 1.2 Background

For the reader who is not familiar with the basic principles and methods in this thesis, a background is provided in this section. This section provides basic knowledge about nucleic acids, why they are important, and how they change. Common techniques used by researchers in the field are presented, including tissue storage, extraction of nucleic acids from tissues, and detection or quantification of nucleic acids by PCR. Each background section also lists any assumptions or special terminology used in the thesis.

### 1.2.1 Nucleic acids

#### 1.2.1.1 What are nucleic acids?

Nucleic acids are biologically evolved macromolecules containing unique sequence information in a variety of lengths. The reader is assumed to be familiar with the basic chemical structure of nucleic acids, including ATGC base pairing, molecular size, sense, double versus single-strandedness, and differences between RNA and DNA. Some of the important features of nucleic acids are highlighted as follows.

- Nucleic acids have a negatively charged backbone under most pH conditions.
- RNA contains the bases adenine (A), uracil (U), guanine (G), and cytosine (C) while DNA contains A,G,C, and thymine (T) bases.
- Nucleotides in two nucleic acids strands hybridize by strong hydrogen bonding to form double-stranded nucleic acids.

- RNA has one more hydroxyl group than DNA, which allows enzymes to distinguish between the two, but which also makes RNA less chemically stable, resulting in faster degradation.
- RNA is normally single-stranded, while DNA is double-stranded.
- Messenger RNA often contains long stretches of adenine sequences at the 3' end of the molecule. This is called a polyA tail.
- DNA in a cell is tightly bound to proteins called histones to compress and structure the DNA into a chromosome.
- Nucleic acid sequences are always created in a 5' to 3' direction by polymerases, therefore sequences are always presented and written using the same 5' to 3' orientation.
- A human cell contains 6.6 pico-grams of DNA.

#### 1.2.1.2 Types of nucleic acids

There are several classes of nucleic acids, with different functionalities, size ranges, and structures.

- **DNA** codes for messenger RNA, contains 6.6 billion base pairs per genome, and is nearly identical in all the normal diploid cells of a human body.
- **Messenger RNA** (mRNA) codes for proteins, is typically 500-10000 bases long, and varies greatly in copy number by cell type. About 1-10% of total RNA is mRNA.

- **MicroRNA** (miR) regulates gene expression, is typically 20-25 bases long, and varies in copy number by cell type.

#### 1.2.1.3 Assumptions and use in the thesis

For the thesis, the following assumptions are used.

- No unintentional artifactual modifications to nucleic acids are expected beyond those due to storage or preservation methods.
- While the methods described in the thesis may apply to studying mitochondrial, bacterial, fungal, plant, and artificial nucleic acids, they were not considered when developing the technique.

For the thesis, the following conventions are used.

- The words “nucleic acids” are used to refer to any mammalian DNA, messenger RNA, and microRNA sequences longer than 20 bases.
- Total RNA includes messenger RNA, microRNA, ribosomal RNA, and transfer RNA.
- The word gene generally refers to nucleic acid sequences that were characterized and curated in a database. Mammalian DNA and mRNA sequences can be found using the NCBI database. MicroRNA sequences can be found using the MirBase database<sup>2</sup>.

#### 1.2.2 Changes in nucleic acids

In order to identify the functions and importance of a nucleic acid, a change needs to be measured between two specific physical states. The states may be a change in

time, a change in space, or a developmental condition (i.e. diseased versus normal).

A change is defined as any of the following listed.

- DNA copy number gain or loss.
- DNA base pair mutations.
- DNA methylation – addition of a methyl group to base pairs.
- mRNA or microRNA expression level changes.

These changes can be significant or not, depending on the nucleic acid and state. Not all of the listed genetic changes can be detected with ISH, as summarized in section 1.3.6. However, all of the listed changes can be detected using variations of PCR. PCR is described in the next section.

### 1.2.3 Detecting genetic changes by the polymerase chain reaction (PCR)

#### 1.2.3.1 What is PCR?

PCR was invented as an in-vitro method for amplifying DNA molecules<sup>19</sup>. By using amplification, as little as one copy of DNA can be obtained at a high enough concentration in solution such that the amplified DNA can be seen with the naked eye using fluorescent staining. PCR is most often used to amplify short target sequences (50 base pairs up to a few thousand base pairs). Only specific molecules are amplified based on the design of the PCR reaction components, allowing for the specific and sensitive detection of almost any sequence from any biological entity. Due to the sensitivity and specificity of PCR, the technique was rapidly adopted in the early 1990s, as demonstrated by a publication history shown in Figure 1.

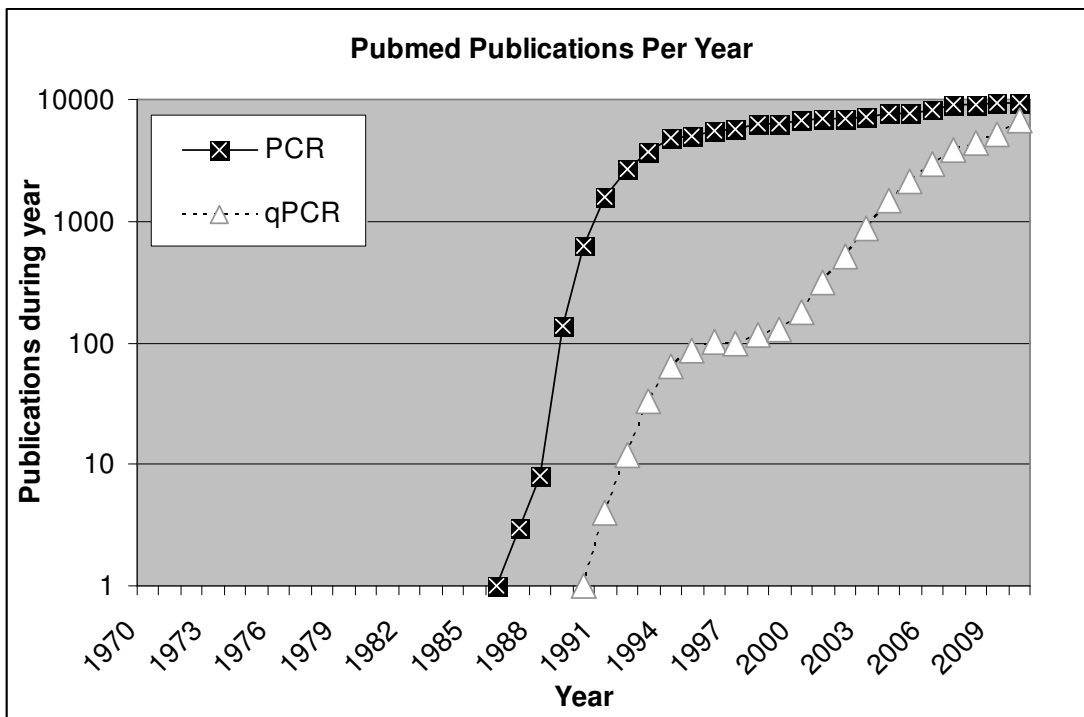


Figure 1 – PCR and quantitative PCR publications by year. Data generated by performing a Pubmed search by year, in title or abstract, for the quoted phrase “polymerase chain reaction” or the phrase [qPCR or "quantitative PCR" or "real-time PCR"].

### 1.2.3.2 How does standard PCR work?

In this section, the fundamentals of PCR are explained, standard PCR reaction components are explained, and terminology common to the field is provided.

PCR works by exploiting the fact that single-stranded DNA sequences naturally hybridize by base-pairing, and that DNA polymerases copy a longer DNA sequence (template) that is hybridized to a smaller DNA sequence called a primer. Three steps are required to amplify a DNA molecule to increase the DNA by a factor of two.

## One PCR Cycle Copies and Doubles DNA

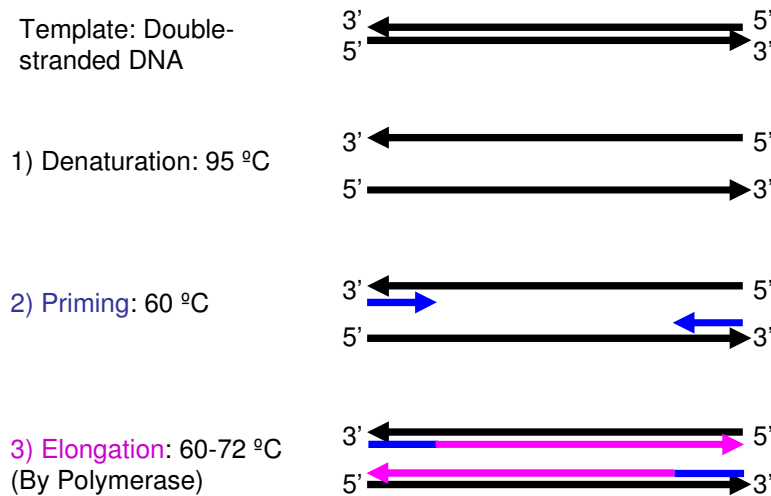


**Figure 2 – The polymerase chain reaction doubles the amount of DNA using the three steps of a PCR cycle. In step 1), the double-stranded DNA is first heated to denature (separate) the two strands. In step 2) primers are hybridized to the target DNA by lowering the reaction temperature. In step 3) the primers are elongated in a 5' to 3' direction by DNA polymerase, copying the template DNA strand.**

1. **Denaturation** – A target double-stranded DNA sequence is first heated to separate the two complementary strands. Typically, this occurs at a temperature of 95 °C and requires 5 to 15 seconds.
2. **Annealing** – Two short DNA sequences added to the reaction mix called primers or oligonucleotides, typically 16-30 bases long, are hybridized to each target DNA strand specifically. The annealing occurs in an aqueous buffer at a specific temperature. The temperature is typically 55 °C- 60 °C, and annealing usually takes 30 seconds.
3. **Elongation** – DNA polymerase extends the primer, in a 5' to 3' direction, by copying the opposite DNA strand and incorporating nucleotides. About 100

bases can be incorporated per second. The temperature range is typically 60 °C - 72 °C for elongation, and elongation usually requires 30 seconds.

The steps of denaturation, annealing, and elongation are called a PCR cycle. Each PCR cycle in theory produces two identical copies of double-stranded DNA for each copy of double-stranded DNA in the reaction. Although the ideal doubling would give a 100% PCR efficiency, in practice PCR efficiencies are typically 80%-90%<sup>20</sup>. The PCR steps are repeated as many times as necessary to be able to detect the target DNA with downstream techniques. The repetition of PCR cycles is called thermocycling. Typically, 20-40 PCR cycles are used. After a certain number of cycles, the PCR reaction reaches a point at which the amplified DNA is no longer copied efficiently due to inhibition of the reaction, caused by binding of the polymerase to its amplification products. Typically, no more than 40 PCR cycles are needed. By the end of a PCR reaction, billions of amplified DNA molecules are present. To verify a successful PCR, gel electrophoresis followed by fluorescent staining is used to validate a PCR product size.

The PCR reaction mixture typically consists of only a few components. The components are mixed before thermocycling. The most basic PCR components for a typical reaction are listed in Table 1. The reaction components are normally optimized and the buffers may need to be modified to enable the use of special polymerases. A demonstration of optimizing reaction components was provided by the Henegariu group<sup>21, 22</sup>.

Table 1 – The essential components, their functions, and typically ranges for a basic PCR reaction. Abbreviations: picogram (pg), microgram (µg), nanomolar (nM), micromolar (µM), nanomoles (nmol).

<b>Component</b>	<b>Low Range</b>	<b>High Range</b>	<b>Function</b>
<b>DNA Template</b>	5 pg	1 µg	Target to detect
<b>Primer 1</b>	50 nM	1 µM	Targets first DNA strand
<b>Primer 2</b>	50 nM	1 µM	Targets second DNA strand
<b>Buffer - Tris pH 8.3</b>	5 mM	20 mM	Stabilizes reaction mixture
<b>Buffer - KCl</b>	25 mM	100 mM	Increases reaction efficiency
<b>Magnesium Chloride</b>	1.5 mM	6 mM	Co-factor for polymerase enzyme
<b>dNTPs</b>	50 µM	500 µM	Single base-pairs to make new template
<b>DNA Polymerase*</b>	0.02 Unit/ µL	0.2 Unit/ µL	Elongates DNA at primers 1 and 2

\* Manufacturers test polymerase activity and defined units to account for variations between lots.

One unit of enzyme incorporates 10 nmol of nucleotides at 74 °C in 30 minutes

The common terminology of the PCR field is provided in the next list.

- **Thermocycling** or PCR cycling – The physical process of heating a sample through a range of temperatures many times to control the number of rounds of DNA amplification.
- **PCR primers** or oligonucleotides – Sequences of single-stranded DNA, usually 16-30 bases long.
- **Template** – The purified sample containing many nucleic acids.
- **Target** – A specific nucleic acid sequence within a template. The PCR primers are designed to anneal to the target.
- **dNTPS** or deoxynucleotide triphosphates – The four individual building blocks needed to copy a DNA strand, including A, T, G, and C.
- **PCR amplicons** – The amplified target products of PCR.
- **Mispriming** – Unexpected PCR priming that creates nuisance or inhibitory PCR products.

- **Primer dimers** – Short PCR products created during PCR that are formed by mispriming of PCR primers to themselves<sup>23</sup>.
- **PCR efficiency** – Actual rate of doubling per PCR cycle, in percent.

PCR has been widely adapted to detect the full range of nucleic acid changes, including DNA methylation, copy number changes, microRNA expression levels, and mRNA expression levels. This wide applicability allows PCR to detect molecules that many other methods cannot, as described in section 1.3. Furthermore, PCR has been modified over the years by providing more advanced detection schemes as described in the next section.

#### 1.2.3.3 Advanced PCR

Due to the robustness of the standard PCR reaction, many advanced modifications have been adopted. This section highlights the different kinds of PCR that are relevant to the thesis.

Quantitative real-time PCR determines the relative or exact amount of template in a PCR reaction. Quantitative real-time PCR, or qPCR, works by measuring the intensity of fluorophores at the end of every PCR cycle, as shown in Figure 3. The fluorophores increase in brightness proportionate to the buildup of DNA in a reaction tube. As the fluorescent signal increases, it is possible to produce a plot of fluorescence versus PCR cycle. This plot can be used to determine how much starting template there was, based on the number of cycles it takes for the

fluorescence to surpass a background threshold level (Cts). By contrast, traditional PCR only looks at the end-products. Because quantitative PCR is widely applicable, it has been rapidly adopted, as shown in Figure 1.

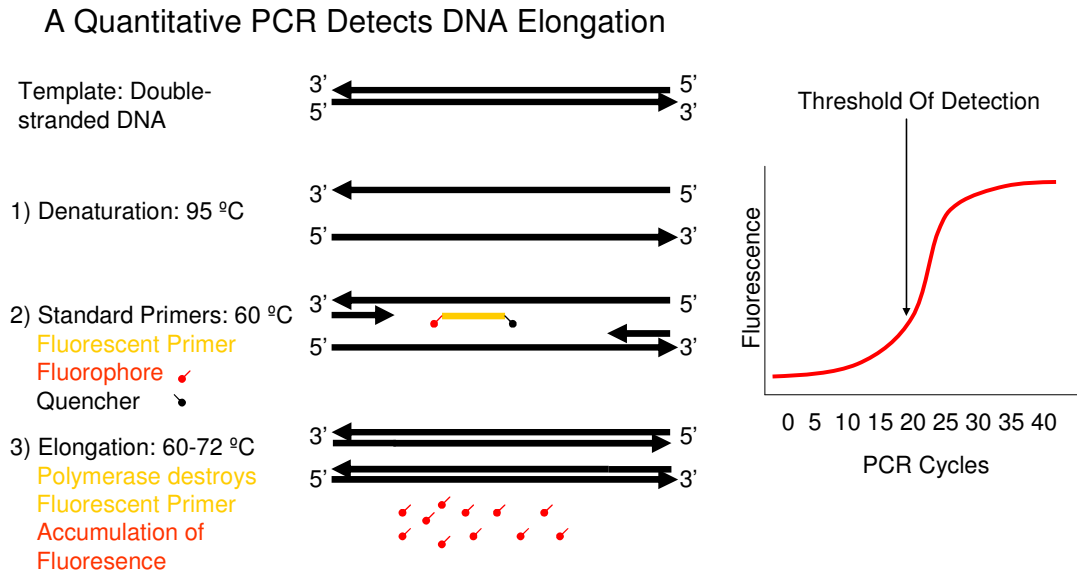


**Figure 3 – The quantitative real-time polymerase chain reaction (qPCR) detects the amount of template by monitoring fluorescence, allowing for the quantification of starting template. The qPCR reaction is based on a standard PCR reaction. However, a molecular probe (TaqMan probe) is added to the reaction mix. Upon elongation, the primer hydrolyses and releases fluorescent molecules into the reaction mixture. The fluorescence is measured at the end of each PCR cycle. The fluorescence intensity is presented as a graph that can be used to determine the amount of starting template relative to another qPCR reaction.**

There are two forms of qPCR. The first form uses a dye that generally increases fluorescence proportionate to the amount of double-stranded DNA in a sample<sup>24</sup>.

These dyes include ethidium bromide, SYBR Green I, or EvaGreen. Since the dye detects all double stranded DNA, the amount of initial double stranded template in a reaction cannot be too concentrated, and the reaction is known for detecting false-positives due to primer-dimer accumulation<sup>23</sup>. It is therefore best suited for solutions containing an abundance of starting template. However, it is popular because it is inexpensive.

The second form of qPCR uses molecular probe (also known as hydrolysis probe or TaqMan probe) chemistry, as depicted in Figure 3. The probe is an oligonucleotide with a fluorescent molecule bound to the 5' backbone of DNA and a quencher molecule bound to the 3' backbone of DNA. Because the quencher and probe are within 10 nanometers of each other, the fluorescence intensity of the fluorophores is reduced. This fluorescence principle is called Förster resonance energy transfer<sup>25</sup>. Since the probe has a 3' quencher, DNA polymerase will not recognize it as a priming site. Instead, a primer upstream from the probe is used as a priming site. As the polymerase elongates the parent strand, the polymerase will hydrolyze the probe, separating and releasing the fluorophores and quencher into solution. Because the fluorophore and quencher are far apart, a fluorescent signal increase can be measured at the end of every PCR cycle, provided that the fluorescence is above the instrument's measurement sensitivity. Because the probe includes a third primer sequence, it adds enough specificity to a PCR reaction to virtually eliminate false positives. As a result, it eliminates the need for gel electrophoresis. However, molecular probes are more expensive than qPCR dyes. Several references containing additional information on qPCR efficiency and qPCR equations are provided<sup>20, 26-29</sup>.

Reverse-transcriptase PCR, another advanced form of PCR, enables the detection of RNA molecules. RNA cannot be amplified by a standard PCR reaction because the DNA polymerase only recognizes DNA templates. Therefore, RNA templates are first converted into complementary DNA (cDNA) molecules using a reverse

transcriptase (RT) enzyme. The RT enzyme converts RNA into cDNA using a primer, and RT enzyme elongates the primer by copying the RNA. The primer is typically an oligo-dT or random oligo (6-10 random bases) to prime all possible mRNA sites. RT reactions are normally prepared using RT enzymes and buffer in a reaction volume in a first tube. Then, the cDNA is diluted into PCR buffer containing DNA polymerase in a second tube so that the RT buffer doesn't inhibit PCR. A typical two-step procedure dilutes an RNA template 10-15 times, reducing the amount of template and sensitivity of the reaction<sup>30</sup>. RT-qPCR refers to quantitative RT-PCR.

One-step reverse-transcriptase PCR uses only one tube for both the RT step and PCR step. However, while the two-step process can turn all RNA into cDNA, the one-step process must use primers that are specific to a few target mRNAs. There is evidence that an optimized one-step RT-qPCR is more sensitive for low abundance targets<sup>30</sup>.

Special considerations are needed when using PCR to amplify low copy number targets. If the number of target molecules in a sample is less than 20, it is not possible to dilute the purified template to quantify more than one gene. This is because the stochastic nature of random sampling (called the Poisson effect) causes the variability of PCR to increase if the sample is diluted<sup>31</sup>. Furthermore, the Poisson effect can be worsened with increasing PCR volume. As a result, if the number of target molecules in a PCR is less than 20, the entire purified template must to be used,

allowing for the quantification of just one mRNA. To quantify the expression of more than one gene, multiple templates would need to be prepared.

Multiplexed Tandem PCR is a technique for amplifying up to 92 nucleic acid targets in a single PCR reaction<sup>32-34</sup>, to detect multiple low-abundance targets (multiplexing). Tandem PCR allows multiple genes to be profiled from a sample by pre-amplifying many transcripts, so that all of these transcripts can be detected in a subsequent qPCR reaction. Because the templates are concentrated during the tandem PCR, sensitivity is not lost, which would be the case if the template was diluted instead (Poisson effect). To perform tandem PCR, a mixture of standard PCR primers is used to prime many targets. The primers are diluted to 100 nM and the PCR anneal time is also increased to 4 minutes to prevent bias – the less efficient amplification of any one target over another.

Methylation-specific PCR uses modifications of DNA before PCR to detect changes in DNA methylation patterns<sup>35,36</sup>. This procedure is beyond the scope of this thesis but is included to demonstrate the wide applicability of PCR for detecting the different changes to nucleic acids.

Fluidigm PCR assay – is a technique for improving the throughput of qPCR. The highest capacity that a traditional qPCR machines provides is 384 sample wells, allowing for the study of about a dozen genes in a few dozen samples. However, as the number of samples and genes studied increases, the number of sample wells

increases by a squared factor. For example, to study 96 genes and 96 samples would require at least 27,648 pipetting steps, 24 384-well plates, weeks of qPCR run time, and thousands of dollars of reagents. The Fluidigm approach solves these problems by using a microfluidic system to reduce the number of pipetting steps, such that the number of pipetting steps scales linearly with the number of sample wells. It also increases throughput by performing qPCR in up to 9216 miniaturized wells per experiment. For example, to study 96 genes and 96 samples would only require 192 pipetting steps. Each sample or primer/probe set is provided to a Fluidigm chip, which uses microfluidic channels and pressure to mix each primer and each probe set into a miniaturized PCR well. However, the Fluidigm system dilutes templates so much that it requires a pre-amplification step (tandem PCR).

#### 1.2.4 Typical methods of tissue sample preservation and storage

##### 1.2.4.1 Need for sample preservation

Solid biological tissue samples are obtained from a living or recently deceased organism. Removing a tissue cuts off its blood supply and starts a process called ischemia. Ischemia causes cellular processes to change due to loss of oxygen and other essential cell growth chemicals in the blood. Therefore the state of nucleic acids in the ischemic tissue partially reflects dying cells rather than a snapshot of the nucleic acids in living tissue.

For molecular analysis, it is very important to preserve samples quickly because gene expression can change or cells can begin to digest themselves (autolysis). It is also

important to preserve samples for storage because it takes many weeks or months to perform a nucleic acid study. It is even common to archive large numbers of tissue samples for future research projects on the scale of years. A survey of best practices for biospecimen handling and a list of existing human tissue/biospecimen repositories was compiled by RAND Science and Technology<sup>37</sup>.

#### 1.2.4.2 Types of sample preservation

Sample preservation most often includes freezing tissues or crosslinking tissues with formalin. Frozen samples are kept at -80 °C for storage, while formalin tissues are stored at room temperature. Less often, fresh tissues are preserved in a solution of ammonium nitrate, fixed with ethanol<sup>38</sup>, or used immediately without preservation. Solid tissue samples may be as small as one centimeter long and 1 millimeter in diameter (cylindrical biopsies), or as large as whole organs and even entire animals. Common sample preservation techniques are described below.

#### 1.2.4.3 Formalin fixation

Formalin fixation uses formaldehyde to crosslink tissue proteins together by covalent bonds<sup>39</sup>. Typically, a solid tissue is placed directly in a solution of formaldehyde for several hours or days. To prevent fixation differences across the tissue sample, formalin needs to penetrate the tissue quickly. Tissues are usually cut so that one dimension is small (< 5 millimeters) to allow faster penetration of formalin. After fixation, the tissues are dehydrated to remove water for long-term storage. Dehydration is the process of placing the tissue in successive baths containing

increasing levels of ethanol, followed by 100% ethanol, and followed by 100% xylene. The tissue is then placed in paraffin wax to “embed” the tissue by filling voids. The embedding also allows the tissue to be sectioned for light microscopy and prevents water from entering the sample during long-term storage.

It is very important to note that formalin fixation is the predominant method of sample preservation, as evidenced by the RAND report<sup>37</sup>. For example, the human cooperative tissue network supplies 5-10 times as many formalin fixed samples than other sample types. There are four reasons for the wide-spread use of formalin. First, the formalin fixation method was available before freezing techniques. Decades before samples were frozen, pathologists studied cells under a light microscope and trained themselves to recognize morphological features of tissue with respect to artifacts caused by formalin fixation<sup>40</sup>. Second, the formalin fixation method does not require a -80 °C freezer to store samples, saving the costs and space of freezer equipment and maintenance. Third, the formalin fixation can inactivate harmful pathogens and viruses in a biological sample, and likewise prevents any external bacteria from entering the sample. Fourth, the formalin-fixation, followed by paraffin embedding (FFPE), can increase the mechanical strength of tissue, allowing the layout of a sample to be preserved. A good example is lung tissue, which is hollow and could not be sectioned unless filled.

There are also disadvantages to formalin fixation. It is common for labs or hospitals to have widely varying protocols, which can impact sample quality<sup>41</sup>. For example, a

sample that is left too long in formalin will over-crosslink, resulting in poor quality RNA<sup>41</sup>. However it is becoming more common for labs to use carefully controlled protocols to preserve tissues with considerations for RNA quality<sup>37, 41</sup>. A second major disadvantage is that for unknown reasons, sample molecular quality degrades over time. Possible causes of molecular degradation include oxidation, hydrolysis, cross-linking, and other chemical modifications. A third disadvantage is that the slow speed of fixation hinders decision-making. A quick decision based on tissue morphology is often needed during the middle of medical surgery. Therefore, intraoperative histology is usually obtained by staining snap-frozen tissues or cells smeared from fresh tissue directly onto a slide. The slow speed of fixation can also cause autolysis or delayed protein immobilization in the center of a large sample, such as a brain.

#### 1.2.4.4 Other forms of sample preservation

There are other ways to preserve tissue samples. After formalin fixation, the most common preservation method is freezing. Tissues can be frozen on dry ice or in liquid nitrogen to rapidly preserve the tissue and the molecules inside. Frozen samples provide much longer (higher molecular weight) nucleic acid sequences than formalin fixed samples and may prevent chemical modifications of nucleic acids<sup>42</sup>. However there are many disadvantages to freezing. First, the samples require great care because once frozen, thawing will cause nucleic acid degradation<sup>43</sup>; freezing followed by thawing ruptures the cell sub-compartments and causes the contents to intermix, resulting in the release of natural enzymes in the tissue called nucleases.

Ribonucleases (RNases) will degrade RNA and deoxyribonucleases (DNases) will degrade DNA. Second, frozen samples require expensive and large freezers to store the samples. Third, any viruses or pathogens in the sample may still be active once the tissue is thawed.

Other tissue fixation methods include RNAlater, which is a solution of ammonium nitrate that preserves molecular quality. Ethanol fixation can also be used to dehydrate a sample, aggregate proteins, and preserve molecular quality<sup>38</sup>. Fresh tissue can also be used, but special tools are required to cut fresh tissues into thin sections.

### **Molecular quality due to preservation**

The quality of nucleic acids, particularly RNA from tissue samples, varies based on preservation methods and storage time. Quality can be defined as the average length of nucleic acids recovered from a sample, but also needs to take into account the possibility of chemical modifications. Fresh samples are known to have the highest quality nucleic acids, whereas long term formalin fixed samples are known to have the poorest sample quality<sup>33, 44</sup>. The quality of nucleic acids from freshly-fixed samples and frozen samples is in between fresh and long-term formalin-fixed samples. The impact of sample molecular quality due to preservation methods is an ongoing subject of debate<sup>45</sup>.

### 1.2.5 Typical methods for recovering nucleic acids

Nucleic acids need to be extracted and isolated from tissues in order to be amplified by PCR. The nucleic acids in a tissue are mixed with other molecules such as proteins, lipids, carbohydrates, and salts, all which can inhibit PCR. Of critical importance, tissues also contain natural (endogenous) RNases and DNases that degrade nucleic acids. Therefore the first step to recovering nucleic acids is to inhibit the action of RNases or DNases. The next step is to break open the cells (lysis). The last step is to purify the nucleic acids from the other cellular components. Care is required to isolate nucleic acids intact from tissues for subsequent analysis. This section describes three common ways to recover nucleic acids.

#### 1.2.5.1 GITC, phenol, chloroform, and isoamyl alcohol

One of the most cited academic papers in history is by Chomczynski and Sacchi (50,000+ citations), which demonstrated a chemical mixture that lyses cells and maintains molecular quality in one step<sup>46</sup>. This technique has been widely adopted because it could isolate total RNA from frozen samples faster (4 hours) than other methods available at the time. Furthermore, the technique recovers high quality RNA from tissue samples rich in RNases, such as pancreas.

The method works by first denaturing and inhibiting RNases using the chemical guanidinium isothiocyanate (GITC). Surfactants and buffers are added to the GITC to help lyse cells. Water-saturated phenol and a mixture of chloroform-isoamyl alcohol are then added sequentially and centrifuged to create three layers – an

aqueous upper phase containing RNA, a middle liquid interphase containing DNA and proteins, and a pink lower organic phase containing proteins and lipids. The aqueous phase is carefully removed without removing any interphase or lower phase components. Alcohol is added to the aqueous phase, and the sample is cooled to -20 °C for an hour to precipitate the RNA. The sample is centrifuged to concentrate the RNA into a pellet, and the supernatant is removed. The RNA is resuspended in ethanol several times to wash it, and is finally vacuum dried. To isolate DNA using this method, the GITC is not included in the initial step.

Although the technique was created in 1987, it is still popular because it isolates nucleic acids from large tissue samples effectively. It also isolates small RNAs very effectively. However it has major drawbacks. First, the technique will not work for small tissue volumes because a sufficient weight of nucleic acids (nanograms to micrograms) is needed to create a concentrated RNA pellet. Second, the centrifugation step requires careful handling and manual inspection to ensure that only the aqueous phase is removed. Otherwise organic solvents will be present in the purified sample that will inhibit PCR. Third, the technique uses chemicals that are labeled as toxic. Fourth, the technique requires special equipment, several tubes, and many reagents.

#### 1.2.5.2 Silica purification technology

A technique using silica to bind and purify nucleic acids was optimized by Boom et al in 1990<sup>47, 48</sup>. The Boom technique is similar to the Chomczynski method, but it

simplifies the centrifugation step, eliminates error from precipitating nucleic acids into a pellet, and eliminates the use of toxic chemicals like phenol. The Boom technique uses GITC buffer to lyse cells in suspension. Silica (glass) microbeads (diatoms) are then added to the lysed sample. The silica captures nucleic acids in the presence of chaotropic salts like GITC due to several effects. Primary effects include the increase of DNA mobility and dehydration in denaturing buffers, the absorption of water at the silica surface, and the reduction of negative silica surface potential in high ionic strength buffers<sup>49</sup>. The silica is centrifuged, holding on to the nucleic acids while allowing other lysed cell constituents to wash away. The nucleic acids are purified further by rinsing with ethanol, without removing (eluting) the nucleic acids from the glass. Finally, water is added to the glass to elute the purified nucleic acids. Because the nucleic acids are bound to particles rather than floating free in solution, this technique is called solid-phase purification.

The Boom method cut the sample preparation time from 4 hours to 1 hour. It also eliminated the need to use phenol-chloroform, which is more hazardous than just using chaotropic salts. The purification efficiency of the method (nucleic acids recovered vs input) is about 50%<sup>47</sup>. This technique is still popular today and modern variations use a silica membrane in a spin-column in place of silica beads to improve handling by eliminating the chance of pipetting microbeads.

However, the technique has the disadvantage that it was designed to lyse cells in suspension. Therefore, whole tissues or even tissue scrapes and tissue sections need

to be homogenized first. Most often, the tissues are mechanically ground, for example in a blender or using a mortar and pestle in liquid nitrogen. If the tissue is not first homogenized, tissue fragments will not fully dissolve and will clog pipette tips and silica surfaces.

The technique also selects for certain nucleic acids. It typically isolates nucleic acids that are larger than 200 base pairs. This means that semi-degraded RNA from formalin-fixed samples and naturally small RNA like microRNA cannot be efficiently purified. The Boom technique also isolates DNA, which may interfere with RNA detection and may need to be degraded by a DNase treatment<sup>47</sup>. Lastly, the fluid flow through the pores in a silica membrane can cause long DNA molecules to shear into smaller fragments.

#### 1.2.5.3 Magnetic beads

Another advance in tissue lysis and nucleic acid purification was the introduction of magnetic beads with a nucleic acid binding surface<sup>50-52</sup>. With the magnetic bead method, tissue is first ground into a frozen powder, or cells in suspension are used as with the Boom method. The tissue is lysed in a lithium chloride buffer with surfactants. Magnetic beads coated with oligo-dT molecules are added to the lysate to specifically hybridize to the polyA tails of mRNA. The magnetic beads are concentrated using a magnet, which pulls mRNA away from other components in the lysis buffer. The mRNA is purified using aqueous salt buffer washes. The purified mRNA is then eluted in water or low-salt buffer. This technique cut the purification

time down from one hour down to 15 minutes by eliminating the need for centrifugation.

The original magnetic bead-based purification used oligo-dT molecules which is limiting. Oligo-dT molecules do not capture DNA, small RNA, or total RNA. They also introduce bias in that the mRNA molecules are only captured if they have polyA tails, and any breaks in the RNA molecule upstream from the polyA tail will not be purified. Therefore, this technique is only good for working with high quality (fresh or frozen) tissue specimens.

To address some of these deficiencies, the company DNA Research Innovations patented a magnetic bead-based surface using a “ChargeSwitch” material<sup>53</sup>. The patent was awarded in 2005 and the technology was licensed to Invitrogen. The ChargeSwitch material is similar to silica beads because they both capture or elute total nucleic acids by changing a single variable (pH or salt concentration of water). For ChargeSwitch beads, the pH is lowered below 4.5 to capture nucleic acids, while the pH is raised above 8.0 to elute nucleic acids. Because the ChargeSwitch surface captures total nucleic acids and because the magnetic beads eliminate the need for centrifugation, the ChargeSwitch magnetic beads were used extensively for our 2D-PCR protocol. However, no literature characterizing ChargeSwitch magnetic beads exists and there is little information about them.

#### 1.2.5.4 Proteinase K

Another method for lysing tissues to recover nucleic acids is the use of proteinase K. The proteinase K method uses a simple buffer to stabilize pH, and proteinase K, an enzyme that digests proteins in tissues to lyse cells. Although proteinase K is a protein itself, it is resistant to the enzymatic denaturants and to the inhibitors SDS, urea, and EDTA<sup>54</sup>. This makes proteinase K ideal for use in denaturing buffers. Once a sample is lysed with proteinase K, the released nucleic acids may be used directly by heat inactivating the proteinase K, but it is more common to mix the lysate with GITC and to purify with one of the previously discussed purification techniques.

#### 1.2.5.5 Special considerations for formalin fixed samples

It should be noted that formalin fixed samples were not originally intended for preserving the molecular integrity of nucleic acids. However, the recovery of nucleic acids from formalin fixed samples is increasing<sup>55,56</sup> because most solid tissues are formalin fixed. Since the proteins are already crosslinked in these tissues, there is little concern about releasing endogenous RNases. Instead the challenge is getting the nucleic acids out of the tissue. For working with formalin fixed samples, proteinase K provides the highest yields of nucleic acids and is the predominant lysis method<sup>42, 44, 56, 57</sup>

Another special consideration for formalin fixed samples is that the effects of fixation should be reversed to allow the recovery of more molecules. Specifically, if heat and

moisture are applied to a formalin fixed sample, the chemical crosslinks will be hydrolyzed. This approach is called antigen retrieval<sup>58, 59</sup>.

#### 1.2.6 A common lab workflow to study changes in nucleic acids

A sample project workflow is provided in order to show how the methods presented in this section (sample fixation, nucleic acid purification, and qPCR) fit together.

Typically, the experiment begins with the hypothesis that a change in nucleic acids confers a biological difference or diseased state. In order to determine the difference, at least two nucleic acids are quantified from normal and non-normal (diseased) tissues. At least one nucleic acid called a housekeeping gene is required. The housekeeping gene is one that does not change between the diseased and normal states and can be used to account for differences in nucleic acid recovery between different samples.

1. Obtain tissue (normal, non-normal) from surgery or biopsy.
2. Preserve tissue (i.e. by freezing).
3. Section tissues with a cryostat microtome.
4. Scrape tissues into different sample tubes (i.e. tumor vs normal).
5. Quickly lyse samples in denaturing buffer (i.e. GITC).
6. Purify the nucleic acids of interest (i.e. RNA using a spin column).
7. Quantify the desired target nucleic acids by qPCR (i.e. tumor promoter).
8. Quantify the “housekeeping” nucleic acids by qPCR.

9. Normalize the amount of target to housekeeping genes to account for and measure differences between two samples<sup>60-62</sup>.
10. Determine the significance - is there a novel finding (i.e. t-test,  $p < .05$ ).
11. Validate findings using other methods (i.e. ISH, IHC, see section 1.3).

### 1.2.7 Summary

It should be noted that the methods described in this section apply to studying nucleic acids from large areas of tissue. Most often gross regions of tissues are analyzed as a whole - on the scale of millimeters or centimeters. However, tissues are made from dozens of cell types and have significant cellular heterogeneity, which may reduce the significance or utility of nucleic acid studies using mixed cell types<sup>63-65</sup>. In the next section, methods intended for studying the layout of nucleic acids in a tissue sample are described.

## 1.3 Current methods for localizing nucleic acids in tissue

### 1.3.1 In-situ hybridization (ISH)

ISH can localize specific nucleic acids at the cellular level. By studying nucleic acids across a tissue sample cellular heterogeneity is preserved, tissue morphology is preserved, and even sub-cellular features can be examined. As a result ISH has become a central tool in molecular biology for explaining fundamental processes<sup>16, 40</sup>.

A publication history of ISH is provided in Figure 4.

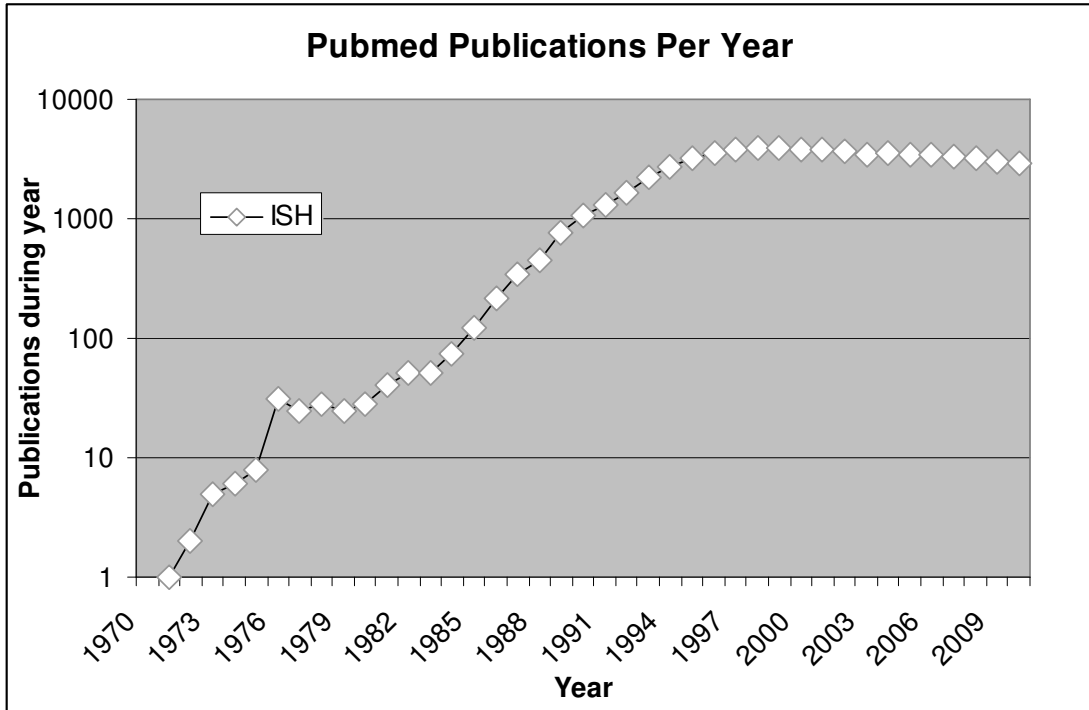


**Figure 4 – *In-situ* hybridization (ISH) publications by year. Data generated by performing a Pubmed search by year, in title or abstract, for the quoted phrase “in situ hybridization.”**

ISH works by hybridizing an artificially created oligonucleotide (probe) with either DNA or RNA in the cell. Initially, ISH required the use of radioactive labeled probes, slowing its growth for almost 20 years until safer and more sensitive fluorescent and indirect labeling methods were created<sup>16</sup>. Today the probe is labeled with either a direct reporter such as a fluorescent molecule, or an indirect reporter, such as biotin or digoxigenin, that is detected at a later stage. A typical ISH involves many steps and days to complete. An exemplary ISH protocol is summarized below based on the whole-mount mouse embryo staining technique by Correia and Conlon<sup>66</sup>.

1. Day 1:
  - a. Place tissue sample on slide.
  - b. Formalin fix samples to lock biomolecules in place.
  - c. Lightly treat cells with proteinase to make cells permeable.
  - d. Hybridize digoxigenin-probe overnight.
2. Day 2:
  - a. Rinse and wash several times.
  - b. Add blocking reagents to reduce non-specific binding.
  - c. Hybridize digoxigenin antibody overnight.
3. Day 3 (up to 5 days):
  - a. Rinse and wash several times.
  - b. Monitor color development under a microscope.
  - c. Wait 30 minutes to 3 days.
  - d. Rinse overnight to preserve color.

There are hundreds of recipes like this one claiming to be the best recipe for a specific tissue. Therefore a key limitation of ISH is that it needs to be re-optimized for every tissue type and fixation method. It was shown to be difficult to reproduce some ISH protocols between labs due to cellular artifacts<sup>67-69</sup>.

A second key limitation is the low sensitivity of ISH. ISH is most commonly reported to have a detection sensitivity of “10-20 copies” of target mRNA per cell<sup>13, 14, 70-72</sup>. If the concentration of probe is increased, background staining becomes too

great to detect the target. Furthermore, whereas a long probe can be made to detect single DNA molecules, several smaller probes are used to detect many more mRNA molecules because mRNA is naturally shorter and degraded. Because most mammalian mRNA is present in low copy numbers (less than 15 per cell) and because low copy transcripts are hard to detect, relatively few studies using ISH focus on gene expression<sup>73</sup>.

A third limitation is that ISH cannot easily detect changes to small nucleic acid sequences. The proteinase K step that makes tissue permeable and the wash procedures will rinse away target nucleic acids. Just as easily as probe can enter the cells, so can the small RNA diffuse out of the cell. This issue has been recently addressed with some success<sup>74</sup>, but the protocol takes 1 week. Similarly, it is not easy to detect DNA methylation (a single base pair modification) with ISH, although one publication has recently addressed this challenge<sup>75</sup>, it is too early to tell if the technique works well.

A fourth limitation is that ISH is most effectively used as an on/off detection tool<sup>76</sup>.

It is not normally possible to quantify the amount of target.

A fifth limitation is that freshly-fixed samples need to be used in order to detect low abundance mRNA transcripts. During a freeze-thaw or storage with formalin fixation, some mRNA transcripts are lost to degradation. Researchers who study low-

abundance transcripts therefore focus on cell culture or mouse models so that fresh tissue is available.

A sixth limitation is that usually only one target is optimized for study per tissue section. This uses more tissue sections than if multiple targets could be detected (multiplexed) from a single tissue section. In principle, ISH can use combinations of up to 6 colors with 21 target probes to detect different regions of chromosomes<sup>76</sup>, but it is normally only multiplexed for 2 or 3 targets for mRNA<sup>77, 78</sup>.

As a result of these critical limitations (summarized in Table 2), ISH is mainly used in clinical medicine to identify viruses<sup>79</sup> or to diagnose cancers using a few highly-abundant mRNAs in cancer when diagnosis by protein-staining methods (see 1.3.5) fail<sup>79-81</sup>. ISH is primarily still a research tool, and its use or significance seems to have plateaued, as shown in Figure 4.

Table 2 – Benefits and limitations of *in-situ* hybridization (ISH).

Resolution	Sensitivity	Time	Complexity	Reproducibility
<5 μM	Low	Days	High	Good
Samples	Targets	Multiplexing	Quantitation	Minimum Target
Fresh-Fixed	DNA, mRNA	1-3 Targets	No	20 copy/cell

### 1.3.2 In-situ PCR (ISP)

In order to circumvent the critical limitation of ISH sensitivity, in-situ PCR (ISP) was developed in the early 1990s<sup>82</sup>. The principle behind ISP is to amplify targets in tissue using PCR to increase the number of targets before staining. PCR

amplification increases the number of targets and increases specificity due to the use of two primer sequences. The use of ISP increases the number of targets available for ISH by about 50 times<sup>72, 82</sup>.

The potential of ISP rapidly popularized the technique, but it soon became clear that ISP is not a reliable<sup>14, 68, 71, 72, 83, 84</sup>. It turns out that the tissue environment is so complex that results are unreliable and irreproducible. ISP is therefore not in widespread use, as illustrated by the number of publications on ISP versus time, shown in Figure 5. Furthermore, just like ISH, quantification using ISP is “extremely difficult” as reported by Komminoth<sup>72</sup>. ISP, like ISH, therefore appears to be best suited for detecting viruses<sup>85</sup>. A summary of the benefits and limitations of ISP are provided in Table 3.

Table 3 – Benefits and limitations of *in-situ* PCR (ISP).

Resolution	Sensitivity	Time	Complexity	Reproducibility
<5 μM	Low	Days	High	Poor
Samples	Targets	Multiplexing	Quantitation	Minimum Target
Fresh-Fixed	DNA, mRNA	1 Target	No	0.1-1 copy/cell

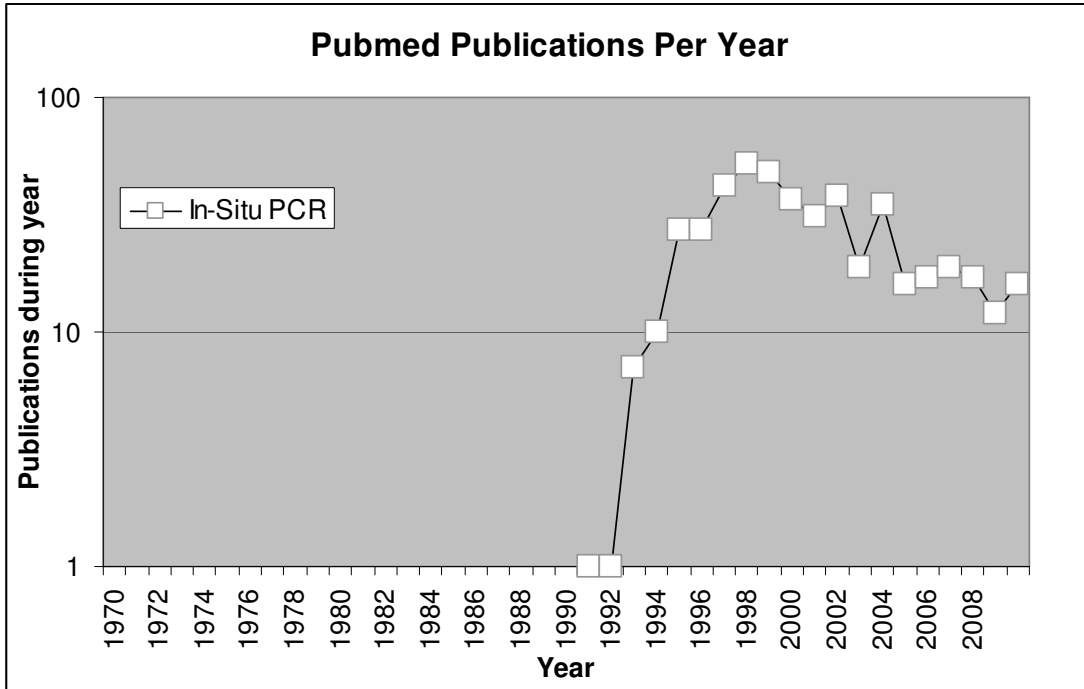


**Figure 5 – *In-situ* PCR publications by year. Data generated by performing a Pubmed search by year, in title or abstract, for the phrase [PCR in situ hybridization or "in situ PCR"].**

### 1.3.3 Laser microdissection & PCR

Laser capture microdissection (LCM) was developed by Emmert-Buck<sup>65</sup> in 1996 to address the need for a more sensitive and widely-applicable technique to study nucleic acids from specific cells. With LCM, a user places an 8 millimeter thermoplastic film (LCM cap) over a dried tissue sample. The user then directs a laser to melt the film over a homogenous group of cells from the heterogeneous tissue. Each laser shot takes about one second and covers a small group of cells, therefore many laser shots are needed to collect enough sample for analysis, typically averaging 10,000 laser shots per sample. Removing the film pulls off the cells of interest. The cells on the film are then lysed using standard GITC methods, and nucleic acids are purified using silica spin column technology<sup>86</sup>. Because the nucleic

acids are purified in solution, they can be used with most available techniques such as qPCR, microarrays, whole-genome amplification, sequencing, etc. However, by far the most common analysis method is qPCR because it is quantitative and because it makes the most use of the small amount of recovered sample.

The LCM technique does not directly preserve the spatial resolution of nucleic acids. In fact, all of the cells captured on an LCM cap are mixed and analyzed together. The purpose of LCM is to enrich for specific cell types (i.e. stromal tumor cells) from the bulk of the tissue, providing enough sample that low abundance mRNAs can be detected by qPCR. In order to preserve the 2D layout of a sample using LCM, multiple caps must be collected from a variety of locations across tissue. Days to weeks are needed to perform the LCM and additional days to weeks are needed to perform the purification and nucleic acid analysis on the large number of specimens<sup>8</sup>. The sensitivity of LCM followed by the quantification of gene expression by qPCR has made LCM a widely accepted technique, as evidenced by its publication history (Figure 6). In addition, because LCM uses downstream molecular techniques, changes in DNA methylation and microRNA expression can be detected - these nucleic acids cannot be detected easily with ISH or ISP.

However, LCM has several limitations. First, many cells are needed to provide sufficient nucleic acids for analysis. Typically, tens of thousands of individual laser shots are needed, requiring hours to dissect enough cells for an average study. 10,000

fresh cells contain about 50 ng of RNA or DNA template. This process is requires continuous operator input and may also be subject to user bias.

A second limitation is the type of sample that can be used. In order to adhere the melted polymer to the cells, the tissue must be dehydrated. Most of the samples are frozen sections that are dehydrated in xylene. The dehydrated tissue also needs to be processed within 30 minutes to prevent the re-activation of RNases by moisture in the air. It is not common to use FFPE samples for LCM because even more laser shots are needed to make up for degradation of RNA in the sample.

A third limitation is that only a small percentage of the whole tissue section can be examined in a reasonable time. To obtain a more global view, it is desirable to obtain data from a significantly larger percentage of a tissue section<sup>8</sup>.

A fourth limitation is that collecting a small amount of tissue causes nucleic acid purification efficiency to drop when using silica spin-columns<sup>87, 88</sup>. Papers have been published showing the use of LCM to capture and study one cell, however special cellulose columns and nucleic acid amplification strategies are required to work with the limited material<sup>89</sup>. While it is not common to work with single cells, these studies demonstrate the wide applicability of providing purified template, allowing the workflow to incorporate novel techniques.

In summary, LCM solved the majority of problems with ISH in that it purifies the nucleic acids, allowing robust downstream detection methods to be used. However, the critical limitation of LCM is the cost of labor and time to isolate, purify, and analyze many samples across a single section. A summary of the benefits and limitations of LCM are provided in Table 4.

Table 4 – Benefits and limitations of laser capture microdissection + PCR (LCM).

Resolution	Sensitivity	Time	Complexity	Reproducibility
>10 $\mu$ M	High	Days	Medium	High
Samples	Targets	Multiplexing	Quantitation	Minimum Target
Frozen	Unlimited	Unlimited	Yes	5-50 ng

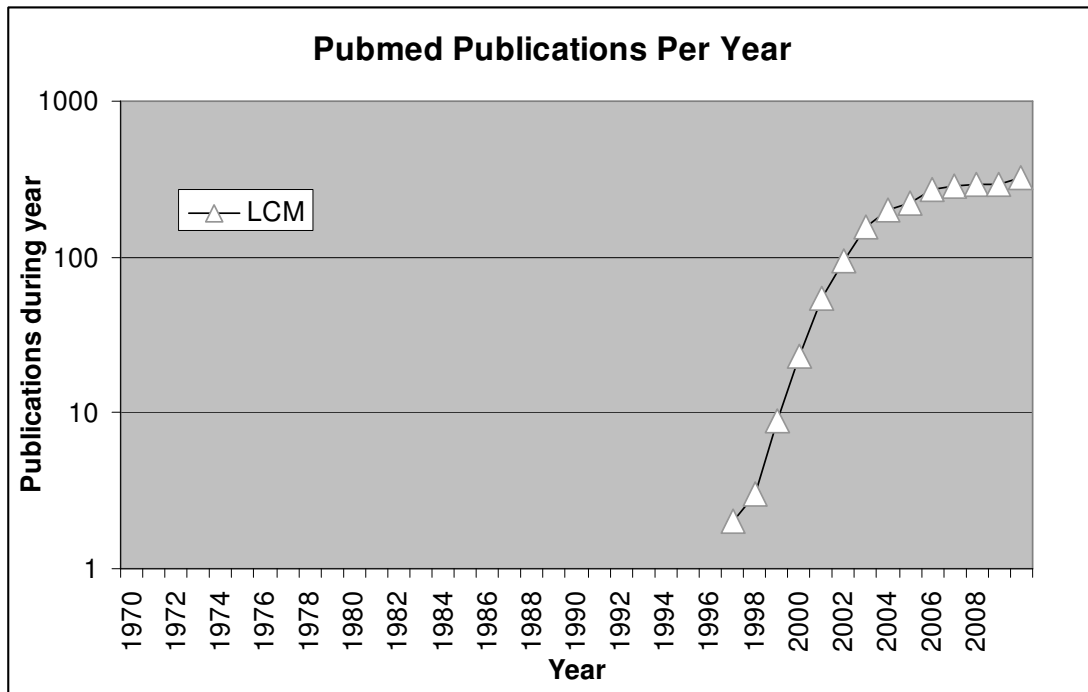


Figure 6 – Laser capture microdissection (LCM) publications by year. Data generated by performing a Pubmed search by year, in title or abstract, for the phrase [laser microdissection or "laser capture microdissection].

#### 1.3.4 Macrodissection or voxelation & PCR

The other alternative to laser capture microdissection is to manually dissect gross regions of tissue to preserve spatial heterogeneity, albeit on the scale of millimeters to centimeters. To perform a macrodissection, subregions of tissue (i.e. tumor vs normal) are scraped into a tube without any regard to sample heterogeneity within the scrape. Alternatively, a garlic-slicer like device can be used to cut the tissue into 1 mm x 1 mm x 2 mm rectangles called voxels<sup>6, 18</sup>. Dissected samples are lysed individually, and the nucleic acids are purified from the lysates and analyzed by methods such as PCR or microarray. Like LCM, changes in DNA methylation and microRNA expression can be detected after macrodissection because the nucleic acids are first purified.

While macrodissection and voxelation may appear crude, studies have obtained useful information with macrodissection that could not have been obtained with other techniques. This is particularly true for mapping gene expression in the brain or for tumor research studies<sup>7, 90</sup>. For example, sufficient sample is obtained from brain voxelation to perform microarray analysis directly. If smaller samples were used, a transcriptome amplification step would be required, adding bias to the results.

In fact, a macrodissection-based method made it into the clinic for diagnostic and prognostic purposes, and it is called the oncoType DX test<sup>91</sup>. In the procedure of this diagnostic test, formalin-fixed tissue sections are made from resected breast tumors, and normal regions are scraped and discarded using a razor blade, such that at least

50% of the sample contains tumor cells. It is possible to use such a heterogeneous sample because the signal from non-tumor cells in a sample do not overwhelm the signal from tumor cells, because tumor cells provide more RNA<sup>92</sup>. Subsequently, six macrodissected tissue sections are lysed, RNA is purified, RNA is amplified by tandem PCR, and pre-amplified targets are quantified by qPCR to determine the expression of 21 genes. 16 of the genes are specific to cancer and are normalized to the average expression of five housekeeping genes. If other techniques were used, such as microdissection, the sample analysis would have taken too long or there would not have been enough sample for a direct analysis. Therefore, despite the millimeter-scale resolution, macrodissection is useful and versatile.

There are only two major limitations with macrodissection. The first is the obvious lack of spatial resolution below about one millimeter. Macrodissection is fundamentally limited by the ability of an individual to scrape subregions of tissue by hand.

The second limitation of macrodissection is the bottleneck caused by having to purify and analyze dozens or hundreds of nucleic acid samples in parallel<sup>87, 93, 94</sup>. Typically, each macrodissected sample is placed into a tube for lysis. Each sample is then placed into another tube for purification, another for recovery, and yet another for qPCR. If hundreds of samples are processed this way, the technique becomes laborious.

It is difficult to estimate how many studies scrape large areas of tissue. However, one can estimate that the vast majority of studies using PCR, qPCR, and microarray detection also use non-cellular resolution techniques like macrodissection. There were only 320 publications LCM in 2009, compared to 22,000 publications on PCR, qPCR, or microarray analysis (Figure 7). Although many of the microarray or PCR studies may use uniform samples such as cells grown in culture, it is likely that thousands of studies each year use macrodissection methods on tissue sections. The main reason for the popularity of macrodissection is the low complexity of the approach. A summary of the benefits and limitations of macrodissection is provided in Table 5.

Table 5 – Benefits and limitations of microdissection + PCR.

Resolution	Sensitivity	Time	Complexity	Reproducibility
>1 mm	High	Hours-Days	Low	High
Samples	Targets	Multiplexing	Quantitation	Minimum Target
Any	Unlimited	Unlimited	Yes	5-50 ng

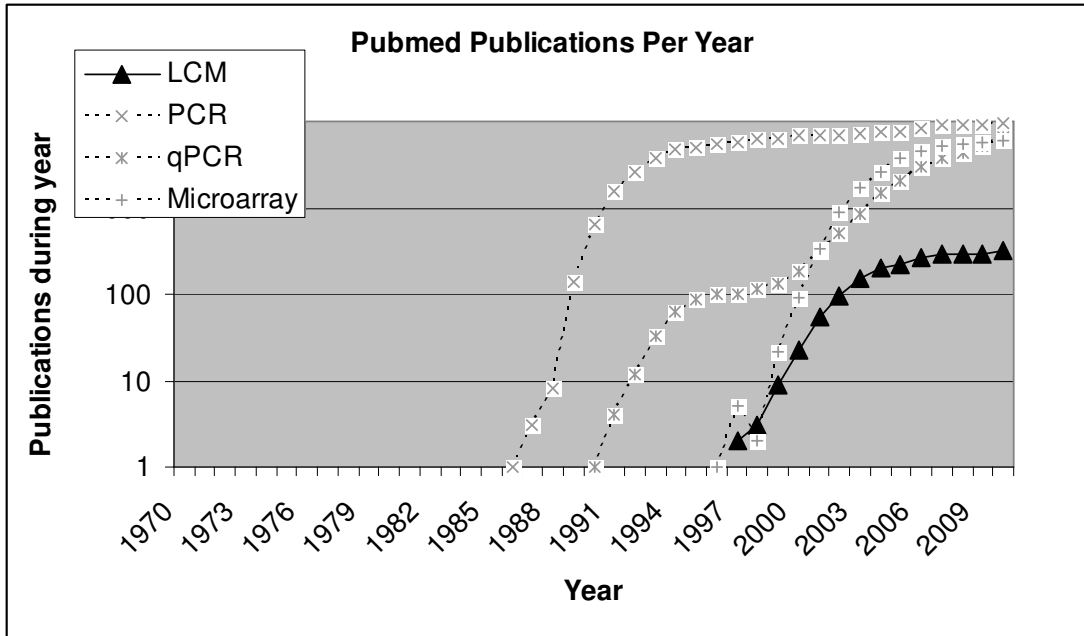


**Figure 7 – LCM, PCR, qPCR, and microarray publications by year.** Data generated by performing a Pubmed search by year, in title or abstract as described previously for LCM, PCR and qPCR. Microarray history was generated using the phrase [gene expression profiling or microarray not "cell microarray" not "tissue microarray"]. The difference in publications between LCM and these other techniques was 21,743 in year 2009. These studies are presumed to use large tissue scrapes, cell culture, or other methods that do not provide spatially resolved information.

### 1.3.5 Immunohistochemistry (IHC)

Although it is intuitive to detect nucleic acids in tissues directly, many researchers will measure the indirect effects of nucleic acids on protein levels. There is in fact a very strong direct correlation between mRNA expression and protein expression for some genes, but no correlation for others, as exemplified in Greenbaum's study<sup>95</sup>.

Immunohistochemistry (IHC) is a staining technique for detecting proteins in tissue samples. Typically an antibody is hybridized to a target protein of interest. The antibody is then indirectly labeled and viewed under a microscope, as with ISH. Like

ISH, the weaknesses of IHC include sensitivity, reproducibility, and inability to quantify the amount of target in a sample<sup>80,96</sup>. As with the transcriptome (RNAs), the proteome is dominated by a few highly abundant proteins<sup>97</sup>. IHC is most often used to provide a yes/no detection of a few medium and high abundance proteins for clinical diagnostic purposes<sup>81,97-99</sup>. A publication history of IHC is provided in Figure 8.

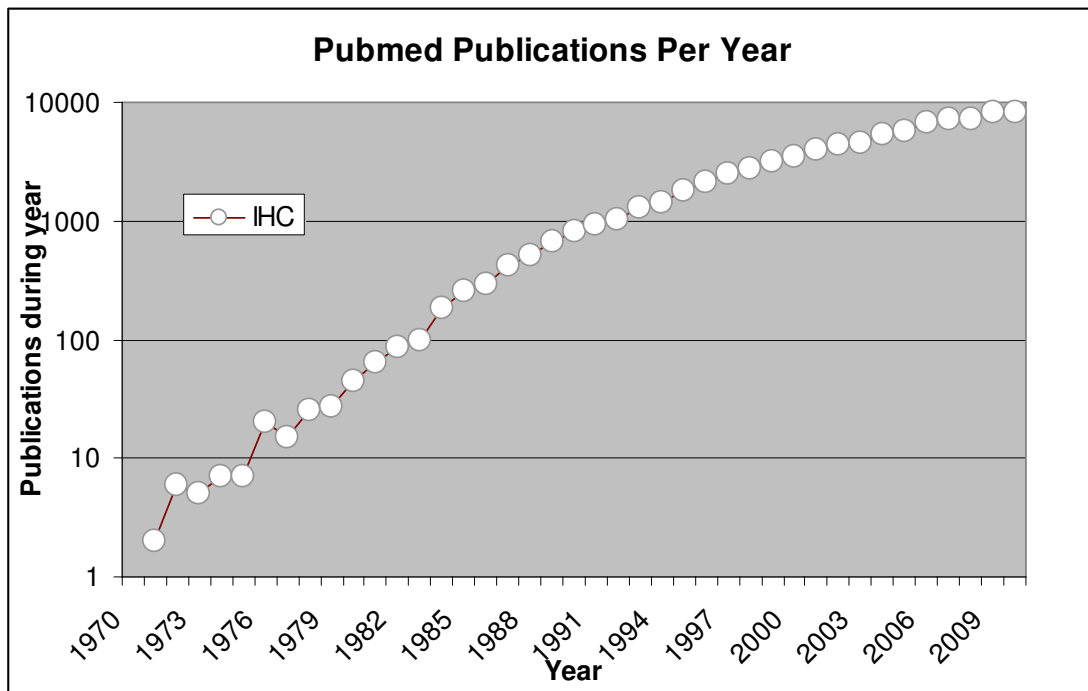


**Figure 8 – Immunohistochemistry IHC publications by year. Data generated by performing a Pubmed search by year, in title or abstract, for the quoted phrase “immunohistochemistry.”**

### 1.3.6 Summary

There are four major methods for localizing nucleic acids in tissues or cells. Each method has major limitations and trade-offs, as summarized in Table 6. ISH is capable of detecting highly abundant nucleic acids at the finest resolution. ISP provides better sensitivity, but it was so difficult to reproduce results that ISP was essentially abandoned by the field. LCM enriches for cells across a subregion of

tissue, is sensitive, reproducible, and allows for multiple downstream methods to be used – thus it is widely applicable. However, LCM is still laborious, complex, and limited to high-quality samples. Finally, macrodissection provides the maximum use of downstream methods and sample types, but it has the lowest spatial resolution.

Table 6 – Benefits and limitations of four methods for localizing nucleic acids in tissues.

	Resolution	Sensitivity	Time	Complexity	Reproducibility
<b>ISH</b>	<5 $\mu$ M	Low	Days	High	Good
<b>ISP</b>	<5 $\mu$ M	Low	Days	High	Poor
<b>LCM</b>	>10 $\mu$ M	High	Days	Medium	High
<b>Macrodissection</b>	>1 mm	High	Hours-Days	Low	High

	Samples	Targets	Multiplexing	Quantitation	Minimum Target
<b>ISH</b>	Fresh-Fixed	DNA, mRNA	1-3 Targets	No	20 copy/cell
<b>ISP</b>	Fresh-Fixed	DNA, mRNA	1 Target	No	0.1-1 copy/cell
<b>LCM</b>	Frozen	Unlimited	Unlimited	Yes	5-50 ng
<b>Macrodissection</b>	Any	Unlimited	Unlimited	Yes	5-50 ng

## 1.4 Aims

### 1.4.1 A robust nucleic acid mapping method

There are many trade offs between the benefits and limitations of current techniques for localizing nucleic acids in a tissue sample, as shown in Table 6. There is therefore a need for a robust method – a technique that preserves spatial resolution but is sensitive, consistent, widely applicable, and not prohibitively expensive or time-consuming.

The focus of this thesis is the creation of a robust method for mapping nucleic acids in tissues. Each of the desired aspects of a robust method are described further in this section, along with an explanation of how the 2D-PCR approach achieved these

goals. Then, three aims achieved by the thesis towards establishing 2D-PCR as a useful technique are presented.

#### 1.4.1.1 Sensitivity

A sensitive method is needed to detect low-abundance mRNAs, because the majority of mRNA is in a low-abundance class, defined as less than 15 copies per cell. By comparing the existing techniques, it is clear that using solution-phase PCR as an end point detection method detects nucleic acids more sensitively than ISP or ISH. The purification step allows cellular artifacts to be removed by purification, improving sensitivity.

Furthermore, because the majority of clinical samples are formalin-fixed and may contain degraded nucleic acids, the copy number per cell is even lower. There is therefore a need to detect RNA from formalin-fixed samples sensitively.

Macrodissection appears to be the only method for studying these samples.

Macrodissection can detect RNA from formalin-fixed samples because it pools hundreds or thousands of cells. Therefore, some spatial resolution must be sacrificed to allow detection and quantification of targets.

Finally, methods are needed for detecting small RNAs, because as these nucleic acids are being increasingly studied and implicated in protein regulation. ISH and ISP do not offer reliable ways to study microRNA. Therefore, purification methods are needed that purify total RNA, including small RNAs.

#### 1.4.1.2 Consistent

A consistent method is needed because techniques like ISP, ISH, and IHC have been unreliable, making it difficult to use them for clinic diagnostic purposes. Because ISP attempted to amplify nucleic acids in cells, it turned out to be inconsistent. A typical solution-phase PCR reaction amplifies molecules up to 1 billion times, but in-situ PCR reported only 50-fold amplification. Furthermore, ISP and ISH require optimization and different protocols for each sample type. Ideally, one protocol should be consistent enough that it works on a variety of tissues types and tissue preservation methods. The only consistent methods appear to be LCM and macrodissection because they purify nucleic acids and use reliable downstream detection methods like qPCR.

#### 1.4.1.3 Widely applicable

Another constraint of existing methods is that they are not applicable to a wide variety of tissue types, targets, and downstream detection methods. There are several desirable traits that fit into this category, and these are listed below.

#### Quantitative

The technique needs to be quantitative. So far, ISH and IHC are the only methods used in the clinic, but they are not quantitative. They only work well on molecules that are abundant or largely over-expressed tissues, so that an on/off detection can be

used to provide unambiguous results. The use of qPCR allows for quantitation of targets and may thereby improve clinical utility.

### Multiplexing

ISP, ISH, and IHC generally look at one or two targets at a time. Once the tissue is used, it is difficult to detect another target, so the sample must be discarded.

However, there are over 20,000 genes, thus it is useful and often necessary to look at more than one gene at a time. An example is the Oncotype DX test, which quantifies the expression of 21 genes per sample to make a diagnostic. Therefore, multiplexing a few targets is inadequate for today's needs. The minimum amount of multiplexing that would be useful may be in the range of 20-100 targets. This is currently possible using Tandem PCR.

### Target types

The ideal technique would detect all of the possible genetic changes listed in section 1.2.2. As stated earlier, microRNA is not normally detected with ISH because the molecules are too small. Furthermore, DNA methylation does not affect hybridization and it cannot be detected readily using ISH. It is possible to detect and quantify all these genetic changes using variations of PCR.

### Tissue fixation methods

The most common tissue preservation methods are formalin fixation and freezing. However, ISH works best on freshly fixed samples while LCM works best on frozen

samples. ISH and LCM methods can be used on other tissues types, but it is not common because different protocols are required. For LCM, it is difficult to use archival formalin-fixed specimens, which require too many laser shots because the nucleic acid degradation. Even for macrodissection methods, entirely different procedures are needed to isolate RNA and DNA from formalin fixed or frozen specimens. Ideally one protocol would be used to work with a variety of different samples.

#### Control of resolution

Although it may be counter-intuitive, it is not always ideal to have the finest possible resolution. The majority of archival clinical samples use formalin fixation. The only way to validate a nucleic acid diagnostic today is by retrospectively analyzing archival patient samples and predicting patient survival. In order to look at the potentially valuable but low-abundant, degraded RNAs from formalin samples, a method is needed that optimizes the level of resolution (size of tissue macrodissection). If the macrodissection size is increased, then the recovery of low-abundance RNA is also increased at the expense of resolution. Currently, there is no method that can control the resolution of recovery while mapping nucleic acids across a sample.

#### 1.4.1.4 Not prohibitively-expensive or time-consuming

The last requirement is a technique that is not prohibitively slow or costly. In particular, it is ideal to use LCM or macrodissection methods because of the wide-

applicability, consistency, and sensitivity of these techniques. However, the major limitation is that they are slow and expensive. For example, the experiments in Chapter 4 showed that macrodissection of just 24 formalin-fixed samples, followed by nucleic acid purification using commercially available kits and analysis using qPCR took 2 days and cost nearly \$1000. For LCM, there is also the problem of user bias and the cost of labor, since a skilled operator is needed. Finally, if a technique has diagnostic potential and is to be used during a medical surgery, it needs to have to potential to be used in under an hour, unlike the days needed for the existing methods.

#### 1.4.2 2D-PCR addresses all of these needs

This thesis will show that 2D-PCR is an approach that solves all of these problems. 2D-PCR works by first cutting a tissue into subregions by pressing a tissue section into a grid of wells, as shown in Figure 9. Then, the steps of tissue lysis, RNA or DNA purification, amplification by PCR, and detection using fluorescent methods are

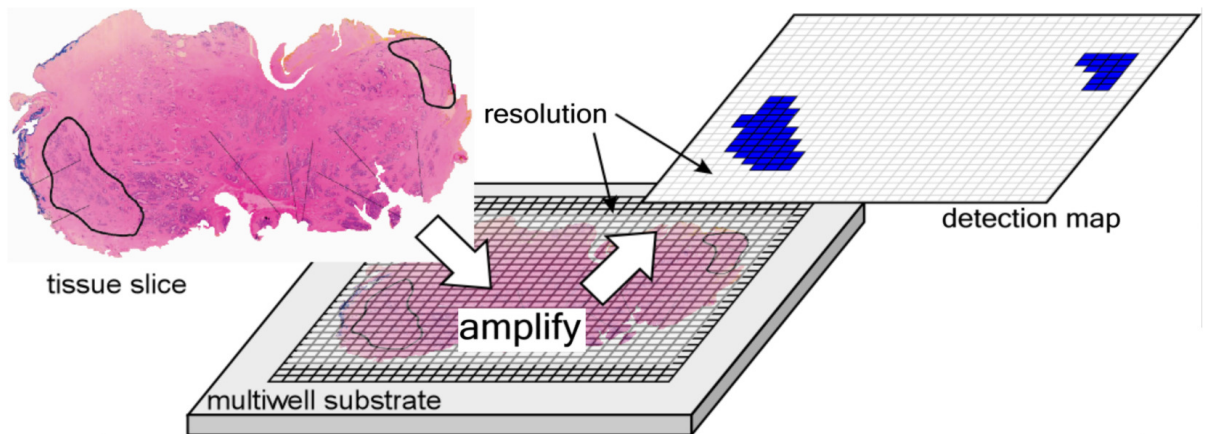


**Figure 9 – Schematic view of the 2D-PCR technique for spatial mapping of changes in genes and gene expression. All of the genes from a tissue section are transferred to a grid of wells, a target nucleic acid is amplified by PCR under clean conditions within each well, and amplified gene products can be detected by staining within the wells using a fluorescent dye. (Figure courtesy of Dr. Smela)**

performed. This approach provides the sensitivity, wide applicability, and consistency of LCM and macrodissection but is faster and uses less reagents and consumables. Therefore, 2D-PCR can be thought of as a high-throughput macrodissection technique that preserves the layout of a tissue.

By dividing the sample into a grid format, 2D-PCR reduces the bottleneck of cutting subregions out of tissues sections and preparing nucleic acids<sup>87,93,94</sup>. By maintaining the layout of tissue sample, time is saved because the relative positions of the nucleic acids are maintained. By using a grid format and scaled-down volumes of reagents, the cost and speed of analysis is reduced by about an order of magnitude compared to existing methods.

The other advantage of 2D-PCR is that in principle the size of grid wells can be scaled down, and the technique was designed with automation in mind. It may be possible to scale down the technique to the resolution of glands (dozens of cells). Work towards miniaturization is described further in Chapter 2. 2D-PCR is the first method that controls the resolution of wells, accommodating samples that may have low-abundance targets and/or degraded or hard-to-recover nucleic acids.

A summary of the advantages of 2D-PCR in comparison to existing methods is given in Table 7.

Table 7 – Benefits and limitations of 2D-PCR and four methods for localizing nucleic acids in tissues.

	Resolution	Sensitivity	Time	Complexity	Reproducibility
<b>ISH</b>	<5 $\mu$ M	Low	Days	High	Good
<b>ISP</b>	<5 $\mu$ M	Low	Days	High	Poor
<b>LCM</b>	>10 $\mu$ M	High	Days	Medium	High
<b>Macrodissection</b>	>1 mm	High	Hours-Days	Low	High
<b>2D-PCR</b>	>1.6 mm	High	Hours	Low	High

	Samples	Targets	Multiplexing	Quantitation	Minimum Target
<b>ISH</b>	Fresh-Fixed	DNA, mRNA	1-3 Targets	No	20 copy/cell
<b>ISP</b>	Fresh-Fixed	DNA, mRNA	1 Target	No	0.1-1 copy/cell
<b>LCM</b>	Frozen	Unlimited	Unlimited	Yes	5-50 ng
<b>Macrodissection</b>	Any	Unlimited	Unlimited	Yes	5-50 ng
<b>2D-PCR</b>	Any	Unlimited	Unlimited	Yes	1-5 ng

The following 2D-PCR aims were achieved for this thesis. The major difficulties overcome are summarized in section Chapter 6 and Chapter 7 and are specified as intellectual contributions 1-8.

#### 1.4.3 Aim 1 – Map DNA using 2D-PCR

Aim 1 was to demonstrate the initial proof of concept of the 2D-PCR technique by mapping DNA from frozen tissue sections at a resolution of 1.6 mm. First, a new process was developed for handling frozen tissue on adhesive films while preserving the layout of the tissue sample. A process was then developed for transferring the tissue into a high-density multi-well plate, which also cuts the tissue into subregions 1.6 mm in diameter (Contribution 1). Throughout the process the sample layout was maintained by using a novel single-well procedure to directly extract, amplify, and detect the DNA, and the use of agarose plus sealing films to prevent the diffusion of DNA (Contribution 2). A novel procedure was also developed for visualizing tissues in wells without affecting PCR (Contribution 3). A 2D map of the gene

glyceraldehyde 3-phosphate dehydrogenase (GAPDH) was created from a tissue section and shown to correlate with the spatial area of the sample. The details of this aim, methods, and results were published in LabChip in 2009 and are presented as Chapter 2.

#### 1.4.4 Aim 2 – Map RNA using 2D-PCR

Aim 2 was to demonstrate a second proof of concept of the 2D-PCR technique by performing the more challenging task of quantifying messenger RNA from frozen tissue specimens. This was done using an industry standard 384-well PCR plate as the device. First, a new process was developed for visualizing frozen tissue on adhesive film without affecting qPCR (Contribution 4). A novel single-well procedure was then developed to extract, purify, amplify, and quantify the mRNA (Contribution 4). Additionally, 2D maps were made for up to three specific mRNA targets in one tissue section. Specifically, a map was created by detecting kidney, liver, or heart using mRNAs specific to these tissues. The details of this aim were written as a manuscript draft to be submitted to Nucleic Acids Research and are presented in Chapter 3.

#### 1.4.5 Aim 3 – Mapping total RNA in FFPE tissue using 2D-PCR

Aim 3 was to demonstrate the utility of 2D-PCR by mapping nucleic acids in real biological tissue samples. However, it was not easy to find frozen human tissue samples for this project. It was, however, significantly easier to obtain formalin-fixed

tissues, but 2D-PCR was not originally developed for formalin-fixed tissues.

Therefore the 2D-PCR method was modified again to allow the detection of total RNA (mRNA and microRNA) from formalin-fixed specimens.

Several constraints were overcome to enable this study. In order to test many tumor and normal samples, a custom tissue microarray (TMA) was created with 25 prostate tumor and 25 matched normal prostate samples from 25 different patients in total. In order to transfer the TMA to the 2D-PCR device, a new adhesive film and procedure for sectioning and dewaxing TMAs onto the adhesive films was developed (Contribution 5). In order to recover mRNA from the formalin fixed samples, a reverse-crosslinking step was introduced to the protocol (Contribution 6). In order to improve the detection of low-abundance microRNA, a novel one-step microRNA amplification and detection procedure was developed that maintains the concentration of microRNA; current techniques dilute the microRNA using two-step procedures (Contribution 7). In order to maximize the use of the precious tissue specimens, a procedure was optimized for pre-amplifying 28 mRNA targets in a single tissue section using tandem PCR. Finally, to simplify the workflow for studying many genes across many samples, 24 of the mRNA samples were assayed by qPCR in duplicate against 42 prostate samples using Fluidigm, a miniaturized high-throughput qPCR system (Contribution 8).

Combining these developments, the 2D-PCR approach for formalin fixed samples improves the throughput and sensitivity of detection from small sample volumes.

Furthermore, the technique validated 15 previously identified gene expression microarray profiles – the overexpression of ALCAM, AMACR, FOLH, and TACSTD1 mRNA in tumors, and the underexpression of ANG, CD69, GSTP1, H1F1A, JAK1, CD10, MUC1, SOD2, STAT5B, TIMP3, and VEGF mRNA in prostate tumors. This result would not have been possible with other techniques in such a short period of time. The results of this aim were written as a manuscript draft, to be submitted to Nature Methods, and are presented in Chapter 4.

## Chapter 2: DNA maps from frozen tissue

In this chapter, the methods and results for mapping DNA from frozen tissue sections are presented, as described in aim 1. This chapter presents these results as the entirety of a journal publication, currently in print<sup>100</sup>.

Intellectual contributions: I drafted the initial manuscript, performed all of the experiments, and developed the experimental methodology (see intellectual contributions 1-3 in Chapter 7). The co-authors on the paper served an advisory role by guiding the project and helped to edit and finalize the manuscript for submission. Dr. Smela also created the first two figures and helped to edit others.

### 2D-PCR: A Method of Mapping DNA in Tissue Sections

Published in *Lab on a Chip* 2009 (9) 3526-34.

Reproduced by permission of The Royal Society of Chemistry (RSC).

<http://pubs.rsc.org/en/Content/ArticleLanding/2009/LC/b910807f>

Michael Armani<sup>abeg</sup>, Jaime Rodriguez-Canales<sup>fg</sup>, John Gillespie<sup>h</sup>, Michael Tangrea<sup>eg</sup>, Heidi Erickson<sup>i</sup>, Michael R. Emmert-Buck<sup>eg</sup>, Benjamin Shapiro<sup>abd</sup>, and Elisabeth Smela<sup>acd\*</sup>

<sup>a</sup>Bioengineering Graduate Program; <sup>b</sup>Fischell Department of Bio-Engineering;  
<sup>c</sup>Mechanical Engineering, <sup>d</sup>University of Maryland, College Park, MD;  
<sup>e</sup>Pathogenetics Unit; <sup>f</sup>Laser Microdissection Core; <sup>g</sup>Laboratory of Pathology, National Cancer Institute, Bethesda, MD;  
<sup>h</sup>SAIC-Frederick, Inc., Frederick, MD;  
<sup>i</sup>University of Texas M.D. Anderson Cancer Center, Department of Thoracic Head & Neck Medical Oncology, Houston, TX  
\*Corresponding author: 2176 Martin Hall, College Park, MD 20742, smela@eng.umd.edu

## 2.1 Abstract

A novel approach was developed for mapping the location of target DNA sequences in tissue sections. The method combines a high-density, multi-well plate with an innovative single-tube procedure to directly extract, amplify, and detect the DNA in parallel while maintaining the two-dimensional (2D) architecture of the tissue. A 2D map of the gene glyceraldehyde 3-phosphate dehydrogenase (GAPDH) was created from a tissue section and shown to correlate with the spatial area of the sample. It is anticipated that this approach may be easily adapted to assess the status of multiple genes within tissue sections, yielding a molecular map that directly correlates with the histology of the sample. This will provide investigators with a new tool to interrogate the molecular heterogeneity of tissue specimens.

## 2.2 Introduction

Variations in DNA status (mutation, epigenetic modification, insertions, deletions) by location within a tissue section are of interest for elucidating their roles in biology and as clinical markers for disease. However, to study the molecular basis of normal and pathological conditions, many researchers identify genes of interest from tissue specimens by examining cell homogenates (all the cells in the sample mixed together). Since tissue comprises a complex milieu of diverse cell populations that define the local microenvironments, combining the multiple cell populations into one measurement masks a tremendous amount of information. Therefore, to achieve a more complete view, DNA variability within a tissue sample needs to be correlated with the type of cell from which it originates (for example, stromal vs. epithelium),

the physical location within the tissue section, and/or histopathological features (for example, a specific disease lesion). This is highlighted by the interest in techniques such as *in-situ* polymerase chain reaction (PCR), and more recently by the increasing use of laser capture microdissection (LCM).

The majority of biological studies that extract, purify, and amplify genes or gene products from homogenized tissue to enable their detection utilize methods such as PCR<sup>19</sup>, RT-PCR<sup>101</sup>, qPCR<sup>24</sup>, qRT-PCR<sup>102</sup>, nano-liter qPCR<sup>103</sup>, digital RT-PCR<sup>104</sup>, DNA microarrays<sup>3,105</sup>, SAGE<sup>106</sup>, oligonucleotide microchips<sup>107</sup>, and OpenArrays<sup>108</sup>. These techniques are capable of impressive sensitivity and high throughput capacity, while also being reliable and consistent among different labs. However, due to the homogenization step, they do not preserve the original 2D histological correlation between the locations of different cell types and their underlying molecular information.

Microdissection methods, including UV cutting<sup>109</sup>, LCM<sup>65</sup>, and its variants expression microdissection (xMD)<sup>110</sup> and immuno-LCM<sup>111</sup>, were created specifically to work with histological tissue sections containing particular cell populations rather than homogenates. These approaches preserve the histological information and can be used in conjunction with sensitive and reliable molecular biology methods, such as PCR, for the molecular analysis of the tissue. For example, LCM has been used to isolate various cell populations of human prostate tissue to identify regional epigenetic alterations associated with the tumor micro-environment

<sup>8</sup>. LCM allows an operator to isolate selected clusters of particular cell populations under microscopic visualization. A large number of like clusters are placed together into a standard 0.5 mL microcentrifuge tube and then studied with the same protocols used on tissue homogenates. As a result of the information on cellular location, as well as its reliability, LCM is now a widely used technique. However, creating a complete molecular profile across an entire tissue section is prohibitively time-consuming with the current microdissection techniques.

There are techniques for in-situ mapping of genes throughout a tissue section, including catalyzed reporter deposition <sup>112</sup>, *in-situ* PCR <sup>82, 113</sup>, rolling circle amplification <sup>114</sup>, or branched DNA <sup>115, 116</sup>. These techniques aim to obtain the molecular profiles of the cells in their original milieu, preserving the correlation with histological and immunohistochemical <sup>117</sup> examination. While this works well for some samples and targets, a widely accepted platform for 2D spatial molecular analysis has not yet emerged due to issues such as background autofluorescence <sup>70</sup> and the need to re-optimize on a case-by-case basis <sup>70</sup>. To overcome these issues, it is typical to either amplify the target genes <sup>82, 113, 114</sup> or the reporter molecules binding to the target genes <sup>70, 112, 115, 116</sup> prior to visualization, and a few studies have even attempted multiple rounds of signal amplification <sup>118, 119</sup> to improve the signal to noise ratio. Nevertheless, the *in-situ* techniques have not seen the same level of acceptance as the well-established techniques for visualizing proteins <sup>117</sup>.

In this paper, we present the first lab-on-a-chip method to visualize target DNA across a tissue section. This will allow, upon further development, the mapping of alterations in genes, such as loss of heterozygosity (LOH), single nucleotide polymorphism (SNP), changes in copy number, and methylation, and correlating these changes with the tissue histology. This novel approach combines the strengths of three existing methods: the amplification power of PCR, the ability to examine clusters of cells using LCM, and the ability to localize molecular targets across a tissue section by in-situ methods. Our approach, which we call 2D-PCR, makes use of a miniature array of wells together with protocols that allow tissue lysis, DNA amplification, and target detection within the same well. Proof-of-concept for this method was demonstrated via the creation of a 2D detection map, showing the presence/absence of the target DNA, on the millimeter scale, but resolution can be further improved to the micro-scale based on our preliminary findings. In principle, this approach can be miniaturized to the level of a few cells per well, the same resolution as achieved with LCM but with more comprehensive study of the tissue section, thereby advancing studies of gene expression as a function of the type of cell and its position within a tissue. We have also established this method of mapping DNA as a step towards the more challenging task of mapping mRNA and microRNA.

### **2.3 DNA Mapping Methodology**

The 2D-PCR concept is illustrated in Figure 10. A tissue is sectioned and transferred into a multi-well array device. The DNA is then extracted from the tissue and subsequently amplified by PCR in the same wells. This method allows mapping of

genes while maintaining the reliability and specificity of PCR for detection. The PCR products can be detected either within the wells or after products are transferred onto one or more detection membranes <sup>120</sup>.

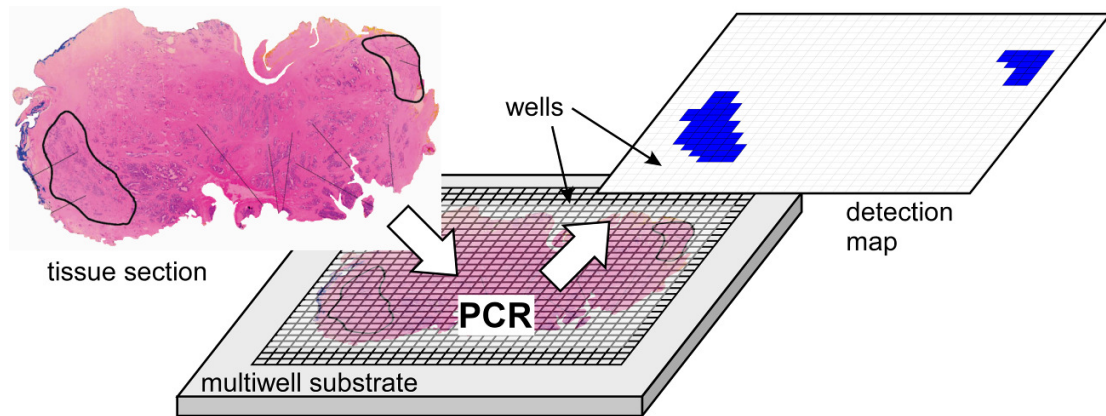


**Figure 10 – 2D-PCR is achieved by transferring a tissue section vertically into a multiwell array device, isolating tissue subregions. The DNA is extracted and then amplified by the polymerase chain reaction. A detection map is created by imaging the amplified DNA, for example using a DNA-intercalating dye.**

The steps to create the 2D map of DNA in tissue are illustrated schematically in Figure 11. The multi-well device consists of a plate with an array of through-holes sealed on the bottom side to form the wells. The wells are pre-filled with agarose, which immobilizes the chemical species to prevent cross-contamination between neighboring wells. In step one, the tissue section is transferred onto the surface of the multi-well array (step 1A) and then pressed onto the surface (1B). The contents of the well are dehydrated to enable the addition of lysis reagents (1C). In step two, the tissue is lysed to release genomic DNA into solution. Lysis reagents are added to the wells (2A), which are sealed and incubated at 65 °C (2B). Sealing prevents evaporation of reagents during the incubation, and heating activates the enzyme in the lysis reagent. The sealing film is removed, and the water in wells is removed by

dehydration at 95 °C (2C) to enable the subsequent addition of aqueous reagents. In step three, the DNA is amplified. PCR reagents are added (3A), and the device is resealed and heat cycled (3B). In step 4, the DNA is imaged. After unsealing the device, an intercalating fluorophore is added and allowed to incubate (4A). After rinsing off the dye solution, the fluorescence coming from the array is recorded and quantified (4B).

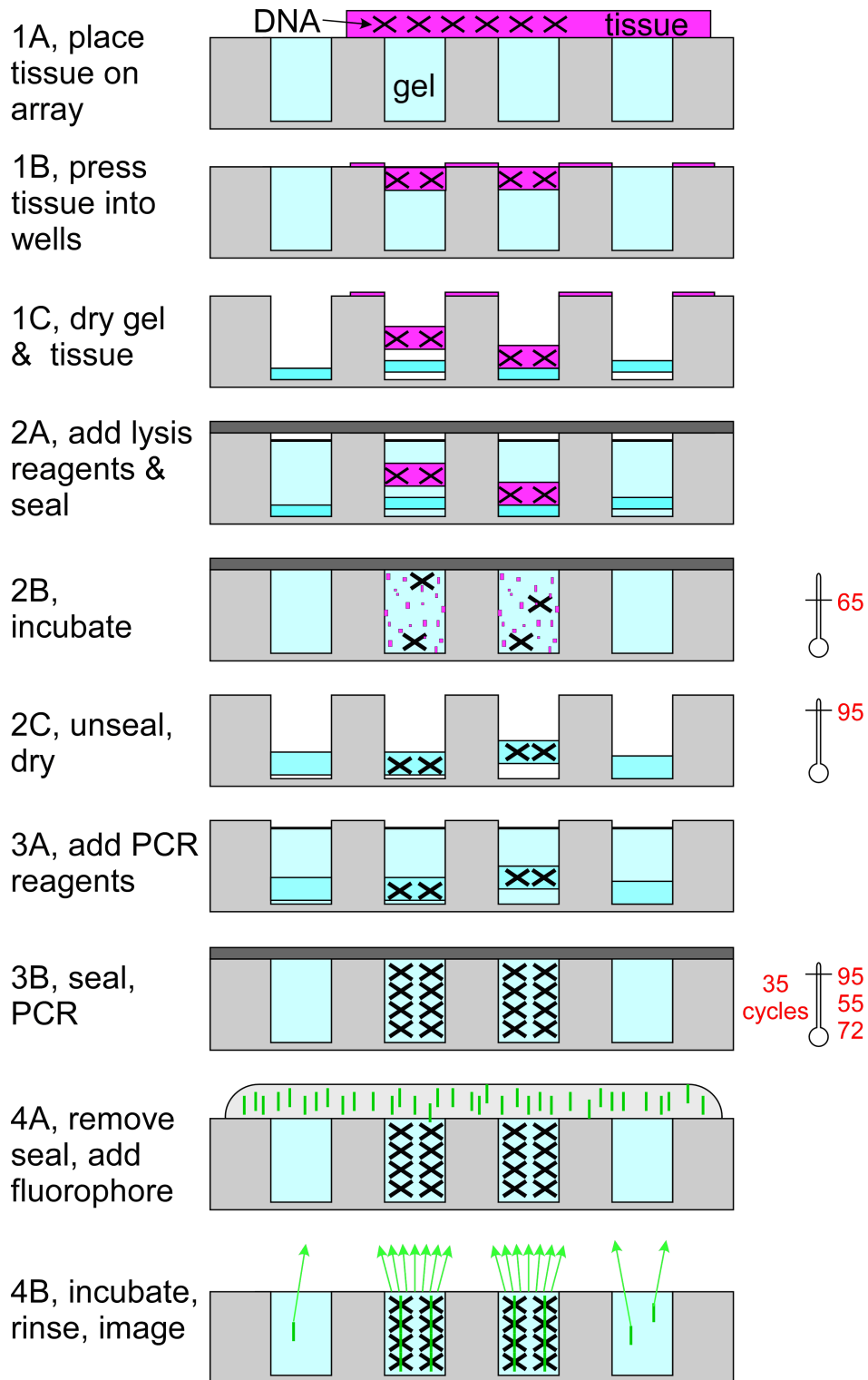


**Figure 11 – Experimental protocol used to demonstrate the 2D-PCR concept. Tissue is transferred into wells, isolated, and lysed to extract the genomic DNA (represented by “x”s). PCR is performed to amplify the target DNA, and the targets are visualized with fluorescent dye (indicated by vertical lines “|”).**

## 2.4 Materials and Methods

### 2.4.1 Device fabrication

Devices were constructed from perforated aluminum (alloy 3003H14, Perforated Metals Plus) obtained in 30.5 x 30.5 cm<sup>2</sup> sheets with 1.27 mm thickness. The through-holes were used as wells/vials and had a 1.6 mm diameter and a 2.38 mm staggered center-to-center spacing. The sheets were cut into 3 x 3 cm<sup>2</sup> pieces for the experiments and cleaned with 100% ethanol. These plates were used because they had the smallest commercially available hole size, near the size of a 1 mm pipette tip. They also had a flat surface and low aspect ratio holes to facilitate the transfer of tissue.

Low melting point (LMP) agarose was added into the through-holes as an immobilizing medium because of its compatibility with a variety of enzymatic reactions<sup>121</sup>, including DNA polymerase and reverse transcriptase. LMP agarose (Lonza 50081) was mixed 2% by weight in 30 mL of water in a sterilized beaker and microwaved at 800 W for 60 seconds. After the solution cooled to 50 °C, the cleaned aluminum plates were dipped into the molten agarose solution for a few seconds to fill the wells by capillary action.

The back (burred) side of the plate was sealed with an 89 µm thick adhesive-backed fluoropolymer film (McMaster 5805T11) that was cut to 3 cm squares. The sealing film was rinsed with ethanol, air dried, and placed in contact with the multi-well device. The plate was then placed film-side-down on a flat surface and pressed

firmly on all corners to ensure sealing. This sealing film remains permanently on the bottom side of the device. A seal of 51  $\mu\text{m}$  thick Kapton film (McMaster 2271K72) was also ethanol cleaned and then added to the smooth top side of the plate. A large, flat, 2 pound weight was placed on top of the seal to create a smooth agarose surface for the tissue to be placed onto in the next step.

#### 2.4.2 Tissue sectioning and transfer

Two types of tissue were used in these studies: frozen tissue samples from a human prostate with benign hyperplasia and breast tissue with lobular carcinoma. Both specimens were obtained at the National Institutes of Health as part of an IRB-approved clinical protocol for molecular analysis. Patient identifiers were removed prior to the study. Tissue specimens were snap frozen and embedded in optimal cutting temperature (O.C.T.) compound embedding medium (Sakura Fine-Tek, Torrance, CA). The tissue histology was evaluated by a pathologist (Rodriguez-Canales) to confirm the presence of viable cells in the tissue blocks. The blocks were then sectioned using a Leica CM1850UV cryostat. Prostate tissue sections measured approximately 40 mm x 20 mm with 8  $\mu\text{m}$  thickness, and breast tumor tissue sections measured approximately 5 mm x 15 mm with 12  $\mu\text{m}$  thickness.

For 2D gene mapping, the lobular breast carcinoma tissue block was stained so that it could be localized in the wells visually after transfer to compare against subsequent fluorescent detection of tissue DNA by 2D-PCR. The tissue block was thawed at room temperature and stained in an Eosin Y (0.05% weight/volume) bath for 2

minutes. It was immersed in 70% ethanol for 5 minutes and 15% ethanol for 15 minutes, and then re-embedded in O.C.T. on dry ice for 10 minutes.

Tissue sections were transferred to the multi-well device immediately after sectioning while still frozen to faithfully preserving the 2D geometry. After removing the top surface Kapton sealing film, the device was placed top side down onto the tissue section. Since the device was at room temperature, the tissue section and O.C.T. compound melted locally, adhering the tissue to the device, in a similar way that cryostat sections are typically adhered to glass slides for histological evaluation. The tissue overlying each well was then pressed into the well by force: the tissue was covered with a fresh Kapton sealing film and the plate/tissue/film was compressed at 150 psi and heated to 95 °C for 5 minutes. The device was then flipped and dehydrated as described below, so that the agarose would dry on top of the tissue to immobilize the DNA and thereby prevent cross-contamination between wells.

#### 2.4.3 Device heating and sealing

To heat the wells for tissue transfer, cell lysis, and PCR while simultaneously preventing evaporation and cross-contamination of the wells due to internal vapor pressure, it was necessary to seal the wells of the device. A standardized procedure was developed to repeatedly remove and reapply these seals. Wells were reversibly sealed with a fresh 51 µm thick Kapton film during each step of the procedure. This sealing film was rinsed with ethanol, air dried, and placed in contact with the multi-well device. The film and multi-well plate were compressed with 150 pounds per

square inch (psi) of force and heated using a customized compression-heating rig. The rig consisted of a steel frame supporting a weight scale, a PCR thermocycler with a flat heating surface, and a screw-type compression plate (see the Supplementary Materials for a figure).

The multi-well plate device was placed on the flat surface of the thermocycler (Alpha Unit Flat Block/PTC-200 DNA Engine, BioRad) and 200  $\mu$ L of mineral oil was applied to the heater surface to improve thermal conductivity. The device was covered with a 1" thick Plexiglass block for thermal insulation and a 1" thick aluminum block for force distribution.

After the heating procedure, the contents of the wells were solidified by cooling to 0 °C for 10 minutes. Solidifying the agarose, which entrapped the DNA and reagents, ensured that the contents from one well did not move into any adjacent wells and that no fluid adhered to the sealing film upon removing the seal. After peeling off the film, the contents of the wells could be dehydrated by heating to 95 °C for 5 minutes.

The reagents for the next procedure were added on top of the previously dehydrated well components. To ensure that the reagents did not exceed the volume of the wells, the water in the reagents was allowed to evaporate at standard room conditions for approximately 10 minutes until the meniscus of the fluid inside the wells became concave by visual inspection. The wells were then sealed with a fresh Kapton film.

We estimate that resulting variations in dilution are at most 5%, the same as that for commercial 96-well PCR plates. It should also be noted that the evaporation of fluid would not affect the yes/no detection of DNA at the levels reported here.

#### 2.4.4 DNA amplification protocol

To perform PCR amplification, PCR reagents were added to wells that had previously been dehydrated. Standard PCR mastermix (Invitrogen 10572-014) was adjusted to 0.1% weight/volume BSA (Fisher BP675-1), 60 U/mL Taq DNA polymerase (ABgene AB-0301a), and 2.75 mM MgCl<sub>2</sub> (ABgene AB-0301a). Primers were added to 200 nM for a GAPDH 167 bp genomic DNA target (5'catcatctctgccccctct and 5'tgagtcctccacgatacca), unless otherwise specified. The device was sealed with Kapton film, compressed, and then thermo-cycled. PCR thermocycling was performed at 95 °C for 2 minutes followed by 35 cycles of 95, 56, and 72 °C for 10, 10, and 15 seconds, respectively, followed by a final 72 °C step for 2 minutes and a 0 °C step for 10 minutes.

#### 2.4.5 Visualization

DNA intercalating dye was used to visualize the PCR amplification products. The top sealing film was removed and 300 µL of a 10X dilution of SYBR Green-I dye (Fisher Scientific BMA50513) was added to the top surface of the device and allowed to diffuse into the agarose for 5 minutes. SYBR Green-I is an intercalating dye that stains double-stranded DNA. The dye solution was rinsed off to reduce background

noise. The device was placed on a blue light transilluminator (Clare Chemical DR45M) and imaged with a CCD camera (Nikon D50) with a shutter speed of 1/15 of a second. An amber screen included with the transilluminator was placed between the CCD and the device.

## 2.5 Results

### 2.5.1 Direct DNA extraction and amplification: protocols and validation

New protocols were developed to isolate DNA from tissue and then to proceed directly to PCR amplification in the wells of the device. This “single tube” approach simplifies the currently-used process of detecting genes from tissue, which requires centrifugation and sample pipetting between multiple tubes. These techniques were initially validated because the device, protocols, and reagents were new. Also, the inclusion of 2% agarose and the small aluminum wells created a novel environment for PCR that necessitated a comprehensive evaluation of system performance.

#### 2.5.1.1 DNA extraction protocol

DNA was extracted directly using water and proteinase K, since the carry over of additional buffer salts is known to inhibit PCR reactions. To prepare the wells for the addition of extraction solution, the agarose and tissue were dehydrated within the device using the heating rig at 95 °C for 5 minutes. To isolate the DNA, the cells were lysed in water mixed with proteinase K (Invitrogen 25530-049) at 2 mg/mL (extraction solution); 2.4 µL of this solution was manually pipetted into each well.

To prepare for device sealing, the reagents were dehydrated at room temperature for 10 minutes and then frozen at -20 °C for 10 minutes. The device was sealed and heated to 65 °C for 30 minutes to digest the tissue and 95 °C for 5 minutes to inactivate the enzyme. The well contents were then solidified and dehydrated.

#### 2.5.1.2 Validation of DNA extraction protocol

The direct DNA extraction protocol was tested using frozen normal prostate tissue that had been snap frozen to a glass slide. Tissue scrapes were placed into 12 randomly chosen wells. The tissue was diluted to 6.7 ng/μL in the extraction solution. The tissue-proteinase K mixture was subjected to the DNA extraction protocol, except without the addition of agarose.

Controls were then added to other wells to semi-quantitatively gauge the efficacy of the direct DNA extraction procedure. First, genomic DNA (BioChain Institute, D1234106) was added as a dilution series of 1.06 ng/μL, 212 pg/μL, and 42 pg/μL, which represents a range of easily detectible to non-detectible levels of starting material. Water was also added to provide a negative control. The contents of the wells were dehydrated as described previously and subjected to PCR. Validation was performed by gel electrophoresis at 100 V for 35 minutes in a 2% gel (NuSieve 3:1) containing 1X TBE and 1X SYBR-Gold dye to see if the 167 bp target DNA was amplified.

An electrophoresis gel (see Supplementary Materials for a photo of the gel) showed a 167 bp DNA fragment from both purified genomic DNA controls above 212 pg/ $\mu$ L and from prostate tissue, but not from the negative control. Furthermore, the observed amplified bands from prostate tissue were of identical size to those from genomic DNA owing to the specificity of PCR. These results demonstrate that the frozen prostate tissue was lysed and the DNA was amplified in the multi-well device without additional purification steps.

#### 2.5.1.3 Validation of DNA amplification protocol

To test that PCR was reliable and robust in the agarose-filled aluminum miniature well environment, a variety of amplifications were carried out simultaneously in 12 wells of the device. Two templates (sources of DNA) were used.

1. Human OsteoSarcoma cDNA at 4.9 ng/ $\mu$ L made from mRNA (Ambion Inc., AM7868) by a standard reverse transcription protocol.

2. A 582 bp PCR target amplified in a thin-walled PCR tube to  $5 \times 10^9$  molecules/ $\mu$ L.

Four sequences on the first template were targeted, and the second template was diluted to four different concentrations. The PCR products were run on an electrophoresis gel (see Supplementary Materials). All the observed gel bands corresponded to primers added to the wells.

In these results a well filled only with water was immediately adjacent to a well that contained previously-amplified PCR targets at a high concentration. The fact that no bands were observed from the water-filled well demonstrates that there was no cross-

contamination between wells. The PCR amplification was effective for both purified targets and mixtures containing many non-specific targets. Taken together, these results demonstrate that PCR within the wells robustly amplifies a variety of targets from a variety of templates including crude genomic DNA, crude cDNA, and PCR-amplified products.

### 2.5.2 2D-PCR mapping

To validate the concept of 2D-PCR, the presence or absence of specific DNA sequences in tissue sections was mapped as a first step towards the more desirable quantification of DNA by real-time PCR methods. To this end, a genomic DNA target sequence (GAPDH) in a breast tissue section was mapped and correlated with the known geometry of the histology. The GAPDH gene is present in the nuclear DNA sequence of every cell, and is thus found throughout the tissue. The map would therefore be expected to show where the tissue was present above the device. Using the 2D-PCR approach, a GAPDH genomic DNA target from breast tissue was extracted, PCR amplified, and visualized by SYBR Green I with 1.6 mm resolution.

#### 2.5.2.1 2D-PCR mapping protocol

To identify the tissue area visually, the sample was stained pink with Eosin Y. The tissue was transferred onto the device surface and imaged (Figure 12). It was then pressed into the wells and dehydrated. The tissue was then lysed to release the DNA as described in the DNA extraction protocol, with the proteinase K concentration reduced to 1 mg/mL. To indicate the orientation of tissue on the device, a diagonal

and square notch were cut out of the sealing film covering the tissue. After dehydration, the GAPDH target region of genomic DNA was amplified. After PCR, the sealing film was removed.

SYBR Green I dye was added. Solidifying the DNA in agarose enabled the DNA to be stained with SYBR Green I dye without losing the DNA from the wells. The fluorescent image of the device is shown in Figure 12. Those wells that were under the tissue fluoresced, demonstrating that the DNA had been amplified to sufficiently high levels. The wells that were completely under the tissue fluoresced the most. The negative control area, which was not covered by tissue, had only a low fluorescent background signal. The detection signal correlated with the known area of the tissue, demonstrating that the 2D-PCR approach was successful.

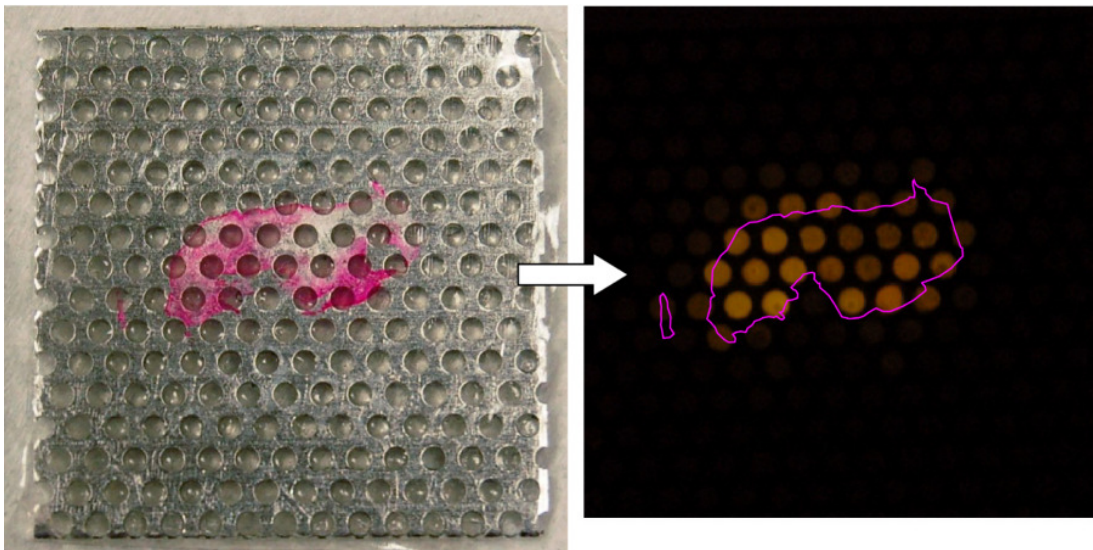


**Figure 12 – Image of a breast tissue section (stained pink for visualization with Eosin Y) after transfer onto the multi-well device, and the visualization map created by fluorescent DNA detection with SYBR Green I after amplification by 2D-PCR. The tissue position is indicated by the pink outline.**

#### 2.5.2.2 Validation of 2D-PCR

To validate that the fluorescent signals correlated with the desired target 167 bp GAPDH PCR product, the well contents were run on an electrophoresis gel. To do this, the device was cooled to 0 °C for 10 minutes to solidify the agarose, and the top sealing film was removed. A pipette (Fisher 02-707-439) was used to obtain gel plugs from six fluorescent and six non-fluorescent wells. Each plug was diluted 100 times with water and melted at 95 °C for 10 minutes to dilute the Eosin dye. Then, to offset the dilution, each sample was amplified by 8 cycles of PCR (110 fold amplification at 90% efficiency) using the same PCR conditions as previously described. Samples were subjected to electrophoresis at 100 V for 35 minutes in a 2% gel containing 1X TBE and 1X SYBR-Gold dye.

A signal corresponding to the 167 bp GAPDH genomic DNA target was observed in lanes 1-6, which correlates with the presence of tissue (Figure 13). There were no observed false positives from wells without tissue (lanes 7-12). Note that the negative well 9 was directly adjacent to wells covered by tissue, yet there was no observed cross-contamination. These results confirm that the 2D-PCR method can be used to isolate tissues, extract DNA, amplify DNA, and visualize DNA in a spatially resolved manner for tissue sections.

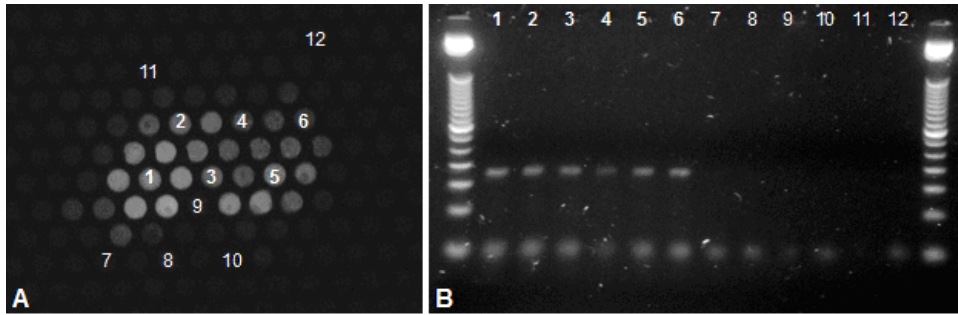


**Figure 13 – A) The wells chosen for electrophoretic validation of the fluorescent signal. B) In wells containing tissue (lanes 1-6) there was a bright fluorescent signal corresponding to detection of a 167 bp GAPDH genomic product, while negative wells (lanes 7-12) had no amplification of the 167 bp target and only weak bands of ~50 bp primer-dimers, an artifact from PCR.**

### 2.5.3 Preliminary work towards miniaturization

A longer term goal of this research is to create a tool with well sizes of 50-100  $\mu\text{m}$ , which would produce 2D maps with a resolution of  $\sim 100$  cells. Such miniaturization has challenges associated with microfabrication, sample loading, rapid fluid evaporation, lower amplification efficiency, and smaller volumes for fluorescence visualization. We have performed some preliminary studies to identify a path to miniaturization. We describe these steps briefly here and give further details in the Supplementary Materials.

Standard microfabrication with deep reactive ion etching (DRIE) in silicon allows the realization of through-hole wells that are tens of  $\mu\text{m}$  in diameter. Multi-well arrays were fabricated in Si using DRIE. They had wells that were 100  $\mu\text{m}$  in diameter and 400  $\mu\text{m}$  deep (the thickness of the wafer); they were spaced 100  $\mu\text{m}$  apart, yielding 2,500 wells/ $\text{cm}^2$  (Figure 14).

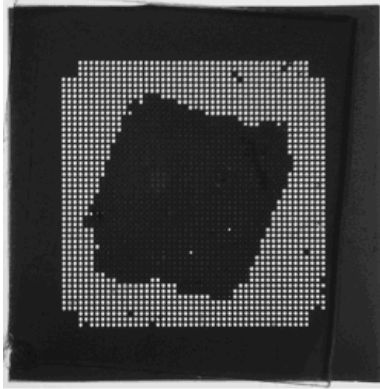


**Figure 14 – Silicon substrate having a 1 cm square area with 100  $\mu\text{m}$  diameter holes spaced 100  $\mu\text{m}$  apart. The surface was pretreated with BSA and spotted with water containing food dye for visualization (dark area in center). The wells filled completely by capillary action.**

It is not possible to pipette reagents into such small wells, but fluid can be pulled into the wells by capillary forces if a wetting agent is added to make the etched walls more hydrophilic. Placing a droplet of water containing BSA, Triton X-100, or Tween 20 of an appropriate concentration (see Supplementary Materials) onto one side of the micro-well plate and allowing it to dry resulted in subsequent complete filling of the wells by both aqueous solutions (Figure 14) and agarose solutions up to concentrations of 1.5%. None of these surface treatments inhibited PCR, consistent with prior work<sup>22, 122</sup>.

The micro-wells must be sealed to prevent spreading and/or evaporation of reagents. This requires a material that conforms to surface variations of the plate to create a good seal, yet that at the same time is not so viscoelastic and adhesive that the sealing material embeds itself permanently into the holes, preventing reversible sealing. Microseal A (MJ Research) was found to prevent evaporation of reagents from most

of the micro-well plate, and it also prevented 99.8% of crosstalk (Supplementary Materials).

To demonstrate PCR in the micro-well plate, the surfaces were pretreated with BSA and loaded by capillary action with a PCR mastermix containing a primer set and cDNA that had been used previously in the mini-vials, as well as additional native Taq DNA polymerase and additional BSA. The additional BSA is needed with large surface to volume ratios to prevent nonspecific adsorption on the walls of the wells. For the negative control, water was substituted in place of cDNA. No gel was used in the wells here, so preventing evaporation was particularly important; the micro-well plate was sealed using Microseal A. The micro-well plate was placed on the flat alpha unit block of the thermocycler, covered with mineral oil to maximize thermal contact, and thermally cycled. For validation, the fluid within the vials was recovered and combined, and loaded onto a 1.5% agarose electrophoresis gel. The gel results (Supplementary Materials) verified successful PCR.

## 2.6 Discussion

Several challenges in using the multi-well array approach were overcome to obtain the DNA mapping results presented here. The first was transferring tissue into the device while segregating tissue subregions (or “pixels”) to preserve overall spatial information. The second was creating a new single-well protocol for extracting the DNA, amplifying the DNA, and detecting the amplified DNA. The third was creating a new technique for sample containment to prevent cross-contamination and

evaporation between wells. The current 2D-PCR technology is now ready for optimization to study specific alterations in DNA, such as LOH, SNPs, and methylation using methylation-specific PCR <sup>35</sup>.

Lab-on-a-chip devices typically use microfluidics on a planar surface to interconnect processing chambers for isolating and amplifying DNA from cells <sup>123-125</sup>, but this consumes too much space on the chip surface to map DNA from tissues with practical density. The single-well procedure for processing samples eliminates the need for fluid movement while providing direct surface access to capture as much tissue as possible.

The first challenge was addressed by loading the tissue vertically, pressing it directly into the array of wells to isolate tissue subregions while preserving the overall 2D spatial relationship. Even though tissue remained on the top of the device between the wells, the 2D-PCR results demonstrated that this tissue does not contribute a signal to the adjacent wells. This tissue loading technique also has the advantage of beginning with traditional histological sectioning and transfer steps, which are familiar to investigators and clinicians who may wish to adopt this technique for research or diagnosis.

A new approach was used to extract DNA from tissue, amplify it, and detect the amplification products with fluorescence visualization. We used a direct DNA extraction protocol so that the reagents could be inactivated and dried without

inhibiting subsequent PCR. Afterward, the PCR products were stained directly with a fluorescent DNA-intercalating dye. This approach streamlines the protocols used in commercially available kits, which require centrifugation and re-pipetting of each sample between three to four tubes<sup>48, 52, 86, 126, 127</sup>. Performing the processes sequentially in a single well not only enables a simple device geometry but is also amenable to further miniaturization. Others have also realized the importance of simplifying and/or miniaturizing commercially-available nucleic acid processing protocols by using fewer steps, tubes, or reagents<sup>87, 94, 123-125, 128-134</sup>, but those techniques do not make it possible to map DNA from tissue.

Directly visualizing the PCR products by staining them with fluorescent dye allows them to be detected across the entire array, creating 2D maps both efficiently and directly *in situ*. There is sufficient DNA in an 8  $\mu\text{m}$  thick tissue sample for detection in a single 1.6 mm diameter well. Given the facts that there were at most 5,000 cells captured per well, that the detection signal was strong, and that detection occurred at 35 cycles, it is anticipated that 2D-PCR can be extended to the level of about 100 cells per well – a limit we expect due to the efficiency of DNA extraction with this method rather than PCR sensitivity (which has been shown to amplify DNA even from single cells<sup>135</sup>). In the future, it would also be desirable to use real-time PCR to detect the PCR products, eliminating the staining step, as others have demonstrated<sup>136</sup>. It is also possible to detect the products by fluorescent hybridization after blotting onto detection membranes<sup>120</sup>.

The single-well protocol depended on a new reversible sealing procedure to contain the samples across an array format and to enable the addition of successive reagents. Without sealing, reagents can evaporate or spread during the heating steps. The vapor was contained within the wells by applying compression to a sealing film placed on top of the entire multi-well array. Suppliers of 96-well or denser multi-well plates also employ reversible seals to prevent evaporation of the water, but this is the first example of reversible sealing across an array of holes in a flat surface. PCR lab-on-a-chip reactors typically employ irreversible seals, such as nail polish or epoxies, to attach glass cover slips onto silicon PCR wells<sup>108, 122, 136</sup>. Reversible sealing was used for 2D-PCR because different reagents needed to be added and dehydrated at different times. This method of sealing was successful with both the aluminum and the silicon substrates.

Sample containment also relied on the addition of 2% agarose gel to the wells before the tissue transfer step to prevent the movement of fluid and to immobilize the DNA. PCR has not previously been reported in the presence of greater than 0.5% agarose, although there have been reports of up to 3% agarose used with other biological enzymes<sup>121</sup>. We note that it is also possible to prevent mixing by freezing the fluids prior to seal removal, but the resulting condensation can prevent future sealing.

It is also of interest to miniaturize the device presented here to provide biomolecular information at the level of a few dozen cells, which would allow pathologists to overlay 2D genetic maps over a tissue histology and see molecular variations as a

function of cell type. We have solved some of the challenges of such miniaturization, but significant challenges still need to be overcome. The greatest challenge will be transferring tissue into the micro-wells in such a way that the tissue does not block the openings, preventing future transfer of fluid. Solutions to this issue may include electro-transfer of DNA from tissue lysates or using a more disruptive tissue lysing process. Another major challenge is designing a batch fluid-loading system that is consistent, prevents cross-contamination between wells, and avoids uneven evaporation.

We are currently working on mapping RNA from tissue, since current visualization techniques for RNA cannot reliably detect below a few dozen copies per cell *in situ*<sup>70,71</sup>. There are many techniques that can currently detect high abundance targets directly in a tissue section, but based on recent publications and personal accounts of researchers in the field, these techniques have failed for lower-abundance targets because they are either unreliable, difficult to reproduce, or too time-consuming. On the other hand, the robustness of LCM has led to widespread acceptance because it can be used to study small cell populations with reliable down-stream techniques. Unfortunately, LCM is only employed to study a limited number of cell populations because of time and cost constraints. Thus, a promising new way to address the need for mapping low abundance genes is via the 2D-PCR method presented here.

2D-PCR opens several other promising avenues for technical research. One ideal 2D-PCR development would be the ability to study formalin-fixed paraffin-embedded

(FFPE) tissue samples in addition to frozen samples. FFPE tissue represents the majority of clinical tissue samples available for study, but these samples contain fragmented and immobilized RNA due to the formalin cross-linking. The technique could also be extended to other 2D samples, such as Southern blot gels, to improve the detection limits and post-staining specificity. Finally, in the future, it would also be desirable to use quantitative real-time PCR (qPCR) to detect the PCR products, eliminating the staining step as others have demonstrated<sup>136</sup>. To account for variations in the number of cells loaded, the PCR would need to be multiplexed to include housekeeping genes to which other signals could be normalized. However, qPCR machines that would be compatible with the setup presented in this work are not commercially available and would require a significant effort to customize.

Currently, biological research is growing with respect to the number of genes and number of patients studied, but it suffers from slow growth with respect to comprehensive tissue analysis. Therefore, a potentially promising avenue for future work is facilitating human genetic anatomy research that would create gene expression maps of human tissue. This can be applied to study tissue heterogeneity and tumor microenvironments, to map the extension of the molecular field effect from cancer into normal regions (the “histological margins of tumors” versus the “molecular margins”, which can have potential clinical use in the surgical resection of neoplasias), and to the study of the molecular anatomy of normal and pathological tissues.

It would be possible to use the 2D-PCR method to create 3D maps of tissue. By combining information from a number of serial cut tissue sections taken from a single tissue block, one can create 3D maps<sup>8</sup>. To facilitate this process, the sample handling should be automated. The practicality of 3D mapping will depend on how quickly, easily, and cheaply the 2D PCR can be performed, a goal for future work.

The spatial genetic data may also elucidate the normal function of human genes, which is known for only 30% of them<sup>137</sup>. To highlight the interest in mapping gene function in tissues, there have been several initiatives for procuring and archiving gene expression images on the mouse, including BGEM<sup>138</sup>, Brainatlas<sup>139</sup>, Genepaint<sup>140</sup>, GENSAT<sup>141</sup>, Mamep<sup>142</sup> and EMAGE<sup>143</sup>.

## 2.7 Conclusions

We have developed a novel approach for creating maps of DNA preserving the 2D architecture of the tissue based on extracting the nucleic acids from a tissue section and then amplifying them within a controlled environment in such a way that the positional information is preserved. To validate this method, we demonstrated that DNA could be mapped from a frozen human tissue section, a result that represents over a hundred successful DNA isolations and subsequent PCR reactions performed in parallel on a single device, in less than a few hours total time.

## **2.8 Acknowledgements**

We thank Rodrigo Chuaqui and Jeffrey Hanson at the NCI for their support for this project. This work was supported in part by the Intramural Research Program of the NIH, National Cancer Institute, Center for Cancer Research.

## **2.9 Supplementary Materials**

The supporting information includes a figure showing the pressure compression rig, the electrophoresis gel validations of the 2D-PCR method, and complete details of the miniaturization studies, including the microfabrication, reagent loading by capillary action, cross-talk studies, demonstration of PCR, and discussion.

## **2.10 Supplementary Information for Mini-Vial Results**

### **2.10.1 Compression Rig**

The compression rig that was used to ensure sealing during thermocycling of the mini-vial substrates is illustrated in Figure 15.

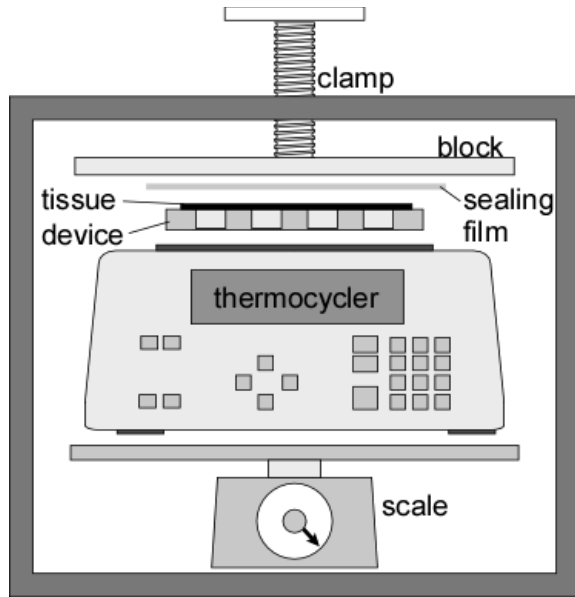


**Figure 15 – Schematic view of the compression-heating rig used for sealing and thermocycling.**

### 2.10.2 Electrophoresis Gels for Validation of 2D-PCR Method

Our tissue DNA extraction protocol was verified by the electrophoresis gel results shown in the next figure.

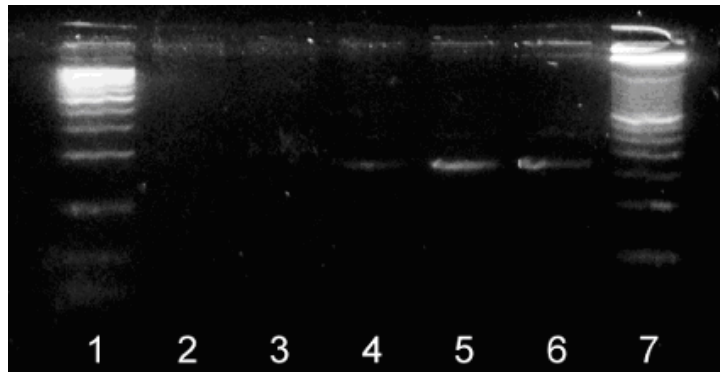


**Figure 16 – Gel electrophoresis from PCR validation experiment. Lanes 1 and 7 show 50 bp molecular weight ladders. Lane 2 had a negative water control, lanes 3-5 had increasing concentrations of purified genomic DNA, and lane 6 had a tissue-derived DNA extract.**

The PCR DNA amplification protocol in the agarose-filled aluminum miniature wells was also verified via an electrophoresis gel. Twelve amplifications were tested (Table 8) for the twelve mini-vial locations shown in Figure 17a with the resulting electrophoresis bands in Figure 17b. All the observed bands corresponded to primers added to the wells thus verifying in-well PCR.

Table 8 – Well contents for validating DNA amplification.

Well	Contents	Concentration	Target	Primers
1	1. cDNA	78 pg/ $\mu$ L	BetaActin – 167 bp	5'tcacctgaagtacccatc, 5'ggtcattctctcgcggttg
2	1. cDNA	78 pg/ $\mu$ L	BetaActin – 489 bp	5'tcacctgaagtacccatc, 5'ccatctcttgctcgaagtc
3	1. cDNA	78 pg/ $\mu$ L	GAPDH – 167 bp	5'catcatctctgccccctct, 5'tgagtctctccacgatacca
4	1. cDNA	78 pg/ $\mu$ L	GAPDH – 582 bp	5'aaatcccatcaccatcttcc, 5'gcctgcttcaccaccttct
5	water	--	GAPDH – 582 bp	5'aaatcccatcaccatcttcc, 5'gcctgcttcaccaccttct
6	1. cDNA	4.9 pg/ $\mu$ L		
7	1. cDNA	20 pg/ $\mu$ L		
8	1. cDNA	478 pg/ $\mu$ L		
9	2. 582 bp target	$7 \cdot 10^2$ molecules/ $\mu$ L		
10	2. 582 bp target	$1.2 \cdot 10^4$ molecules/ $\mu$ L		
11	2. 582 bp target	$1.9 \cdot 10^5$ molecules/ $\mu$ L		
12	2. 582 bp target	$3.0 \cdot 10^6$ molecules/ $\mu$ L		

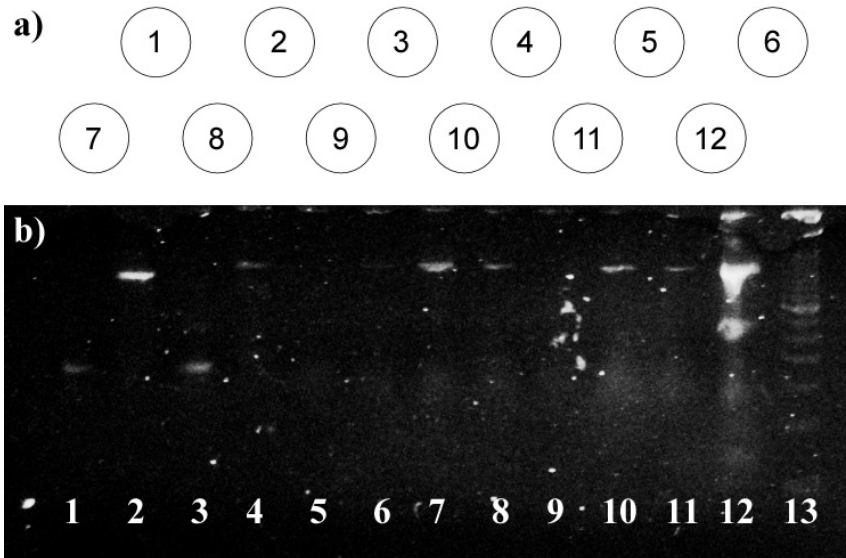


**Figure 17 – a) Geometric arrangement of the wells. b) Gel electrophoresis validation of DNA extraction experiment. The lane numbers correspond with the well numbers in Table 8. Lane 13 had a 50 bp ladder. The gel lanes show bands at (1) 167 bp, (2) 489 bp, (3) 167 bp, (4) 582 bp, (5) no bands, (6) no bands, (7) 582 bp, (8) 582 bp, (9) no bands, (10) 582 bp, (11) 582 bp, (12) 582 bp.**

Here all the gel bands corresponded to the primers added to wells. These results demonstrate the robustness of PCR in the device since there was specific amplification of four different PCR target regions (lanes 1 to 4). Well 5, filled only with water as a control, showed no bands. This well was directly next to well 12, which contained previously-amplified PCR targets at a high concentration. The fact that no bands were observed demonstrates that there was no cross contamination between wells. To further demonstrate the robustness of PCR, lanes 6-8 contained a genomic DNA dilution series, and lanes 9-12, a PCR product dilution series.

## 2.11 Supplementary Information for Further Miniaturization

### 2.11.1 Purpose of Further Miniaturization

The current device was developed with a resolution of 1.6 mm as a proof-of-concept for the 2D-PCR approach. This initial effort demonstrated a substantial improvement in resolution (over 100 fold) compared to a whole tissue scrape. However, our long term goal is to create a tool that can map 2D tissue sections for gene expression with a resolution of about 100 cells, or well sizes of 50 to 100  $\mu\text{m}$ . This finer-resolution device would have applications in all areas of biology, including developmental biology, cellular-level studies of genes expressed at low abundance, and animal models. However, miniaturizing 2D-PCR has the additional challenges of microfabrication, batch fluid loading by capillary action, containment of samples that evaporate quickly, lower amplification efficiency, and a smaller volume for fluorescence visualization. All of these have been addressed by the preliminary studies presented here. However, the challenges of loading tissues into the smaller vials and adding reagents while avoiding cross-contamination have not yet been examined.

### 2.11.2 Challenges Addressed

#### 2.11.2.1 Fabrication

Standard microfabrication with deep reactive ion etching (DRIE) in silicon allows the realization of through-hole wells tens of  $\mu\text{m}$  in diameter, thus providing micro-scale spatial resolution for 2D-PCR. Using DRIE, multi-well arrays were fabricated

comprising 1.3 cm x 1.3 cm areas separated by a 1.5 mm wide border for mechanical support on the outer edge. The wells were 100  $\mu\text{m}$  in diameter and spaced 100  $\mu\text{m}$  apart, yielding 2,500 wells/ $\text{cm}^2$ . The wells had a depth of 400  $\mu\text{m}$  that was determined by the thickness of the silicon wafer. Assuming a biological cell diameter of 10-20  $\mu\text{m}$ , and noting that tissue can be sliced down to single cell thicknesses, wells of 100  $\mu\text{m}$  could contain nucleic acids from a localized population of just 25-100 cells from the tissue.

Micro-well plates (Figure 18a,b) were produced from double-side polished, 4" diameter, 400  $\mu\text{m}$  thick <100> Si wafers. SU8-50 (Microchem), a negative resist, was used as a mask to protect those areas not to be etched. After dehydrating the wafers at 180  $^{\circ}\text{C}$  for 10 minutes, the SU8 was spun onto the wafer, ramping up to 2,500 rpm and holding for 40 seconds. The resist was prebaked at 65  $^{\circ}\text{C}$  for 5 minutes and 95  $^{\circ}\text{C}$  for 10 minutes, then cooled to room temperature over 5 minutes. The SU8 was exposed through a mask that included the 100  $\mu\text{m}$  wells and lines of 20  $\mu\text{m}$  width between micro-well areas to aid later dicing. The resist was post-baked using the same procedures as for prebaking. The SU8 was developed (MicroChem SU8 Developer) for 2 minutes, then rinsed in isopropanol, methanol, and de-ionized water. The wafer was attached to a second "handle" wafer with a layer of spin-coated Shipley 1813 resist. The holes were etched all the way through the wafer by DRIE using an etch cycle of 10 seconds and a passivation cycle of 6.5 seconds, for a total of 4 hours. A small percentage of holes did not etch all the way through (black dots in

Figure 18a,c), and we assume this was due to defects in the SU8 mask. Lastly, the handle wafer was removed in acetone, and the SU8 mask was peeled off.

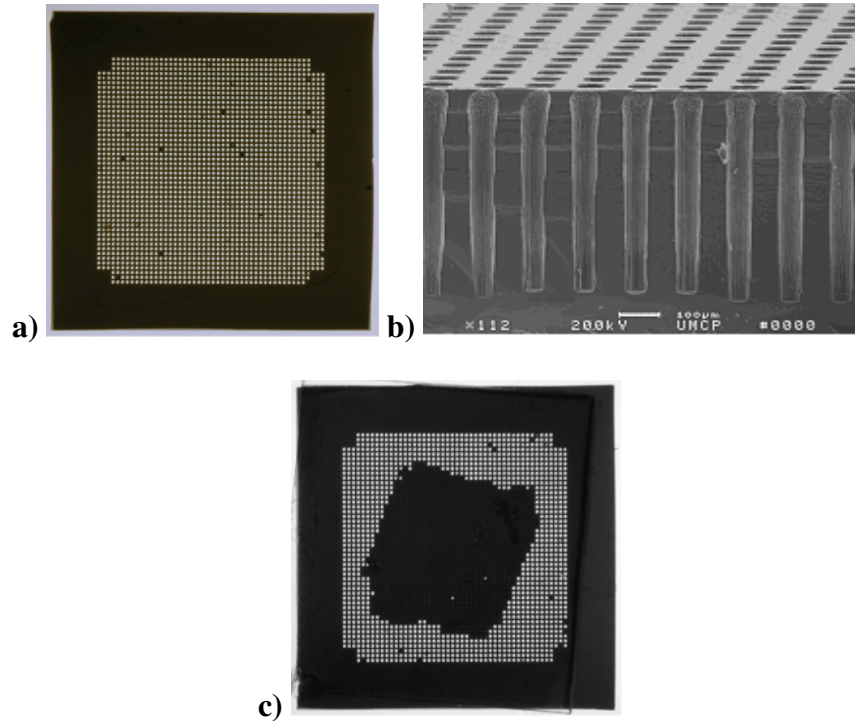


**Figure 18 – a) Silicon chip having a 1 cm square area with 100 μm holes spaced 100 μm apart. b) SEM sidewall profile of 50 μm wide holes made by DRIE. c) Silicon chip with 100 μm holes that was pretreated with BSA and spotted in an arbitrary diamond-shaped pattern with water containing food dye. The wells filled completely by capillary action.**

#### 2.11.2.2 Loading reagents by capillary action

Since it is not possible to pipette reagents into these 100 μm wells, capillary action was used to draw the fluid into them. The driving force,  $F$ , for capillary action is related to the radius of the well,  $r$ , by  $F = 2\pi r \sigma_{LG} \cos\theta$ , where  $\sigma_{LG}$  is the surface tension of the liquid-gas interface and  $\theta$  is the contact angle. If the surface is hydrophobic and the contact angle goes above 90°, there is a negative force for filling the wells; this is the case for Si, necessitating a surface coating to lower the contact

angle. Several surfactants were tested for their ability to facilitate fluid transfer: bovine serum albumin (BSA) (20 mg/mL, BP675-1), Triton X-100 (NC9903183), and Tween 20 (BP337-100), each diluted to 0.2%, 1.0% and 5% of their stock concentrations in 50% ethanol-water (0.04, 0.2, and 1.0 mg/mL BSA, respectively). A 10  $\mu$ L droplet was coated on one side of the micro-well plate and allowed to dry. 5  $\mu$ L of water-based food coloring (for ease of visualization) was placed on the surface, and the percentage of filled holes determined (Figure 18c). The 5% BSA (1 mg/mL) and all the Triton X-100 and Tween 20 coatings resulted in complete filling.

The surfactant inhibition limit in PCR was also tested by drying the various surfactants in standard PCR tubes. None of the surfactants inhibited PCR up to the 5% concentration (from stock) that was tested. This is consistent with the well-known observations that Tween 20 stabilizes the Taq enzyme and that surfactants such as X-100 or BSA can be used to improve PCR specificity<sup>22, 122</sup>. Since BSA in the reaction mix has previously been used for PCR in silicon plates this was the surface treatment chosen for the remaining work. These experiments allow us to conclude that the use of 5% BSA allows the transfer of reagents into the wells and does not interfere with the PCR processes.

To test the loading of reagents into the (BSA-pretreated) micro-well plate by capillary action, samples of molten agarose at 0.5, 1.0, 1.5 and 3.0% weight/volume were spotted on four different plates, and each plate was covered on both sides with the same sealing film. A 1" plexiglass substrate was placed on top of the plate with a 200

g weight for even spreading. The micro-well plate was placed in a 4 °C refrigerator for 15 minutes to solidify the agarose. The agarose could be seen in all of the micro-wells for concentrations up to 1.5%. The 3.0% gel hardened too quickly to be drawn into the chip by capillary action.

#### 2.11.2.3 Sample containment in micro-wells

As mentioned in the main text, the micro-wells must be sealed to prevent spreading and/or evaporation of reagents (Figure 19). The challenge is to identify a material that conforms to surface variations of the plate to create a good seal yet at the same time is not so viscoelastic and adhesive that the sealing material embeds itself permanently into the holes, preventing reversible sealing. A number of sealing materials were tested by measuring the fluid loss from a fixed initial fluid volume under the same temperature, pressure, and time. This provided measurements of the total percentage of evaporation 1) before loading and 2) after heating.

The sealing materials (Table 9) were rinsed with ethanol and air-dried, then placed in contact with one side of the plate. Before use, the sealing materials were compressed at 100 psi and 98 °C for 15 min to reduce their thickness and avoid later plugging of the wells. Wells were filled with aqueous food dye by pre-treating the devices as described above and pipetting 8  $\mu$ L of dye over the wells so that they would be filled by capillary action. The fluid was then frozen by placing the plate on dry ice. The other side of the plate was covered with the same sealing material. The plate was then subjected to thermocycling conditions. The sealed chip was placed on a

thermocycler heating block, covered in 200  $\mu\text{L}$  of mineral oil, covered with a 1" plexiglass block and a 1" aluminum block, and compressed using a custom-built pressure rig (100 psi force). The plate was heated at 98  $^{\circ}\text{C}$  for 15 min, then cooled to room temperature. Temperatures were verified to within 2  $^{\circ}\text{C}$  using a type J thermocouple. The plate was placed on dry ice for several seconds, the top seal was peeled off, and the plate was brought to room temperature. To measure the change in fluid volume, the total volume of fluid in the 10 vials was collected with a 30  $\mu\text{L}$  pipette tip.

To determine fluid loss in micro-wells, plates were photographed with a digital camera using a macro lens before and after annealing, and the images analyzed with a custom-designed MATLAB script. The results are summarized in Table 9.

Microseal A prevented evaporation of reagents from most of the micro-well plate, and it prevented 99.8% of crosstalk. Thus, for the micro-wells, Microseal A is the best choice, since preventing crosstalk is essential. The sealing process still requires some additional optimization to consistently and uniformly prevent evaporation across the plate.

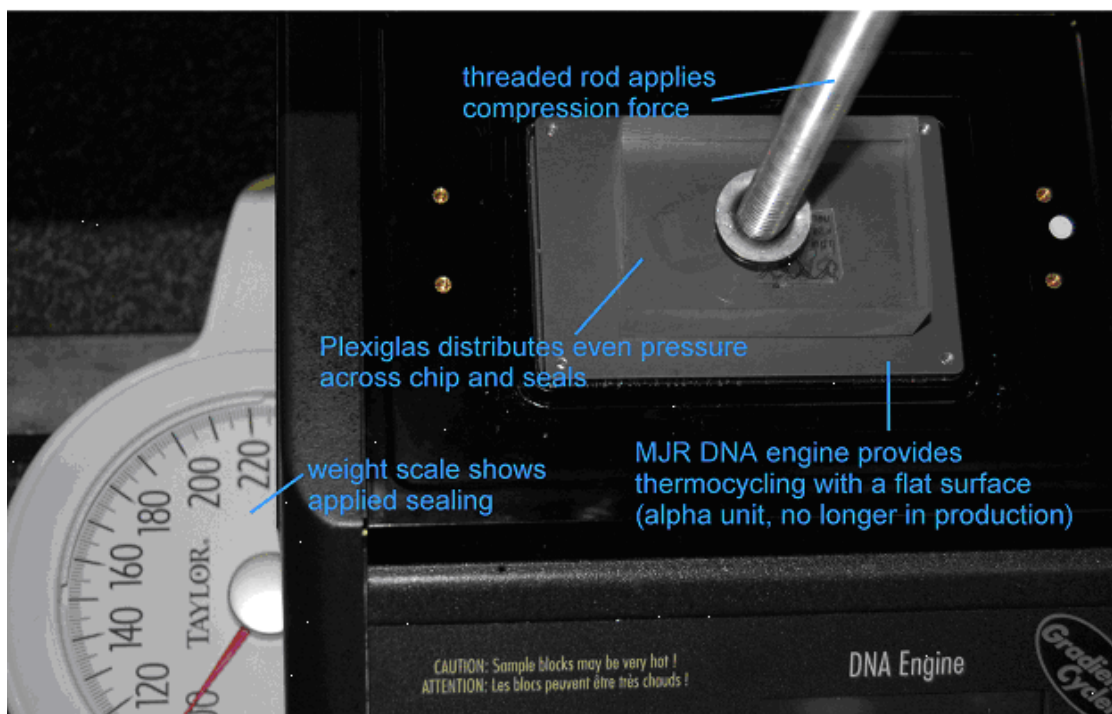


Figure 19 – Compression-thermocycling rig showing PCR machine on a weight scale.

Table 9 – Testing evaporation and spreading for different micro-well sealing films.

Material		Micro-Wells		
Sealing Material	Description	Evaporation	Spreading	Comments
Parafilm	thick, viscoelastic	N/A	N/A	plugs wells
Microseal A	clear, proprietary	~11%	<1%	
Microseal B	clear, proprietary	N/A	N/A	plugs some wells
Alum sticky foil	adhesive	N/A	N/A	removal breakage
Adhesive FEP	adhesive fluoropolymer	0%	~5%	
Silicone	medical grade	N/A	N/A	Inconsistent

### 2.11.3 PCR

To demonstrate PCR in the micro-well plates, they were pretreated on one side as previously described and then loaded by capillary action with 8  $\mu\text{L}$  of the following mixture: 50  $\mu\text{L}$  of PCR supermix containing an additional 2  $\mu\text{L}$  of native Taq DNA

polymerase, 3.5  $\mu\text{L}$  of 25 mM  $\text{MgCl}_2$ , 250  $\mu\text{M}$  of the 587bp GAPDH primer set, and 1  $\mu\text{L}$  of the cDNA (5 ng/ $\mu\text{L}$ ) used previously, as well as an additional 2 mg/mL BSA. A second PCR supermix contained the same reagents with 1  $\mu\text{L}$  of water in place of cDNA as a negative control. Since no gel was used in the wells here, particular attention had to be paid to prevent evaporation. The micro-well plates were sealed as described above using Microseal A. The micro-well plate was then placed on the flat alpha unit block of the thermocycler, and covered with mineral oil. PCR was performed with the following parameters: 95.0  $^\circ\text{C}$  for 2 min, 30 repeated cycles of 1) 95.0  $^\circ\text{C}$ , 30 sec, 2) 56.0  $^\circ\text{C}$ , 30 sec, and 3) 72.0  $^\circ\text{C}$ , 45 sec, followed by 72.0  $^\circ\text{C}$ , 2 min, and cool down to 4  $^\circ\text{C}$ , 10 min. The pressure lid was removed and the sealed plate was placed on dry ice. The seals were removed within a box containing dry ice.

To yield enough sample for visualization on an electrophoresis gel, the fluid in all of the micro-wells was combined. To extract the fluid, the mini-well plate was broken into pieces, placed in a 1 mL tube with 50  $\mu\text{L}$  of 50% ethanol-water, shaken, and heated to 70  $^\circ\text{C}$  for 5 minutes. The recovered fluid was dried at 95  $^\circ\text{C}$  to remove the ethanol and reconstituted with 10  $\mu\text{L}$  water to match the original reaction volume.

This mixture was combined with 2  $\mu\text{L}$  of concentrated gel-loading buffer and loaded onto a 1.5% agarose electrophoresis gel for validation. A second pair of positive and negative PCR controls performed in a test tube were also included.

As expected, the positive micro-well control and the standard plastic tube control both correctly displayed a band at the 587 base pair location, and no non-specific or

primer-dimer bands were observed (Figure 20). The negative control plate showed no band at 587 bp, for either the test-tube negative control or micro-well plate negative control. A fifth lane was included containing unamplified PCR super mix. These results confirm that we can perform PCR in the silicon micro-well plates, which was expected given the prior work by others<sup>108, 122, 136</sup>. The band intensity is weaker from the micro-well plate, and it is not clear whether this is an artifact from the fluid recovery method or if the micro-well plates perform somewhat less efficiently than standard plastic tubes.

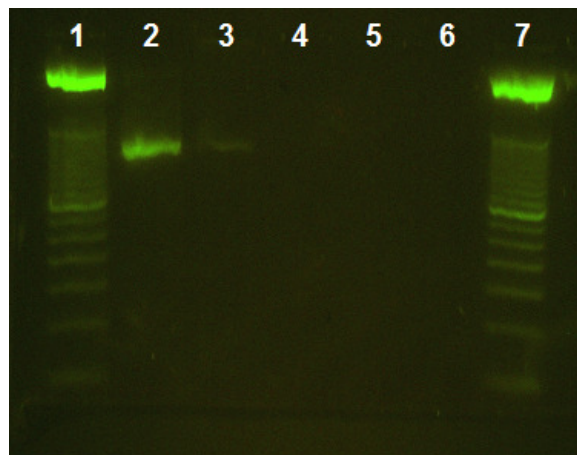


**Figure 20 – PCR results from (lane 2) a standard plastic PCR tube with control DNA added, (3) a micro-well plate with control DNA added, (4 and 5) a plastic tube and another micro-well plate containing only water, and (6) a lane containing unamplified PCR supermix. Lanes 1 and 7 contained 50 bp ladders.**

If our technology was able to map and quantify the levels of nucleic acids, rather than just detecting target molecules above or below a pre-determined threshold, it would be more valuable. This capability would potentially be useful for applications such as clinical determinations of tumor margins or identifying cancer in biopsies.

Quantification can be done using standard qPCR techniques<sup>103</sup>. However, one

question concerning qPCR in micro-wells is whether there is enough volume for fluorescent detection of PCR products with standard fluorescent imaging machines. To address this question, we loaded micro-wells with previously amplified PCR products containing either TaqMan or Sybr-Green I fluorescent probes, and imaged the devices using a Typhoon 9410 set to 10 micron resolution. There was a measurable and clear difference in signals between positive and negative controls (Figure 21). In another plate (not shown) run with SYBR gold probe chemistry, there were similar results, indicating feasibility at the microscale.

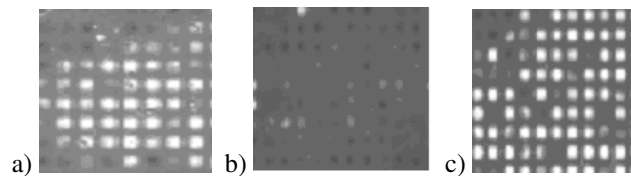


**Figure 21 – TaqMan in 100  $\mu\text{m}$  micro-wells, looking at different areas on one plate. a) Strong positive control with Ct value of 24. b) Negative control with no Ct value. c) Strong positive control with Ct value of 29.69.**

The image pixel intensities were directly related to the amount of DNA. These results demonstrate that it should be practical to use quantitative real-time methods (Ct values, point of curve inversion) to determine the approximate initial expression level of mRNA in single wells of a multi-well device.

#### 2.11.4 Discussion of Miniaturization Results

These preliminary results demonstrate that extending the 2D-PCR concept to miniaturized devices, which have 256 times the well density, requires further optimization. Despite the small size of these wells, which were 1,000 times smaller

in volume (2.4 nL) than our aluminum device (2.4  $\mu$ L), there was still enough fluid volume to detect a strong positive signal from post-PCR products, and a clear difference in signal between positive and negative samples. The PCR efficiency in these devices still remains to be determined.

In the future, work will focus on loading tissue and reagents into these wells. In particular, the silicon device needs a stronger inner hydrophilic coating and a stronger surface hydrophobic coating, both to prevent evaporation of fluid and to prevent spontaneous wicking of fluid out of the wells. Tissue loading may suffer from clogging of the wells, which would prevent subsequent loading of reagents by creating an air bubble that prevents fluid movement by capillary action.

2D-PCR is expected to be scalable because the single-well procedure requires no pipetting of reagent out of the wells, enabling reagents to be added by capillary action. Since the volume of sample is always proportionate to number of cells, we do not expect a loss of efficiency in these devices when trying to amplify the same concentration, even if there is smaller number of transcripts per well. To support this hypothesis, the results of testing quantitative fluorescent dyes showed that there was plenty of fluorescence to distinguish positive and negative samples (Figure 21).

## Chapter 3: RNA maps from frozen tissue

Nucleic Acids Research, full article, draft

In this chapter, the methods and results for mapping and quantifying mRNA from frozen tissue sections are presented, as described in aim 2. This chapter presents these results as the entirety of a manuscript still in preparation, which is expected to be submitted for publication to Nucleic Acids Research Methods Online.

Intellectual contributions: I drafted the initial manuscript, performed all of the experiments, and developed the experimental methodology (see intellectual contributions 3-4 in Chapter 7). The co-authors on the paper served an advisory role by guiding the project and helped to edit and finalize the manuscript for submission.

### Quantifying mRNA across a Histological Section with 2D-RT-PCR

Michael Armani<sup>acd</sup>, Michael A. Tangrea<sup>d</sup>, Benjamin Shapiro<sup>ac</sup>, Michael R. Emmert-Buck<sup>d\*</sup>, and Elisabeth Smela<sup>bc\*</sup>

<sup>a</sup>Fischell Department of Bio-Engineering

<sup>b</sup>Mechanical Engineering

<sup>c</sup>University of Maryland, College Park, MD

<sup>d</sup>Pathogenetics Unit, Laboratory of Pathology, National Cancer Institute, Bethesda, MD

\*Corresponding authors:

2176 Martin Hall, College Park, MD 20742, [smela@umd.edu](mailto:smela@umd.edu)

Pathogenetics Unit, Laboratory of Pathology, NCI, Bethesda, MD 20892,

[buckm@mail.nih.gov](mailto:buckm@mail.nih.gov)

### 3.1 Abstract

The ability to visualize nucleic acids across a tissue sample would lead to a greater understanding of the biological function of genes. This requires a high-throughput process to prepare tissue for PCR and to perform the amplification while maintaining the layout of individual tissue subregions. In this paper we present 2D-RT-PCR, a method for performing cell lysis, nucleic acid purification, and quantitative RT-PCR amplification across a tissue section while maintaining spatial relationships. A single-well protocol for tissue lysis and nucleic acid purification was developed that is as efficient as commercially available bench-top scale reactions and that has greater consistency and lower detection thresholds. It uses a GITC-based buffer and works with as little as 5  $\mu$ L of starting lysate. As an example of the utility of this method, a frozen tissue section containing mouse liver, kidney, and heart was mapped in multiplex to quantify three tissue-specific mRNAs.

### 3.2 Introduction

The standard approach for understanding the biological role of nucleic acids is to visualize proteins and nucleic acids by *in situ* staining techniques. *In situ* staining includes the “gold standard” Hematoxylin and Eosin (H&E) staining, protein staining by immunohistochemistry (IHC), and nucleic acid staining by *in-situ* hybridization (ISH). However, IHC and ISH have poor sensitivity, as exemplified by difficulties in using these techniques to obtain a clinical diagnosis<sup>13-15, 17, 80, 81, 99</sup>. To address this need for greater sensitivity, *in situ* PCR was invented in the early 1990s, combining the benefits of PCR amplification with subsequent staining of PCR amplicons *in situ*<sup>82</sup>. Despite initial excitement over the technique, *in situ* PCR proved to be too variable to consistently amplify many desired targets within a range of complex tissue milieus<sup>13-15, 63, 84</sup>, and it has been found that the *in situ* PCR technique is best suited for detecting high-abundant targets such as virus DNA<sup>85</sup>.

Researchers who seek to both quantify and localize nucleic acids have first isolated tissue subregions and then performed PCR on each subregion separately. For example, brain tissue has been cut into a grid on the mm scale using the voxelation method<sup>18</sup>, and larger regions of tissue have been manually isolated using macrodissection<sup>90, 91</sup>. The approach has provided significant useful information by maintaining the spatial information concerning the source of the nucleic acids. Laser microdissection is another technique for isolating subregions from a tissue section, but it does so on the length scale of individual cells<sup>8, 10, 65</sup>. However, this approach is labor intensive because each PCR data point is individually generated.

Microdissection typically involves a four-step workflow of macrodissection, tissue homogenization and lysis, RNA purification, and RT-qPCR.

We have previously demonstrated 2D-PCR for mapping genomic DNA across a tissue section<sup>100</sup>. This approach married the desirable features of *in situ* measurements with the advantages of solution-based molecular analysis. In 2D-PCR, the tissue section is transferred into a multi-well plate, using the grid format of the plate to mechanically subdivide the entire section at once. Simultaneously within all the wells, the tissue subregions are lysed and the DNA is amplified.

In this paper we present a version 2D-PCR, 2D-RT-PCR, that performs the more complex task of mapping and quantifying mRNA. The technique includes RNA purification, reverse transcription, amplification and qPCR (Figure 22). After showing experimental proof-of-concept, we introduce a new single-well tissue lysis and RNA purification method that enables the use of a chaotropic buffer with ChargeSwitch magnetic purification beads. We then demonstrate the utility of the single-well technique combined with 2D-RT-PCR as a high-throughput approach to quantifying three organ-specific mRNAs across a tissue section containing three different mouse tissues.

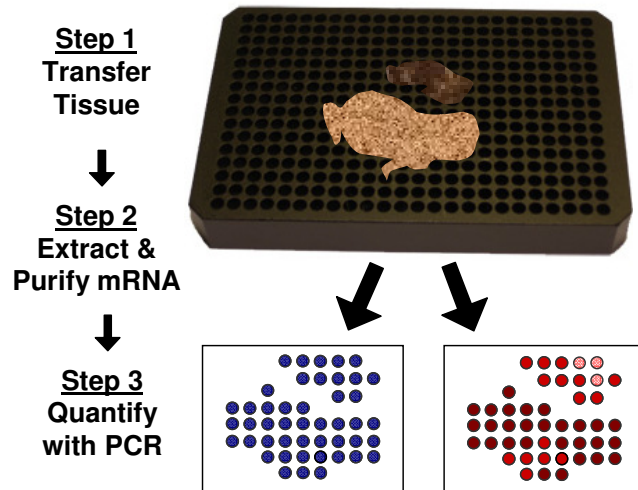


Figure 22 – 2D-PCR is achieved by transferring a tissue section vertically into a multiwell array device, thereby isolating tissue sub-regions. RNA is extracted by cell lysis, captured and purified on ChargeSwitch beads by rinsing steps, and quantified by one-step reverse-transcriptase PCR in each well. Visualization of targets is performed within the wells using standard molecular probe chemistry.

### 3.3 Materials and Methods

#### 3.3.1 Quantitative PCR Primers and Probes

Multiplex PCR primers and hydrolysis probes for mouse GYS2, KCNJ1, and HPRT1 targets (see section 3.7.1) were generated using the Primer3 web application, version 4.0<sup>144</sup>. Primers and probes were obtained from Biosearch Technologies<sup>[ESI]</sup>. The 5' and 3' fluorophores ordered for each probe were Quasar 670/BHQ-2 for HPRT1, Cal Fluor Orange 560/BHQ-1 for GYS2, and FAM 520/BHQ-1 for KCNJ1.

#### 3.3.2 Tissue Sections and Scrapes

Frozen mouse liver, kidney, heart, and brain organs and chicken thymus glands were obtained from Pel-Freez Biologicals. Individual organs or composites of multiple

organs were embedded in O.C.T. Compound (Tissue-Tek) in a cryostat at -24 °C.

Tissues were sectioned to 10 µm thickness using a Leica cryostat microtome. Tissue scrapes were obtained by sectioning tissue onto glass slides, heating the slide at 90 °C for 30 seconds, and scraping the dried tissue using a razor blade into tubes.

### 3.3.3 Materials and Equipment

Heat-activated adhesive film ARSeal 90697 was provided by Adhesives Research.

Industry standard 384-well clear PCR plates were utilized (Applied Biosystems, 4309849); each well had a volume of 40 µL. A Sorval RT7 swinging bucket centrifuge was used with these plates. In place of a multiplexing real-time PCR machine, plates were imaged on a Tecan Infinite 200 fluorescent microplate reader as described in section 3.7.4.

### 3.3.4 Buffers and Commercial Purification Kits

A custom lysis buffer was prepared that contained 3.33 mL guanidinium isothiocyanate (GITC, 6 M, Fluka Part 50983), 1.1 mL Triton X-100 (MPBio part 807426), 5 µL 2-mercaptoethanol (Sigma M3148), and 565 µL double-distilled water. Buffer RLT was obtained from Qiagen (RNeasy kit). Extraction buffer was obtained from Molecular Devices (PicoPure RNA extraction kit). ChargeSwitch lysis, magnetic binding, wash, and elution buffers were obtained from Invitrogen (ChargeSwitch total RNA cell kit 45-7006). Ag-Path ID one-step PCR mix was

prepared according to the manufacturer's protocol (ABI, AM1005M) and included final concentrations of 250 nM primers and 125 nM probes.

### 3.3.5 Determination of Nucleic Acid Purification Efficiency

Sheared herring sperm DNA (10 µg/µL, Invitrogen 15634-017) was added to the lysis buffers of different purification kits (specified in section 3.4.1). The loading ranged from 2.5% to 50% of the maximum binding capacity of the purification system. Amounts of input and recovered DNA were measured in triplicate using a Nanodrop Spectrophotometer (Thermo-Scientific) using a test volume of 1 µL. The efficiency was calculated as the  $100 * \text{recovered DNA} * \text{recovery-volume} / [\text{input DNA}]$ .

### 3.3.6 2D-PCR Method

The 2D-RT-PCR method is illustrated in Figure 23. The tissue section is transferred onto an adhesive film, placed tissue-side down over a multi-well plate, and sealed. The plate, which has wells pre-loaded with lysis buffer, is inverted to distribute the lysis solution over the tissue. An incubation is performed. Magnetic ChargeSwitch beads are added, which bind the nucleic acids. A magnet is brought close to the wells, attracting the beads and holding them in place for RNA purification by washing and DNase treatment steps. One-step reverse-transcriptase PCR mix is added to the wells, and thermocycling with real-time detection is used to quantify the amounts of RNA transcript in each well. This produces a quantitative map of mRNA

at each well location, which corresponds to histological subregions of the tissue section.

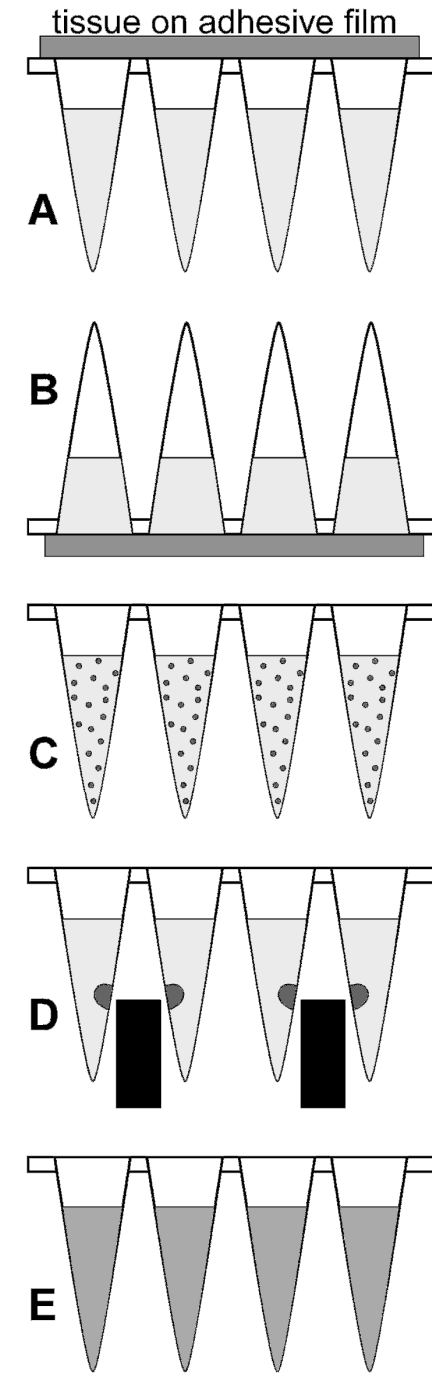


**Figure 23 – Cross-sectional schematic illustration of 2D-RT-PCR method. A) Tissue transfer. B) Tissue lysis. C) Addition of magnetic beads. D) Purification by washing, DNase. E) Amplification by qPCR.**

### 3.3.7 Optimal 2D-PCR Protocol for Quantifying mRNA Across Tissue Sections

#### 3.3.7.1 A) Tissue Transfer

Wells of a 384-well plate were loaded with 5  $\mu$ L of lysis buffer (either custom GITC buffer, section 3.3.4, or others). Tissues were sectioned (section 3.3.2) and covered with a 40 mm x 40 mm piece of heat-activated adhesive film, to which the tissue adhered. Tissues were dried at 50 °C for 2 minutes, rinsed in a bath of 70% ethanol for 2 minutes (containing either 1% Eosin Y or 1% Acid Fuchsin Red stains for visualization), and dried at room temperature in a fume hood for 10 minutes. The tissue was placed face-down onto the PCR plate. To seal the adhesive film against the plate, the adhesive was activated by a combination of 200 pounds of compressive force and 90 °C heat for 5 minutes<sup>100</sup>.

#### 3.3.7.2 B) Tissue Lysis

After sealing, the plate was cooled to room temperature for 2 minutes. To distribute the lysis buffer over the tissue at the top of the wells, the plate was inverted. To provide a flat, heated surface for incubating the tissue in the lysis buffer, an 8 mm thick aluminum block was placed on top of a thermocycler heating plate. The back of the plate was covered with a rubber pad, and the plate was compressed as described previously to keep fluid from leaking. The contents of the wells were incubated for 15 minutes, applying 60 °C on the tissue side and 70 °C on the back side to prevent condensation. The plate was cooled to 30 °C and centrifuged at 3000 rpm for 3 minutes to pull the fluid back down into the bottoms of wells.

### 3.3.7.3 C) Nucleic Acid Isolation

To isolate the released nucleic acids, acidic buffer containing magnetic capture beads was added to each well (15  $\mu\text{L}$  of 0.33  $\mu\text{L}$  ChargeSwitch magnetic beads, 0.4  $\mu\text{L}$  acetic acid, 5.75  $\mu\text{L}$  ChargeSwitch binding buffer, and 8.52  $\mu\text{L}$  water).

### 3.3.7.4 D) Purifying the RNA

To purify the RNA, the magnetic beads were immobilized against a magnet and the fluid removed. For the first rinse, ChargeSwitch wash buffer 13 (20  $\mu\text{L}$ ) was added to each well and removed. ChargeSwitch DNase buffer (15  $\mu\text{L}$ ) with DNase I (0.15  $\mu\text{L}$ ) was added and incubated (10 minutes at room temperature). ChargeSwitch binding buffer B9 (5  $\mu\text{L}$ ) was added to each well, and the plate was sealed (ARseal 90697 at 90  $^{\circ}\text{C}$  for 1 minute). The plate was inverted several times to mix the contents, after which the plate was centrifuged as before. The DNase buffer was removed, and two washes were performed using ChargeSwitch wash buffers 13 and 14, respectively (20  $\mu\text{L}$ ). To isolate DNA from frozen tissues, the DNase step is omitted.

### 3.3.7.5 E) Quantification Using PCR

To quantify RNA across the multi-well plate, PCR reagents were added to each well and the plate thermocycled and imaged according to standard procedures. First, the wash buffer from the previous step was removed. Ag-Path ID one-step PCR mix was added to each well of the plate (5  $\mu\text{L}$ ). Amplification was performed by thermocycling (50  $^{\circ}\text{C}$  for 10 minutes, 95  $^{\circ}\text{C}$  for 10 minutes, and 30 total cycles of 95  $^{\circ}\text{C}$  for 15 seconds and 60  $^{\circ}\text{C}$  for 30 seconds). The plate was imaged on the fluorescent microplate reader after every 5 cycles of PCR starting at cycle 10.

Threshold cycles of detection (Cts) were determined using a standard curve formula (See section 3.7.4).

## 3.4 Results

### 3.4.1 Validation of Efficient Purification at Small Scales

In order to test an initial proof of concept of 2D-PCR using 384-well plates, a lysis and purification protocol was required that would work within those 40  $\mu$ L well volumes. Since it uses magnetic beads instead of purification columns, the ChargeSwitch purification kit was chosen for adaptation. Those reactions are based on volumes of 800  $\mu$ L, however, so the feasibility of scaling this protocol down 20-fold had to be established. Furthermore, because the ChargeSwitch protocol recommends repipetting in each well, which would be too laborious across a 384-well plate, vortexing of magnetic beads was tested in place of repipetting. To provide two points for comparison of our protocol, the efficiency of another purification kit, PicoPure, was also determined.

Sheared DNA was selected as the input nucleic acid because it is a closer representative of RNA than unsheared DNA, but unlike RNA it is stable and inexpensive enough to be used for quantification purposes at the level of 50  $\mu$ g per sample. It was assumed that relative recovery efficiencies would be similar for sheared DNA and RNA. Sheared DNA was spiked into the lysis buffer (this experiment began at step B) at 2.5% and 50% of the maximum reported binding

capacity of the beads (ChargeSwitch – 1 µg/µL) or purification column (PicoPure - 100 µg). Loadings throughout this range are typical in the literature.

After the purification (step D), elution buffer was added to the tubes to recover the DNA and obtain purification efficiency. Experiments were performed at least three times to determine variability. The results are shown in Table 10.

Table 10 – Rows 1-4: Comparison of sheared herring sperm DNA recovery efficiency with two commercially available kits: CS – ChargeSwitch Total RNA Cell Kit, PP – PicoPure. Rows 5-6: Recovery efficiency of 20x scaled-down ChargeSwitch protocol. Rows 7-9: The same protocol with the addition of acetic acid (AA).

Row	Kit	DNA% Load*	Max (µg)	Recovery Efficiency%	Stdev%	N
1	PP	2.5	100	31	11	3
2	PP	50	100	8	3	3
3	CS	2.5	100	86	3	3
4	CS	50	100	47	7	3
5	CS/20	2.5	5	86	12	3
6	CS/20	50	5	30	4	6
7	CS/20 + 1% AA	50	5	50	3	3
8	CS/20 + 2% AA	50	5	38	1	3
9	CS/20 + 4% AA	50	5	37	2	3

\* Load as a percentage of the reported maximum nucleic binding capacity of the kit.

The ChargeSwitch (CS) protocol yielded more DNA than the PicoPure (PP) protocol, but for both kits recovery efficiencies were higher at 2.5% loading than at 50%. At 2.5%, the 20-fold scaled-down protocol provided the same purification efficiency (86%) as the unmodified CS protocol. At 50%, however, the recovery was only 30% for the scaled-down protocol vs 47% for the standard one. In order to mitigate the loss of efficiency at higher loading, acetic acid (AA) was added to the lysis buffer based on the fact that the magnetic beads require a pH of less than 4.5 to bind nucleic acids. All three AA concentrations improved the efficiency, with the 1% solution

raising the efficiency the most, to 50%, the same as that of the standard protocol.

These results demonstrate that a scaled-down purification can be performed without sacrificing efficiency by an appropriate adjustment of the pH.

### 3.4.2 Enabling GITC Buffer Use in Magnetic Bead-Based Purifications

The current method to lyse frozen tissues is mechanical grinding followed by the application of strong denaturing lysis buffers and then centrifugation or filtering to separate remaining tissue fragments. If the nucleic acids are not separated from tissue artifacts, reactions like PCR are inhibited<sup>145</sup>. However, grinding, centrifugation, and filtering are incompatible with the 2D-RT-PCR protocol, so lysis had to be achieved using buffers alone. The lysis buffer supplied with the ChargeSwitch kit was not intended to lyse tissue, and in initial purification tests it in fact did not fully lyse the tissue. This caused the beads to flocculate unpredictably, clogged pipette tips, and prevented the beads from being rinsed uniformly. The beads therefore required careful visual inspection for flocculation followed by repipetting to resuspend the beads to ensure a successful purification. Because GITC lysis buffers are more aggressive (GITC is a powerful chaotropic denaturant), three different buffers were tested to determine whether they were compatible with the CS magnetic beads: PicoPure, Qiagen RLT, and a custom buffer. The concentration of GITC typically found in commercial buffers is 4-8 M, but above 4M GITC is known to prevent hybridization of nucleic acids<sup>146</sup>. Therefore GITC was used at stock concentrations during lysis, but the solution was afterward diluted 4-fold with water to permit

hybridization to the magnetic beads. As in the previous section, the buffers were evaluated for purification efficiency at 50% loading with sheared herring DNA.

As shown in the first column of Table 11, none of these buffers was compatible, showing efficiencies of only 0% to 5%. Therefore, the pH was adjusted by adding acetic acid or the buffer was diluted four times with water. The purification efficiencies were still poor (columns 2 and 3), ranging from 0% to 19%, with the best performance from the custom buffer. Finally, the buffers were both diluted and pH-adjusted (column 4). Under these conditions, the recovery efficiencies rose to between 8% and 31%.

Table 11 – Recovery efficiencies of GITC-based buffers with sheared herring sperm DNA.

<b>GITC Buffer</b>	<b>Without Adjustments</b>	<b>75% H<sub>2</sub>O</b>	<b>pH 4.0</b>	<b>75% H<sub>2</sub>O + pH 4.0</b>
<b>PicoPure</b>	1%	0%	2%	8%
<b>Custom</b>	0%	1%	19%	31%
<b>Qiagen RLT</b>	5%	1%	2%	30%

This is the first demonstration of the use of GITC-based lysis buffer with subsequent nucleic acid capture on ChargeSwitch beads. Even though the ChargeSwitch lysis buffer efficiency with pure DNA was higher (47% versus 31% at 50% loading), because the GITC based buffer provides more consistent lysis, it may actually produce more initial template from tissue.

### 3.4.3 Single-Well Lysis and Purification on Tissue Samples

After lysis, commercially-available kits for RNA recovery from solid tissues typically transfer the sample from the lysis tube to a second tube for purification and a third for amplification. The lysing and transfers steps are a bottleneck for the isolation of nucleic acids, particularly RNA<sup>87, 93, 94</sup>. To increase throughput, robotic automation or microfluidic chips have been utilized for the transfer steps. A single-well approach, however, would prevent loss of nucleic acids to non-specific binding in each tube, decrease the risk of cross-contamination, and reduce processing time.

To determine whether the previously-developed procedures could be performed with tissue, thus enabling a single-well lysis and purification protocol, four lysis buffers were tested with three different mouse tissue scrapes (brain, kidney, and liver). The ChargeSwitch buffer contained 200  $\mu\text{L}$  lysis buffer, 100  $\mu\text{L}$  binding buffer, and 50  $\mu\text{L}$  ChargeSwitch magnetic beads. The others contained 87.5  $\mu\text{L}$  of GITC-based lysis buffer during the lysis step, and after lysis buffers were added (59  $\mu\text{L}$  water 100  $\mu\text{L}$  ChargeSwitch binding buffer, and 50  $\mu\text{L}$  magnetic beads).

The tissues were incubated in the various buffers at 65 °C for 15 minutes. The RNA was purified as described previously and eluted. One-step reverse-transcriptase PCR reactions were run on 1/60<sup>th</sup> of each eluted sample to determine the level of HPRT1 (a housekeeping mRNA), generating standard curves from which threshold-cycles of detection were obtained. Table 12 shows the relative percent of HPRT1 mRNA, normalized to the best performing buffer overall.

Table 12 – Relative effectiveness of single-well lysis and purification using different lysis buffers determined by quantitative reverse-transcriptase PCR.

	<b>Custom Buffer</b>	<b>Qiagen RLT</b>	<b>PicoPure</b>	<b>ChargeSwitch</b>
<b>Brain</b>	66	100	70	70
<b>Liver</b>	29	8	4	39
<b>Kidney</b>	70	17	8	56

For liver and kidney tissues, the PicoPure and Qiagen RLT lysis buffers, which were not designed for this system, recovered substantially less HPRT1, with relative recoveries of 4% to 17%, compared to the ChargeSwitch and custom GITC lysis buffers, which had relative recovery efficiencies of 29% to 70%. With brain tissue, the Qiagen buffer worked the best and the other three were comparable.

Based on visual observation, only the PicoPure and custom GITC buffers fully homogenized the tissues and prevented bead flocculation. However, the PicoPure had poor relative recovery of mRNA, and the ChargeSwitch and Qiagen buffers required manual removal of undissolved tissue from well. Therefore, custom GITC buffer was the best lysis buffer overall for good relative recovery and ease of tissue processing.

#### 3.4.4 Proof of Concept for 2D-PCR

To demonstrate the feasibility of 2D-PCR, the expression levels of two genes were quantified across a tissue section containing frozen mouse brain, mouse kidney, and chicken thymus. Empty wells between mouse tissues served as no-sample controls. The tissue was stained with Eosin Y to permit visualization during transfer. A

multiplex PCR reaction was performed using primer and probe targets for KCNJ1, a kidney-specific gene, and HPRT1, a housekeeping gene specific to all mouse tissues. The KCNJ1 primer/probe set can detect either RNA or DNA. A detailed protocol is provided in Supplemental Information <sup>90</sup>.

Figure 24 shows the results. KCNJ1 was detected only in wells containing mouse kidney and HPRT1 only in wells with either mouse tissue. No false positives were detected in any of the negative control wells, demonstrating perfect well sealing during the initial lysis, effectiveness of DNase treatment (because no KCNJ1 DNA was detected in mouse brain), and the overall cleanliness of this technique. The Eosin Y staining did not affect the subsequent PCR reaction. This experiment shows that it is possible to map two mRNAs across a tissue section using the 2D-PCR approach.

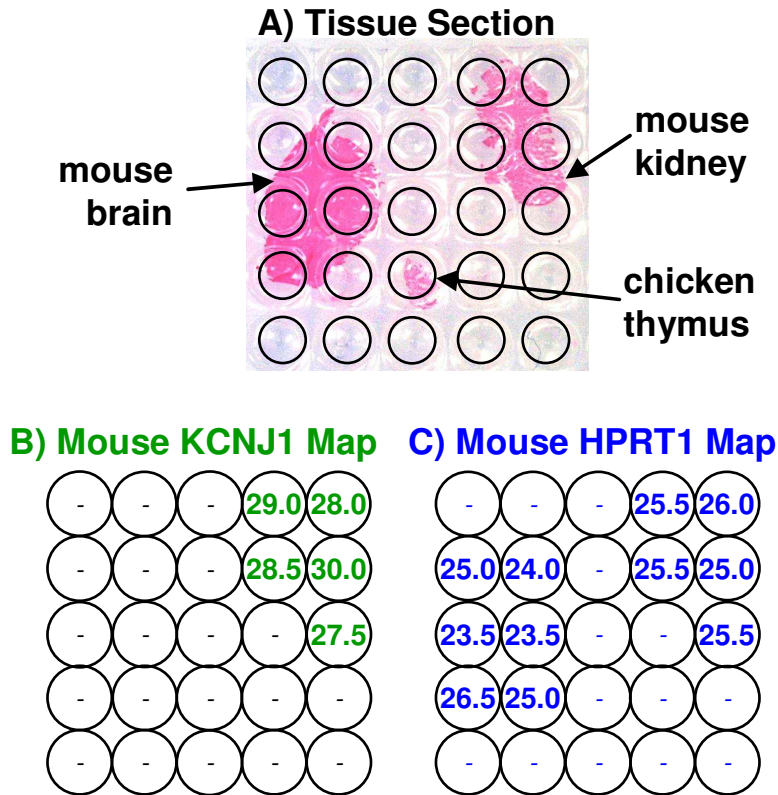


**Figure 24 – A) Mouse brain, mouse kidney, and chicken thymus on an adhesive film, stained red with Eosin Y and transferred onto a 384-well plate. A) The layout of a 384-well format plate is outlined over the tissue. B) KCNJ1 mRNA detection and C) HPRT1 detection showing quantitative cycles of detection thresholds (Cts) determined by qPCR.**

### 3.4.5 Identification of the Best Lysis Buffer for 2D-PCR

The lysis buffers were optimized in section 3.4.3 using tissue scrapes (compacted tissues) loaded into the vials, while the 2D-PCR method instead provides tissue held flat at the tops of the wells, which may change the lysis performance. Therefore, 2D-PCR was used with two different buffer systems, the custom GITC buffer and the ChargeSwitch buffer, to map three mRNAs in serial recuts of a tissue section containing mouse heart, liver, and kidney. Tissue sections in these experiments were stained red with Fuchsin red for visualization. A multiplex PCR reaction was

performed using primer and probe targets for KCNJ1, HPRT1, and also GYS2, a liver-specific gene. A detailed protocol is in the Supplemental Information<sup>[ESI]</sup>.

Cts are shown in Figure 25. HPRT1 was detected in all the wells containing mouse tissue, KCNJ1 only in wells with kidney tissues, and GYS2 only in wells with liver tissues. Both lysis buffers worked well. However, on average KCNJ1, HPRT1, and GYS2 were detected 2.3, 1.4, and 0.3 PCR cycles earlier when using the custom buffer. The GITC buffer completely solubilized tissue (Figure 25A2) while the ChargeSwitch buffer did not (Figure 25A1). These results demonstrate that 2D-PCR can map three targets at once across a tissue and, based on earlier detection of targets, that the custom GITC-based buffer results in greater combined recovery and purification of mRNA template from tissue when used in the 2D-PCR protocol.

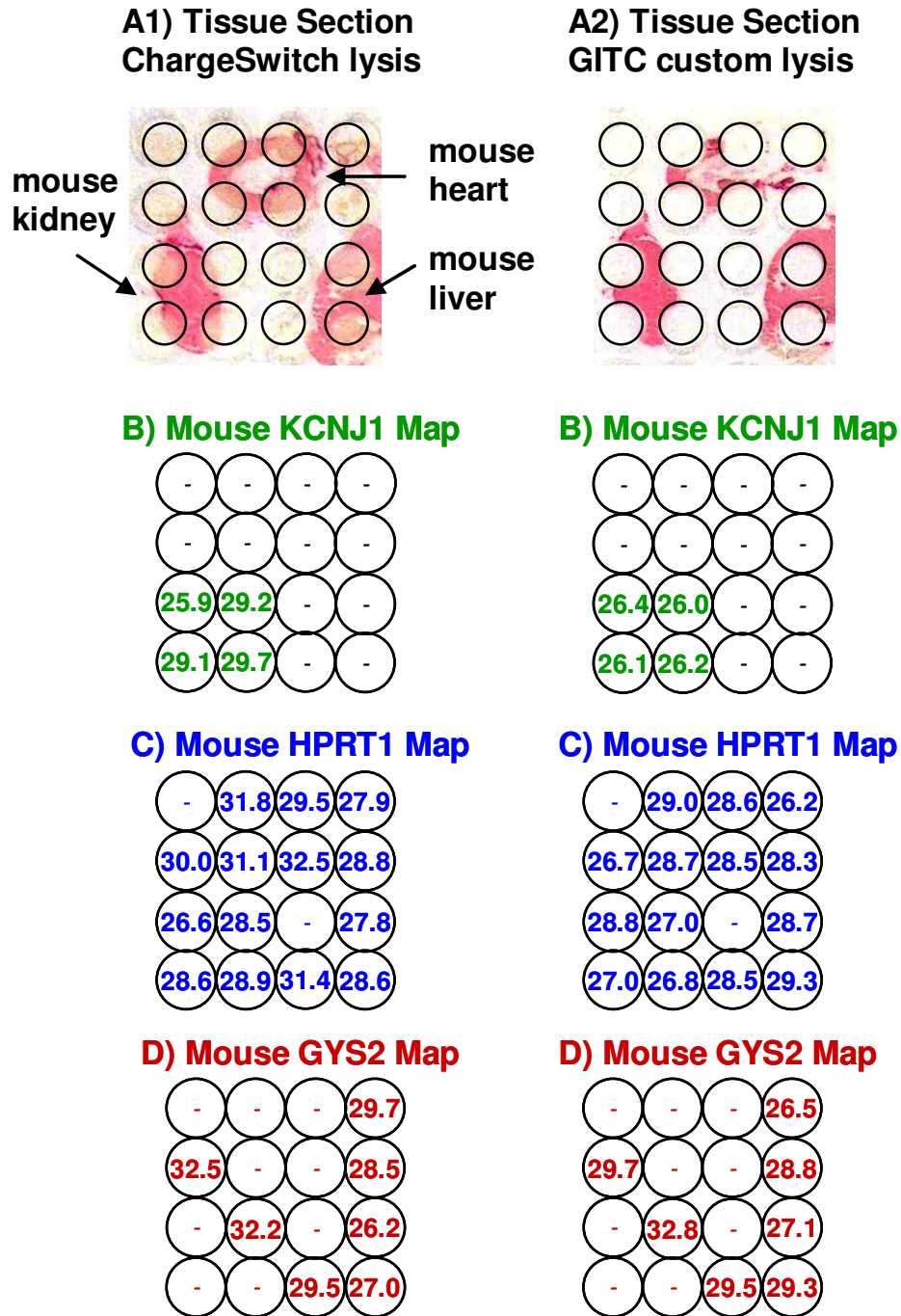


Figure 25 – Two serial recuts of a tissue sample containing mouse brain, kidney, and heart tissue, stained red with acid Fuchsin and transferred onto the wells of a 384-well plate containing either ChargeSwitch or custom buffer (image of tissue after lysis). A) The layout of a 384-well format plate is outlined over the tissue. B) KCNJ1 mRNA detection, C) HPRT1 mRNA detection, and D) GYS2 mRNA detection showing quantitative cycles of detection thresholds (Cts) determined by qPCR.

## 3.5 Discussion and Conclusions

### 3.5.1 Single-Well Lysis and Purification

For the first time, a procedure was developed for using GITC-based lysis buffers with ChargeSwitch magnetic beads, which enabled frozen, dried tissue to be fully lysed, homogenized, and purified using a single-well protocol. The protocol developed was shown to be as efficient as commercially available bench-top scale reactions, which typically require hundreds of microliters of reagents, numerous pipetting steps, and multiple transfers between tubes. The single-well protocol works well with as few as 5 microliters of starting lysate. The protocol can thus save a significant amount of time and cost for purification and may reduce inconsistencies arising from using multiple tubes, for example due to binding of nucleic acids in a tube or purification column<sup>87-89</sup>. Finally, the custom GITC buffer developed for 2D-PCR outperformed the ChargeSwitch lysis buffer in terms of consistency and lower detection thresholds.

### 3.5.2 2D-RT-PCR

We have shown an initial proof of concept of 2D-RT-PCR at the resolution of a 384-well plate, demonstrating that as many as three mRNA targets can be detected in a multiplex qPCR reaction. The technique should have immediate utility with the voxelation of tissue<sup>6, 7, 18</sup> and high throughput macrodissection and RNA template preparation. 2D-RT-PCR will have increasing utility as the resolution is increased

through miniaturization to a sub-millimeter scale and via automation with robotic pipetters.

In a multiplex qPCR, a housekeeping gene should be included to account for differences in the amount and type of material loaded into each well, providing a normalized “delta ct” measurement. This approach has been validated by others<sup>60, 102</sup>.

Using multiplex tandem PCR<sup>32-34</sup>, it has been shown that up to 92 genes can be studied from a single sample of purified mRNA. This approach may increase the number of genes that can be studied across a tissue section. By converting the RNA to pre-amplified DNA, tandem PCR only requires a qPCR step for detection, decreasing the costs and reaction times compared to using a one-step RT-qPCR protocol.

2D-RT-PCR is expected to complement methods such as LCM and in-situ hybridization for validating the expression of mRNA in tissues. Correlation of quantitative mRNA levels with traditional histopathological techniques should lead to a greater understanding of the biological roles of mRNA and the identification of crucial spatial gene signatures for the clinical diagnosis of diseases such as cancer.

### 3.5.3 Conclusions

We have developed a high-throughput technique to quantify the expression of mRNA across tissues using solution-phase PCR. Up to three mRNAs were quantified across

a tissue section using this technique. A novel single-well protocol for lysing frozen tissues with GITC and purifying RNA with ChargeSwitch magnetic beads was developed and optimized to enable this approach. A custom GITC lysis buffer was created and was found to detect more mRNA than three other lysis buffers tested.

### 3.6 Acknowledgements

This work was supported in part by the Intramural Research Program of the NIH, National Cancer Institute, Center for Cancer Research. We would like to thank Adhesives Research for providing samples of ARseal 90697 sealing films.

### 3.7 Electronic Supplementary Information (ESI)

#### 3.7.1 Primer sequences used in this study

Table 13 – Primer sequences  
Primer Sets (Biosearch Technologies)

<b>Target</b>	<b>Forward (5' to 3')</b>	<b>Reverse (5' to 3')</b>
Mouse Liver GYS2	GCCAGACACCTGACACTGA	TCCGTCGTTGGTGGTGATG
Mouse Kidney KCNJ1	GGCGGGAAGACTCTGGTTA	GTGCCAGGAACCAAACCTA
Mouse Control HPRT1	GCAAACCTTTGCTTCCCTGG	ACTTCGAGAGGTCCTTTTCACC
<b>Target</b>	<b>Probe (5' to 3')</b>	
Mouse Liver GYS2	5'CalFluorOrange560-TTCCAGACAAATCCACCTAGAGCCC-BHQ1	
Mouse Kidney KCNJ1	5-FAM-AAGCACCGTGGCTGATCTTCCAGA-BHQ1	
Mouse Control HPRT1	5'Quasar670-CAGCCCCAAAATGGTTAAGGTTGCAAG-BHQ2	

#### 3.7.2 Specific protocol for duplex mRNA mapping (ChargeSwitch buffer)

Tissue was thawed at 90 °C for 15 minutes and the film was transferred into a section of a 384-well plate covering a 6x5 grid of wells pre-loaded with ChargeSwitch lysis buffer, using a sealing time of 2 minutes. In this experiment, the fluid was distributed over the tissue by manually inverting the plate 5 times (as opposed to using a

centrifuge). After lysis, ChargeSwitch beads and binding buffer was added to each well. Next, a wash was performed using 12.5  $\mu$ L of wash #14, 6.25  $\mu$ L of DNase was added and incubated for 10 minutes and 2  $\mu$ L of ChargeSwitch binding buffer (B9) was added. After removing the DNase buffers, two washes were performed using 20  $\mu$ L of wash #13 and 12.5  $\mu$ L of wash #14 buffers. AgPath-ID one-step RT-PCR mix was prepared according to the manufacturer's protocol. It included final concentrations of 250 nM primers and 125 nM probes for both HPRT1 and KCNJ1 targets. Five  $\mu$ L of the PCR mix was added to the 6x5 grid of wells. The thermocycling parameters were 50 °C for 10 minutes, 95 °C for 10 minutes, and 30 total cycles of 95 °C for 15 seconds and 60 °C for 30 seconds. The plate was removed and imaged on the Typhoon 1410 flatbed scanner every 5 cycles from cycles 15 to 30.

### 3.7.3 Specific protocol for triplex mRNA mapping (ChargeSwitch or custom GITC buffer)

Two 5x5 grids within a 384-well plate were pre-loaded with lysis buffer. The wells in one grid were preloaded with a mixture containing 12.5  $\mu$ L ChargeSwitch lysis buffer, 6.25  $\mu$ L binding buffer, 0.5  $\mu$ L beads, 0.2 mg/mL proteinase K, 5 mM DTT, and acetic acid to a final concentration of 1% by volume. The wells in the second grid were preloaded with 5  $\mu$ L of custom GITC-based lysis buffer. The two sections on the film were transferred to the 384-well as described in Methods. The plate was inverted, centrifuged, and lysed, and the wells were washed. AgPath-ID one-step RT-PCR mix was prepared according to the manufacturer's protocol. It included final

concentrations of 250 nM primers and 125 nM probes for each of the HPRT1, GYS2, and KCNJ1 targets. 7.5  $\mu$ L of PCR mix was added to the wells containing beads. The thermocycling parameters were 50 °C for 15 minutes, 95 °C for 15 minutes, and 40 total cycles of 95 °C for 10 seconds and 60 °C for 30 seconds. The plate was removed and imaged at cycles 10, 25, 28, 31, 34, 37 and 40 using the Tecan 200 plate reader.

#### 3.7.4 Determination of Cts

It was necessary to perform PCR in a 384-well plate machine but to determine fluorescence values using a plate reader to achieve multiplex qPCR data. An ABI 7900HT 384-well plate qPCR machine was tested but it was not able to multiplex even two colors without spectral overlap. Therefore the following calculation was used to determine Cts based on the standard curve formula.

Fluorescent data was provided at cycles  $N_{1-7} = 10, 25, 28, 31, 34, 37$  and 40 for the triplex mRNA map, or cycles  $N_{1-4} = 10, 20, 25,$  and 30 for the duplex mRNA map. In order to determine Cts, the difference between two cycles was calculated as  $D_i = \log(\text{data}_{\text{cycle}(N_{i+1})} / \text{cycle}(N_i))$ , based on the standard curve formula of PCR. The cycle (C1) was determined when  $D_i$  was greater than a threshold value; thresholds defined as 0.04 for KCNJ1, 0.06 for GYS2, and 0.08 for HPRT1. Finally, the Ct value was calculated as  $C1 - A1 * D_i / 0.2$  for KCNJ1 and GYS2 or  $C1 - A1 * D_i / 0.25$  for HPRT1. The value A1 was the number of cycles skipped during PCR cycles (3 or 5).

Based on negative controls and background values, Cts above 30, 32.5, and 35 were ignored (for KCNJ1, HPRT1, and GYS2 respectively).

For example, the raw data and calculation to determine the Ct for HPRT1 from a single well is presented in Table 14. In row three, the raw fluorescence data from a PCR cycle is divided from the cycle before it and a log operation is performed to give the value of Di; because a previous PCR cycle is needed for a baseline, there is no value for the first PCR cycle. Next, the cycle at which Di is above a user-defined threshold (.08 for HPRT) is determined to be 28 PCR cycles. Therefore the value of C1 is 28, and because the previous data point was 3 cycles before it, the value of A1 is 3. Using the formula for Ct give a value of 25.86, the approximate value at which the increase in fluorescent signal was above baseline levels.

Table 14 – Example calculation of Cts from raw data.

<b>PCR Cycle</b>	10	20	25	28	31	34	37	40
<b>Raw Well Fluorescence Data</b>	2516	2564	2700	4074	6808	9961	11331	12811
<b>Di = log(cycle(Ni+1)/cycle(Ni))</b>		0.01	0.02	0.18	0.22	0.17	0.06	0.05
<b>Di &gt; .08 threshold?</b>				yes				
<b>Ct = C1-A1*Di/0.25</b>				<u>25.86</u>				

## Chapter 4: RNA and microRNA maps from FFPE tissue

In this chapter, the methods and results for mapping and quantifying mRNA and microRNA from formalin-fixed tissue sections are presented, as described in aim 3. This chapter presents these results as the entirety of a manuscript still in preparation, which is expected to be submitted for publication to Nature Methods.

Intellectual contributions: I drafted the initial manuscript, performed most of the experiments, and developed the experimental methodology (see intellectual contributions 5-8 in Chapter 7). I also started and led a collaborative team to work on this project, therefore many authors contributed to this work. These authors' contributions are described here, referring to them by their initials.

BY and AR are two summer students I mentored while at the NCI. BY performed part of the experiments shown in Figure 27A, and helped develop the idea to use varying core sizes. AR performed RecoverAll experiments which comprise half each of Figure 27A and C. KY and JM worked in the TARP lab and manufactured all of the TMAs. JRC validated the pathology of prostate tumor samples. The co-authors (BS, ES, MT, MEB, SH) served an advisory role by guiding the project and helped to edit and finalize the manuscript for submission. ES edited the second figure, and MT and MA created the first figure.

# Quantitative Validation of RNA Expression Profiles in Tissue Microarrays

Nature Methods, full article, draft

Michael Armani, Michael Tangrea, Brian Yang, Alex Rosenberg, Kris Ylaya, Jennifer Martinez, Jaime Rodriguez-Canales, Benjamin Shapiro, Elisabeth Smela, Michael R. Emmert-Buck, and Stephen Hewitt\*

## 4.1 Abstract

mRNA and microRNA tumor profiles are validated by quantifying the expression of dozens of genes against hundreds of samples. However, current workflows take days to complete and require large volumes of formalin-fixed tissue. We demonstrate a faster and more sensitive approach by quantifying the expression of 24 mRNAs in duplicate across 42 archival prostate cases by using just one 10 micron-thick tissue microarray (TMA) section to validate microarray profiles. The TMA was transferred into a 384-well plate where a single-well lysis and solid-phase purification method was used to recover total RNA in each well. The RNA was assayed directly with PCR or indirectly using a Fluidigm assay. In principle our approach can quantify 96 mRNAs against 96 cases in less than a day, improving the speed and accuracy of traditional workflows such as those used by the MammaPrint or Oncotype DX tests.

## 4.2 Introduction

Currently, there is no streamlined technique for validating the expression profiles of many genes from many samples. Global gene expression profiles are initially

determined by performing microarray analysis on a few dozen tissue samples. Validating the results requires measuring the expression of dozens of genes in hundreds of additional cases<sup>147</sup>. Normally, each case is studied using a laborious four-step workflow whereby tissues are 1) individually sectioned 2) homogenized and lysed, followed by 3) RNA purification and 4) RT-qPCR. The same four steps are also used for the diagnostic application of expression profiles, as in the Oncotype DX breast cancer assay<sup>91</sup>. Although the throughput of RT-qPCR can be improved with the Fluidigm and Biotrove platforms, there is no workflow that simplifies the sample preparation aspect. The tissue lysis and RNA purification is recognized as the rate-limiting step in gene analysis<sup>87, 93, 94</sup>. Furthermore, precious tissue is wasted from each block to align them during sectioning. Complicating gene expression profile validation is the fact that most archival clinical specimens are formalin-fixed<sup>37</sup>. This makes it difficult to obtain many high-quality samples for validation. Using formalin-fixed tissues for validation studies necessitates mixing the nucleic acids across a large volume of tissue to compensate for RNA degradation.

To address these challenges, we report a new method (Figure 26) that can in principle quantify 100s of RNAs in 100s of cases in a single day. The method transfers a 10 micron thick tissue microarray section into a 384-well PCR plate and uses a solid-phase extraction/purification method to prepare RNA from tissue cores. The RNA can be analyzed using traditional PCR techniques or pre-amplified for use with the Fluidigm system. This approach is based on the 2D-PCR method, which was previously used to detect DNA<sup>100</sup> and quantify RNA across frozen tissue sections, as

shown in Chapter 3. To recover mRNA, a reverse-crosslinking step was also added. To further increase sensitivity, a one-step microRNA RT-qPCR was used to prevent the dilution of templates and optimized for use with Fluidigm.

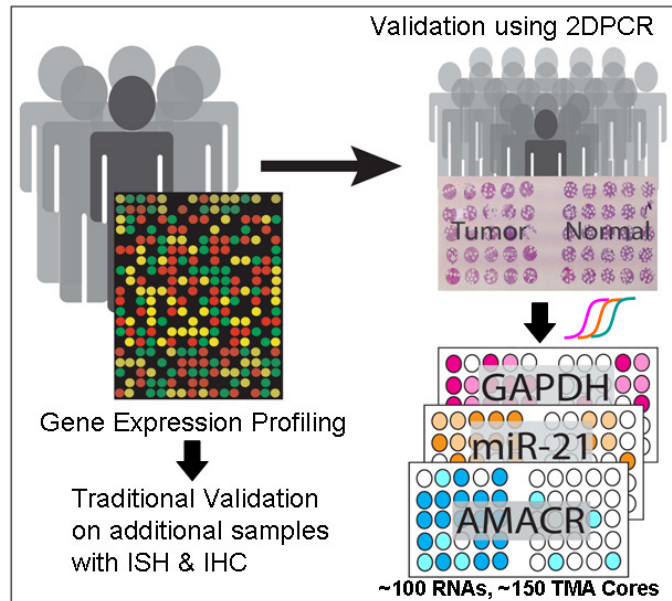


**Figure 26 – 2D-PCR can be used to validate up to 100 RNAs in multiplex from each core in a single 10 micron thick tissue microarray.**

#### 4.3 Results and Discussion

The 2D-PCR method was optimized for detecting microRNA or mRNA from formalin-fixed TMA samples. Speed and sensitivity were compared between 2D-PCR and a traditional workflow using the commercial RecoverAll kit. The reproducibility of 2D-PCR on serial recuts of tissue was also tested. To demonstrate the dynamic range and specificity of 2D-PCR, high-abundance and low-abundance mRNA was detected in 5 types of formalin-fixed mouse tissues. Specificity was also demonstrated by mapping a TMA containing human and mouse tissue for mouse-

specific or human-specific RNA. Finally, the 2D-PCR technique was used to quantify a panel of 24 prostate tumor mRNAs from a TMA containing human normal and tumor prostate tissues. By normalizing gene expression to the average of 4 housekeeping mRNAs, 15 significant gene profiles were validated.

#### 4.3.1 Speed and sensitivity 2D-PCR vs. a four-step workflow for microRNA detection

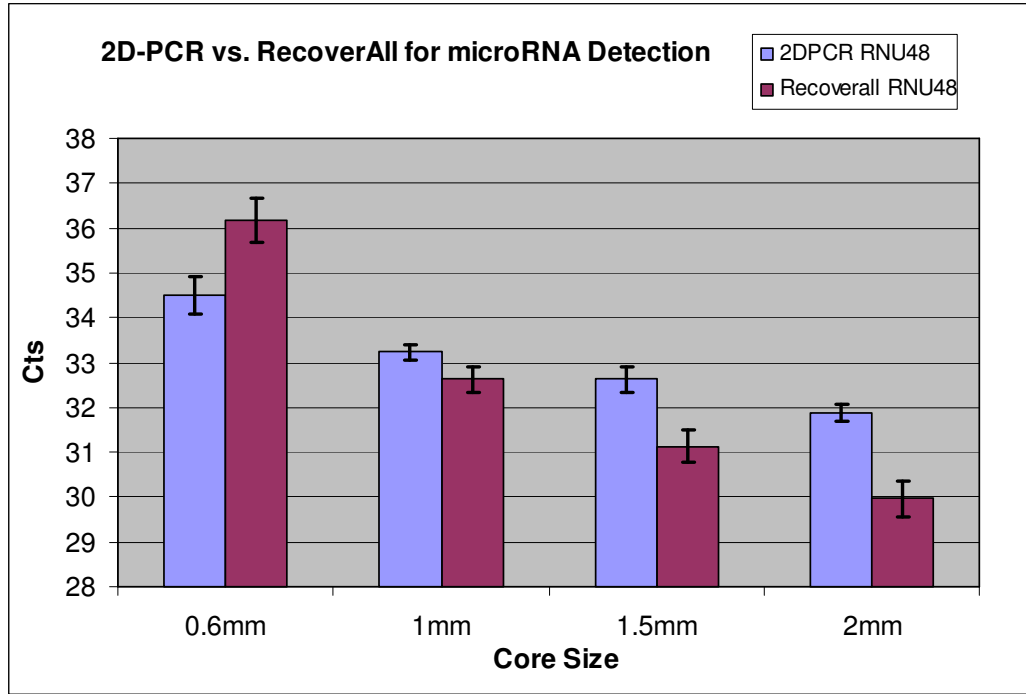
The 2D-PCR workflow was compared to the standard workflow of the commercial RecoverAll kit, because this kit was widely cited for FFPE RNA recovery. A TMA was made from a single human liver tissue block to provide homogenous tissue cores. To assess sensitivity, the TMA included 6 liver cores for each of four different diameters (0.6 mm, 1 mm, 1.5 mm, and 2 mm - method 4.5.1). To perform the RecoverAll workflow, a 10 micron TMA section was placed on glass, the 24 cores were macrodissected, and the RecoverAll procedure was followed according to the manufacturer's instructions. To quantify microRNA, a two-step RT-qPCR Applied Biosystems microRNA assay was used. To perform the 2D-PCR procedure, a 10 micron TMA section was sectioned and transferred into a 384-well plate (method 4.5.2) and a scaled down single-well lysis and RNA purification protocol was used (method 4.5.4). To transfer TMA's into 384-well plates, an adhesive was carefully selected (see 4.6.2). MicroRNA quantification was performed directly on the 2D-PCR templates using a novel one-step microRNA RT-qPCR to detect Mir-191 sensitively (method 4.5.5).

### Speed

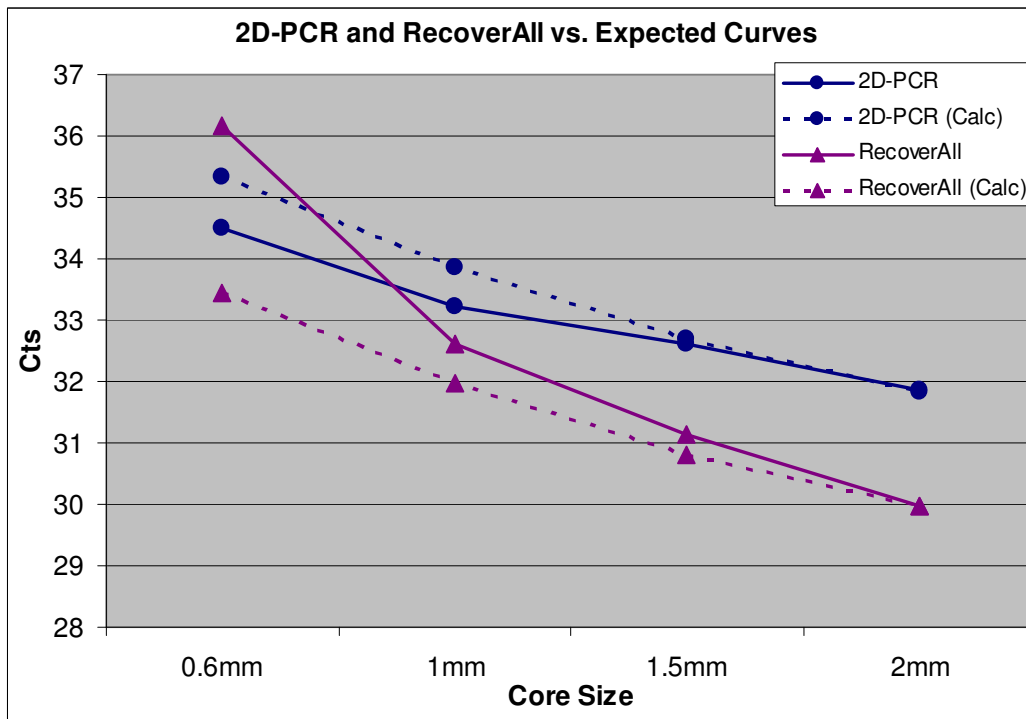
The 2D-PCR workflow took about 4 hours, requiring an actual handling time of about 60 minutes. The RecoverAll procedure took two work days to complete (about 12 hours) and required a handling time of about 6 hours. The 2D-PCR procedure was faster because it did not require macrodissection or manual pipetting of samples between many tubes. Based on these results, 2D-PCR is expected to be about an order of magnitude faster than a traditional workflow for studying 100s of samples.

### Sensitivity

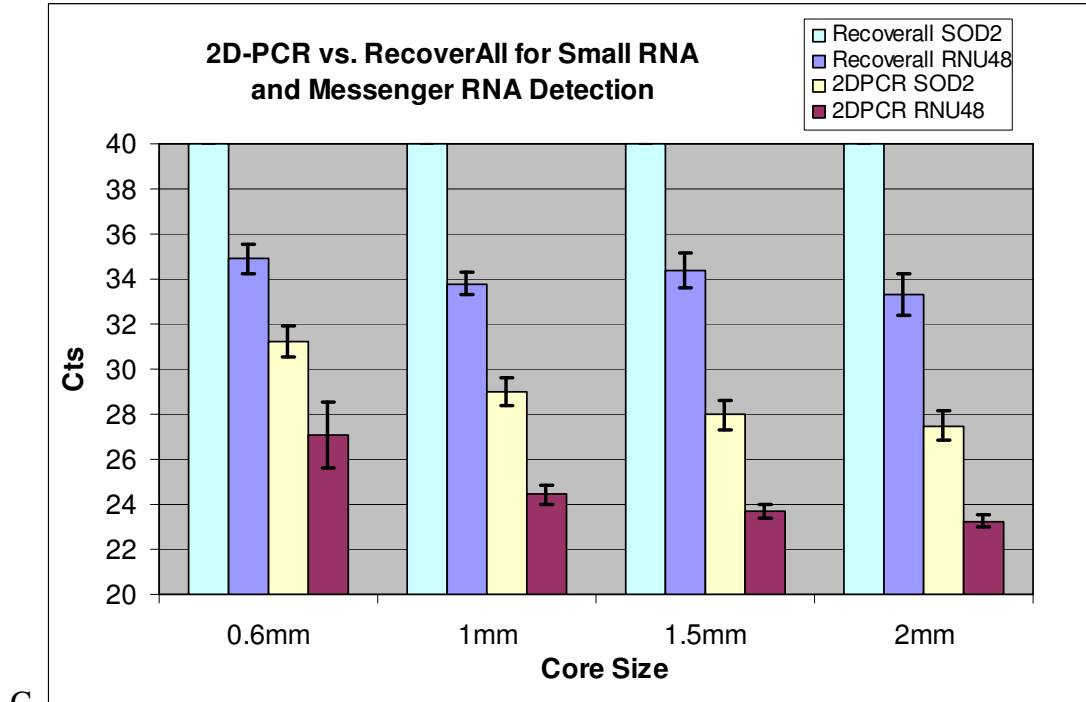
Using different tissue core sizes allowed us to test the sensitivity of 2D-PCR versus a traditional workflow. For example, a 1 mm diameter tissue should provide 4 times less RNA (or 2 Cts) than a 2 mm diameter tissue. Figure 27A shows the Cts determined by each method. As shown in Figure 27B, the RecoverAll loses RNA (higher Cts) as the size of tissue cores decreased, whereas 2D-PCR provided a much less steep drop off in Cts. 2D-PCR also had lower variability than RecoverAll. These differences can be explained by RNA losses in the RecoverAll purification columns and by the dilution of RNA template when using standard two-step microRNA RT-qPCR.



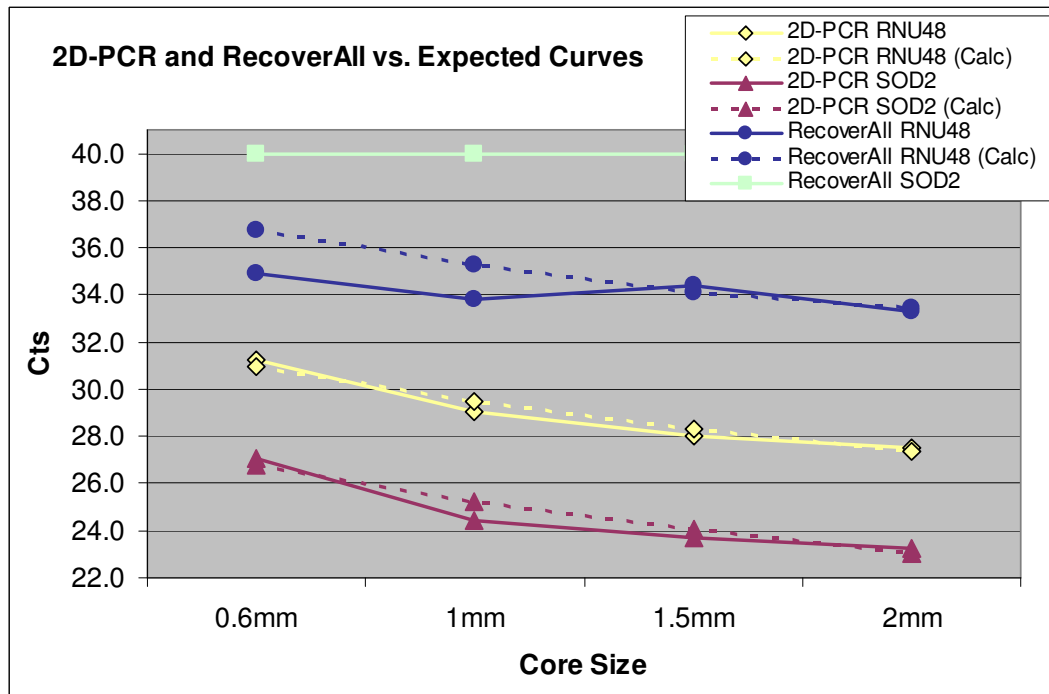
A



B



C



D

Figure 27 – A) Comparison of RecoverAll and 2D-PCR for the recovery of microRNA (mir-191) and B) mRNA (SOD2) and smallRNA (RNU48). Mir-191 is a stable microRNA normalizer<sup>148</sup>. Panels C and D show a plot of the measure Ct versus the calculated Ct as predicted by  $\log_2(\text{core size})$ .

#### 4.3.2 Sensitivity 2D-PCR vs. a four-step workflow for mRNA detection

A similar procedure as in section 4.3.1 was used to compare RecoverAll and 2D-PCR workflows for detecting mRNA. However, a reverse-crosslinking procedure was added before the tissue transfer step to extract mRNA with 2D-PCR (method 4.5.3). Both procedures used a standard one-step mRNA RT-qPCR procedure (method 4.5.5) to detect SOD2 mRNA or RNU48 small RNA.

Figure 27C shows the Cts of detection for SOD2 and RNU48 versus core diameter for the two approaches. The results showed that the RecoverAll did not detect mRNA from these samples. To be sure, RNU48 was quantified. RNU48 was detected from RecoverAll samples, but there was a poor correlation with core diameter (as shown in Figure 27D) and it was detected about 10 cycles later than with 2D-PCR. 2D-PCR detected mRNA and small RNA with a similar correlation to sample size as detected for microRNA. The variability was also lower using 2D-PCR.

#### 4.3.3 Reproducibility of 2D-PCR for microRNA and mRNA detection

SOD2 mRNA and mir-191 microRNA was quantified between two serial recuts of TMAs on two different days. The results showed Pearson  $R^2$  correlations of 0.70 to 0.72 for the microRNA and larger RNAs tested, respectively, therefore 2D-PCR has very good assay reproducibility.

#### 4.3.4 Dynamic range and specificity of 2D-PCR in different tissues

To demonstrate the dynamic range and specificity of 2DPCR, it was tested on a range of tissue types and qualities. One TMA was made with low-quality cooperative

human tissue network (CHTN) breast samples and high-quality 4-month old mouse tissues (brain, liver, kidney, spleen, and lung). Specific RNAs were quantified from serial recuts of this TMA – HPRT1, a low-abundance mouse target, and RNU48, a high abundance human target (Table 15). In another experiment, mRNAs highly-expressed in mouse liver (GYS2) or mouse kidney (KCNJ1) were mapped in a triplex PCR reaction with HPRT1 to show detection specificity and dynamic range for these tissues (Figure 30). Lastly, 2D-PCR was tested using worst-case human autopsy samples and decalcified tissues as negative-controls (Figure 31).

The results showed that 2D-PCR can accurately detect mouse or human tissues by using PCR and probe sets specific to each species. The results also showed that at least 6 different tissue types could be detected by 2D-PCR. However, no RNA was detected in one of the CHTN samples (Table 15), showing that clinical tissues need to be screened for RNA quality before use. The experimental map of GYS2 and KCNJ1 targets, normalized to HPRT1, showed the specificity of 2D-PCR for tissue-specific mRNA, and also showed a dynamic range of at least 12 cycles of detection across the different tissue types (Figure 30). The results from the autopsy samples showed that no RNA could be recovered from decalcified autopsy samples demonstrating the specificity and cleanliness of 2D-PCR (Figure 31).

**Table 15 – Cts of mouse-specific amplification of a low-abundance gene (HPRT1) in well-controlled FFPE mouse samples that are 4-months old. Three triplicate samples of human breast tissues from the cooperative human tissue network were also used and two showed amplification of human-specific small RNA (RNU48).**

<b>Samples</b>	Mouse Brain			Mouse Liver		
	Mouse Kidney			Mouse Spleen		
	Mouse Lung			Human Breast 1		
	Human Breast 2			Human Breast 3		
<b>Target 1</b>	28.12	28.07	28.43	29.03	28.61	29.38
	28.79	29.75	29.71	28.96	28.43	29.40
	29.83	29.28	29.35	-	-	-
	-	-	-	-	-	-
<b>Target 2</b>	-	-	-	-	-	-
	-	-	-	-	-	-
	-	-	-	29.24	28.81	29.04
	-	-	-	29.32	30.08	29.24

#### 4.3.5 Validation of microarray data using human prostate cancer and normal samples

To validate mRNA expression profiles, a panel of two dozen mRNAs were quantified from a TMA containing 25 human prostate tumor and 25 normal prostate samples. A pathologist verified that the majority of the cores were 100% tumor and graded them on a Gleason scale from about 5 to 9. These samples were at least a decade old but were known to have good mRNA quality. As described in methods, the TMAs were sectioned onto adhesive film, dewaxed, reverse-crosslinked, transferred to a 384-well plate, lysed and the RNA was purified.

A few mRNAs were directly assayed using one-step RT-qPCR. However, to measure the expression of 24 mRNAs in duplicate across many samples required a high-throughput assay. Therefore, using a second recut of tissue, total RNA was prepared and then pre-amplified using an optimized one-step tandem reverse-transcriptase

PCR. A control human RNA dilution series was also pre-amplified. The pre-amplified RNA was then assayed using a 48x48 fluidigm plate and an optimized PCR supermix was developed to improve the detection of templates in the fluidigm system. The expression of each gene in Cts was normalized to the average of expression of four housekeeping genes (B2M, GUS, GAPDH and CYPA) to account for differences in total RNA and degradation from each sample<sup>33, 91, 102</sup>. The results are shown in Figure 28. The linearity and variability of the pre-amplification and the correlation between pre-amplified and directly assayed mRNAs was also determined as described in section 4.6.6.

The results showed the validation of several prostate cancer mRNA profiles, including the significant ( $p < .025$ ) overexpression of AMACR, ALCAM, FOLH1, and TACSTD1, and the under-expression of ANG, CD69, GSTP1, JAK1, CD10, MUC1, SOD2, STAT5B, TIMP3, and VEGF in prostate tumors. AR, VHL, H1F1A, and HPRT1 (a housekeeping gene) were not significantly differentially expressed.

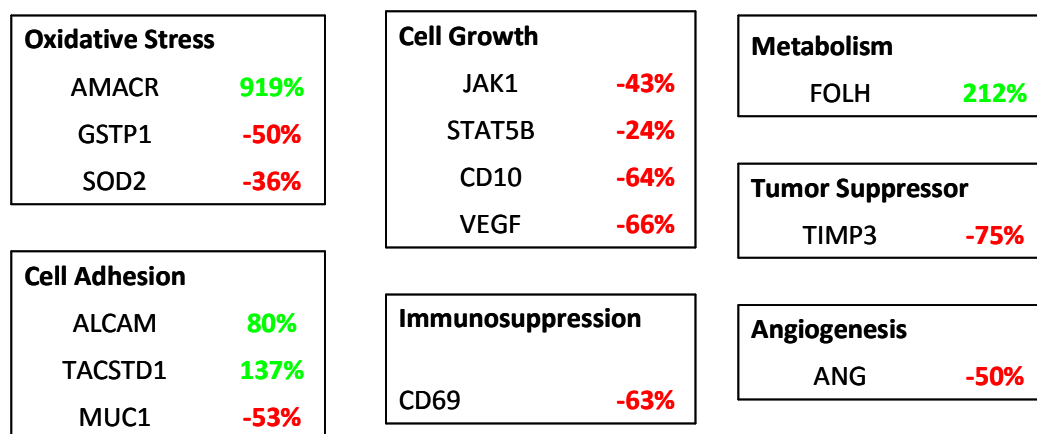


**Figure 28 – Significant differential expression (percent changes determined from Cts,  $p < .025$ ) of 14 genes, each normalized to the average of 4 housekeeping genes in 24 prostate tumor cases versus 18 normal prostates.**

As shown in Section 4.6.6, despite the pre-amplification process, the fluidigm assay was consistent and linear. The Pearson  $R^2$  linearity of the fluidigm assay on tandem RT-qPCR pre-amplified control RNA ranged from 0.9931 to 0.9998 for 21 of the 24 mRNA targets. The remaining 3 probe sets had a poor linearity and were dropped from the study. The average standard deviation of Cts was 0.2.

#### 4.4 Discussion

##### 4.4.1 RNA quality and detection from TMAs

Formalin-fixed paraffin-embedded (FFPE) tissue is the dominant method of fixation in clinics because it allows for high quality histomorphology<sup>39</sup>. However, FFPE was not originally intended for RNA preservation, thus studies have recently optimized FFPE fixation for RNA preservation<sup>41,56</sup>. A TMA consisting of hundreds of samples may represent specimens from numerous hospitals with differing fixation procedures. Samples should be processed in a similar fashion to reduce artifacts due to the fixation method itself<sup>96</sup>, however the use of a housekeeping gene for normalization also allows analysis of samples from different sources<sup>33</sup>.

RNA quality is also highly dependant on sample preparation and age<sup>44</sup>. We showed that sensitive detection of low abundance transcripts and high dynamic range is possible using 2D-PCR and a reverse-crosslinking treatment on prostate samples over a decade old. Some considerations include using the smallest possible amplicon sizes<sup>45</sup>. Furthermore, sample dilution should be avoided since below 20 target copies Poisson effects introduce significant qPCR variations<sup>31</sup>. For mRNA amplification we

used the tandem PCR approach to maximize the concentration of all targets tested. Since most microRNA detection scheme require two-step protocols and a 1:15 fold dilution, we also introduced a new one-step PCR procedure for quantifying microRNA.

#### 4.4.2 Challenges in the application of TMAs to RNA expression analysis

Tissue sample/core heterogeneity and divergence from the intended cell types must be assessed and considered. With some tissues, core loss or "drop out" also results in the loss of cases for analysis as the TMA block is sectioned deeper. Therefore, it is routine practice to stain and visually check every 50th TMA section to ensure that tissue is still present and that the tissue type has not changed. Despite these issues, TMAs provide the best platform today for high-throughput analysis of patient samples.

#### 4.4.3 Potential use for Validation Studies and Clinical Diagnosis and Prognosis

We demonstrated an initial proof of concept for using TMA's and 2D-PCR as a high-throughput sample preparation technique. We also optimized a one-step pre-amplification procedure and use of the Fluidigm assay for the detection of dozens of mRNAs from dozens of prostate samples. The most significant impact of this approach is that it requires only one 10 micron thick tissue section to detect so many mRNAs sensitively. In principle, this approach could be tailored to clinical diagnostic cancer tests that calculate results from less than 96 mRNAs such as the MammaPrint<sup>149-151</sup> or Oncotype DX<sup>91</sup> to increase throughput and sensitivity of

existing workflows. Furthermore, diagnostic tests like MammaPrint and Oncotype DX may depend on the fact that tumor specimens have more RNA than the surrounding normal tissue<sup>92</sup>, which allows the use of simple macrodissection techniques for sample preparation as opposed to microdissection. However, van de Vijver found that several specimens did not have a sufficiently large proportion of tumor cells to use with existing macrodissection workflows and could not be diagnosed<sup>150</sup>. The use of 2D-PCR may allow more patients or multiple smaller tumors from the same patient to be diagnosed because it can use such small volumes of tissue.

In principle, it is possible to use the TMA, 2D-PCR, and Fluidigm approach to study hundreds of genes in hundreds of patient samples (or many tumor regions from a patient) in a single-day. This would decrease the current diagnostic time of about 5 days, and possibly reduce the costs significantly. Furthermore, because the approach is streamlined, the entire RNA preparation aspect could be automated. There are no other workflows that streamline the quantitative molecular analysis of so many genes from so many samples, let alone from archival formalin-fixed specimens. This technique can also be used in principle to detect hundreds of microRNAs by using the ABI MegaPlex pooled microRNA primers and a modified Fluidigm protocol.

## 4.5 Methods

### 4.5.1 Crafting of 384-well format TMAs

Tissue microarrays (shown in Figure 29) were constructed using slight modifications of to standard methods. First, a 384 well format grid (Bio-Rad, 384-well hard-skirted plates) was cut and customized to fit in an aluminum macro-embedding mold (Leica, super metal base molds) approximately 2" x 3" in diameter. The base grid was covered in a thin layer of paraffin (Oxford, paraplast X-tra) and allowed to cool to room temperature. Next, individual TMA cores of various sizes ranging from 0.6 mm to 3.0 mm were extracted from archival tissue blocks and centrally embedded vertically into each hole in the grid. Subsequently, the base mold was completely filled with paraffin, chilled at 4 °C for 15 minutes, removed and sectioned at 5-10 µm thickness using a standard rotary microtome (Leica RM2255).

### 4.5.2 Tissue sectioning and transfer to 2D-PCR Plates

TMA blocks were cut in a microtome onto adhesive films to obtain a uniform thickness tissue section for the transfer step. The film used was Adhesives Research ARCare 7759 film (which was selected as shown in Table 16) was placed adhesive-size against the TMA and pressed with a roller to create consistent contact. The TMA was sectioned at 10 microns thickness, yielding an adhesive bound tissue section. The TMA on the adhesive was then dewaxed in fresh xylene for 60 seconds at room temperature, and then placed in a fume hood for at least 10 minutes to dry. The adhesive containing TMA cores was then aligned over a clear 384-well flat-top PCR plate (KBioscences), which was preloaded with lysis buffer (see next step). This

plate was then placed in a PTC-200 thermocycler in a special compression rig<sup>100</sup> to apply 200 pounds of force and 60 °C to the adhesive for 3 minutes.

#### 4.5.3 Reverse crosslinking treatment for recovering mRNA

After dewaxing, tissues were treated in an un-pressurized steam vessel using double-distilled water for 30 minutes. Without this treatment, no mRNA recovery was possible. Optimization of the reverse-crosslinking treatment is further discussed in supplemental materials (section 4.6.5).

#### 4.5.4 2D-PCR lysis and purification

Each well of the plate was preloaded with 14 µL of ChargeSwitch lysis buffer (Invitrogen ChargeSwitch RNA cell kit) containing 0.2 mg/mL proteinase K and 5 mM DTT. After the adhesive film was sealed, the plate was inverted, placed back into the compression rig under 200 pounds of force, and heated to 60 °C for 30 minutes to lyse the tissue. Alternatively, the procedure was used at 50 °C for 24 hours to increase the RNA yield (for the prostate tumor TMA) approximately 2-4 times. After the lysis, the plate was centrifuged and the adhesive containing residual tissue cores was discarded. A 7 µL solution (containing 0.33 µL ChargeSwitch magnetic beads, 1% acetic acid, and 6.6 µL ChargeSwitch binding buffer) was added to each well. Total RNA was bound to the solid phase of the magnetic beads. The magnetic beads were then concentrated using a magnet, and the wells were subsequently washed twice with ChargeSwitch wash buffers 13 and 14. Samples containing wash 14 were either used directly in PCR reactions or the wash 14 was removed and the total purified RNA on the beads was assayed either directly by one-

step RT-qPCR (section 4.5.5) or indirectly by pre-amplification and Fluidigm qPCR (section 4.5.6).

#### 4.5.5 One-step microRNA or mRNA reverse-transcriptase PCR

To detect microRNA in a single-plex reaction, standard TaqMan microRNA probe sets and RT primers were used with a new protocol. A one-step reverse-transcriptase PCR (AgPath ID, ABI) was prepared according to instructions, and microRNA probes and primers were both diluted 80-fold in the final reaction volume. This dilution works on the majority of TaqMan probes tested, however some probes need to be optimized further. To detect microRNA in multiplex, custom probe sets (see 4.6.8) were also created using different colored fluorophores and diluted to the same concentration (250 nM primers, 125 nM probes, and 3.125 nM RT primers). This one-step reaction was either added to standard 96-well plates, and 1  $\mu$ L of wash 14 containing beads was added to each well. A similar protocol was followed for mRNA. The reproducibility and PCR efficiency was determined for quantifying 6 mRNAs as shown in section 4.6.6.

#### 4.5.6 Tandem mRNA Pre-amplification (to detect up to 100 targets)

Alternatively, the wash 14 buffer from the previous step was removed from the beads, and a pre-amplification mixture was added to the beads, in order to provide the maximum concentration of low-abundance targets for multiplexed detection. The pre-amplification procedure is similar to the one used by Stanley<sup>32</sup>, but was optimized to give higher yields and less bias. One-Step AgPath ID reverse-transcriptase PCR mix was prepared according to the manufacturers instructions, except that twice as

much enzyme mix was used, and TaqMan primer/probe sets (see section 4.6.8) were diluted 450-fold (to 40 nM) for each primer set. 10  $\mu$ L of this reaction mix was added to each well in the 384-well plate. The plate was then thermocycled at 50  $^{\circ}$ C for 60 minutes, 95  $^{\circ}$ C for 15 minutes, and was subjected to 14 cycles of 95  $^{\circ}$ C for 15 seconds and 60  $^{\circ}$ C for 4 minutes. The final product was diluted 20-fold, and 2  $\mu$ L samples were used in standard qPCR reactions in a real-time PCR machine. Alternatively, the templates were diluted only 4-fold for use in the Fluidigm 48x48 assay. The linearity of the combination of pre-amplification of a control human RNA dilutions followed by quantification by qPCR is shown in section 4.6.7.

#### **4.6 Electronic Supplemental Information (ESI)**

##### **4.6.1 TMAs tested**

Tissues originated from wide range of different preservation qualities, including maximum preservation quality from 4-month old mouse samples, high quality surgical prostate and liver samples, medium to low quality cooperative human tissue network samples, and autopsy samples with cores treated by decalcification to serve as worst-case and negative controls.

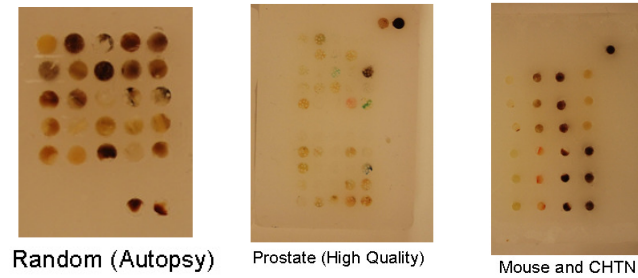


**Figure 29 – Overhead view of TMA blocks embedded in paraffin wax with tissue core sizes ranging from 0.6 mm to 3 mm.**

#### 4.6.2 Selection of adhesive films

Ten adhesive films were tested for their compatibility with the 2D-PCR approach, particularly since xylene is a harsh treatment for most adhesives. The adhesive film needs to be transparent enough to allow visualization of the tissue, it needs to be strong enough to adhere to the TMA block during sectioning and dewaxing, the adhesive needs to survive the xylene treatments without dissolving, and the adhesive needs to maintain its tackiness once the xylene is dried. To determine the best film, sealing was tested on standard 384-well PCR plates which are difficult to seal due to the lip over each well, however a flat-top PCR plate is essential to proper sealing and allows for more adhesives to seal properly. Leaks were detected by sealing ChargeSwitch lysis buffer plus the addition of eosin dye, and imaging for the dye using a Typhoon 1410 flat bed scanner. The best performing film was ARcare 7759, which is an acrylic based adhesive with very high tack; its only disadvantage is that it will begin to disintegrate in xylene after about 10 minutes. A green high-temperature silicone (Caswell PCTAPE2) also performed well, and even survived in xylene for at least 24 hours; however, it loses some tack and is not completely transparent.

McMaster Carr FEP (5804T11) adhesive film also performed well, however polymer backing shrank after xylene treatment.

Table 16 – Selection of adhesive film for TMA sectioning, dewaxing, and transfer to 384-well plates

Material	Clarity	Tack	Sealing	Sealing	Xylene
			Before	After Xylene	Max
ARCare 9020 10mil white acrylic	Opaque	NO	LEAKS	-	-
ARCare 90374 10mil goeey	Translucent	OK	LEAKS	-	Fail
ARCare 7759	Clear	STRONG	OK	OK	5 min
ARSeal 90697	Clear	NO	OK	-	-
Casswell Green Silicone	Green Trans	STRONG	OK	OK	24 hr
Mcmaster Kapton 5mil 2271k73	Orange Trans	OK	OK	LEAKS	24 hr
McMaster Kapton 1mil 2271571	Dark Orange	OK	OK	WEAK	24 hr
McMaster PET 8689k42	Clear	OK	LEAKS	-	-
McMaster PTFE 2208T11	Clear	OK	LEAKS	-	-
McMaster FEP 5805T11	Clear	STRONG	OK	OK	2 min

#### 4.6.3 Validation of mRNA specificity and dynamic range in mouse tissues in a triplex reaction

To validate the specificity and dynamic range of the 2D-PCR technique, high-quality FFPE mouse tissues were amplified using a triplex reaction, which was previously tested for specificity on mouse liver, mouse kidney, and all other tissues (see Chapter 3). The results show the delta-ct (kidney specific and liver specific genes minus housekeeping HPRT1, see 4.6.7 for sequences) demonstrate a wide dynamic range of about 12 delta-CTs for both targets. Indeed, the highest specificity for GYS2 was liver, and for KCNJ1 was kidney, as expected.

	FAM	GYS2
Brain	4.4	5.9
Liver	nd	<b>0.9</b>
Kidney	<b>-2.7</b>	3.9
Spleen	9.3	14.8
Lung	5.3	6.4

**Figure 30 – Demonstration of tissue specific amplification in high-quality mouse FFPE samples using a triplex qPCR reaction from the purified template. Delta Cts are shown. KCNJ1 (FAM) was shown to be highest in Kidney and GYS2 was shown to be highest in Liver as expected. There is also a large dynamic range demonstrated which is owed to the high quality of these samples.**

#### 4.6.4 Worst-Case and negative control tests using autopsy and decalcified tissues

To validate the sensitivity of the 2D-PCR technique, a TMA was made with random autopsy samples, and 4 samples which were heavily decalcified. Tissues were verified independently by a pathologist (JRC). The results show that even in highly degraded autopsy samples, which should not be used for molecular analysis, abundant levels of the small RNA RNU48 were detected in most tissues, with a dynamic range of about 7 Cts. As expected, the 4 decalcified samples did not provide RNA because decalcification (formic acid) hydrolyses nucleic acids. However, one brain specimen did not provide RNA, as the specimen was fixed for a minimum of two weeks.

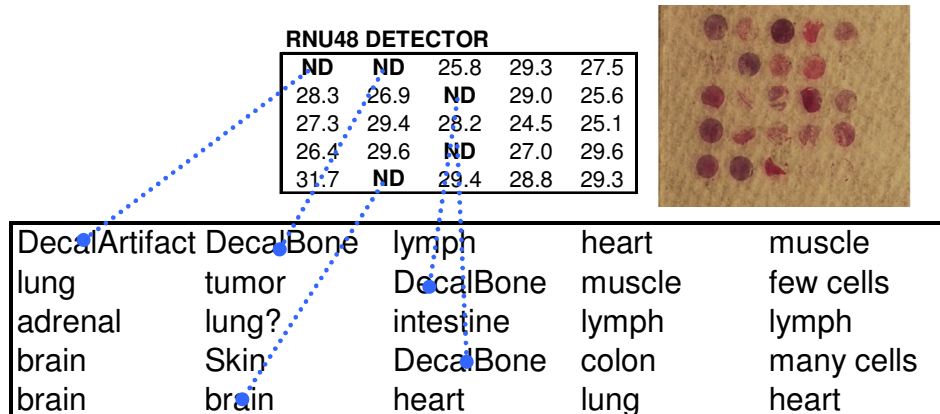


**Figure 31 – Failure to amplify RNU48 in negative tissue controls (decalcified bone).**

#### 4.6.5 Optimization of reverse-crosslinking strategy

We initially observed that without a heating step, no mRNA was recoverable from tissues. Several reverse-crosslinking were tested to identify the best conditions, including dry treatment at 70 °C for 30 minutes, steam treatment for 10, 30, 60, or 120 minutes, and 10 mM tris 1 mM EDTA bath treatments at 60 °C for 30 minutes or 125 °C for 15 minutes using a DAKO pressure vessel. The optimal conditions appeared to be a steam treatment in a non-pressurized vessel for 30 minutes.

Although longer treatments may increase the mRNA yield slightly, there is a risk of hydrolysis of low-abundance targets (results not shown).

#### 4.6.6 Pre-amplification linearity and PCR efficiency (Direct PCR – not Fluidigm)

The one-step mRNA pre-amplification was performed on triplicate samples of human esophagus total RNA (BioChain) containing 1000 ng, 125 ng, 15 ng, or 1.5 ng of RNA. The pre-amplified samples were then quantified using qPCR in singleplex, or multiplex reactions (with B2M) to provide an internal housekeeping reference gene. By determining the PCR efficiency, delta Ct values can be properly adjusted. As shown in Table 17 and Table 18, the results demonstrated good consistency (pearson  $R^2$  ranging from 0.878 to 0.991) for the combination of pre-amplification and quantitative PCR. Furthermore, the results showed that an endogenous (internal multiplexed) reference gene could be included as a normalizer without affecting linearity much ( $R^2$  of .931 to 0.977 with multiplex vs  $R^2$  of 0.98 in singleplex). The results also showed that delta Ct calculations using the internal reference provides

greater consistency ( $R^2$  of .889 to 0.970) than using two reactions ( $R^2$  of 0.773 to 0.954).

Table 17 – PCR efficiency of single-plex amplification after pre-amplification

Target	PCR Efficiency %	$R^2$ Linearity
VHL	77.5	0.88
ALCAM	74.7	0.97
GUS	91.9	0.99
AMACR	90.9	0.91
B2M	83.2	0.98
GAPDH	65.9	0.96

Table 18 – PCR efficiency of B2M as a multiplex endogenous control

Targets	PCR Efficiency %	$R^2$ Linearity
B2M&VHL	61.8	0.95
B2M&AMACR	59.4	0.93
B2M&ALCAM	66.9	0.98

#### 4.6.7 Pre-amplification linearity and PCR efficiency (Fluidigm)

Linearity was also determined by performing a Fluidigm assay on a dilution series of control mRNA subjected to pre-amplification. To perform a Fluidigm assay, 48 Taqman probe sets (24 in duplicate) were mixed with Fluidigm loading buffer and a custom made PCR mix and added to the assay wells of a 48x48 Fluidigm plate. The PCR mix consisted of 30 mM KCl, 25mM Tris, 3mM  $MgCl_2$ , 1mM Dithiothreitol, 0.4mM dNTPs (New England Biolabs) and 0.04 U/ $\mu$ L Dynazyme II DNA polymerase. Then, 48 pre-amplified samples were mixed with Fluidigm loading buffer and added to the sample wells of a 48x48 Fluidigm plate. The samples included 24 prostate tumors, 18 normal prostates, a dilution series of 4 samples, and 2 negative controls.

The results showed linearity above 0.98 for all targets and PCR efficiency above 90% for all targets. Therefore, the Fluidigm assay was more consistent and more efficient than a standard 384-well PCR. As a comparison, the Cts for three genes were compared between a direct one-step RT-qPCR and an indirect pre-amplification and Fluidigm qPCR (see Figure 32). Despite the differences in assay approach, and the fact that the TMA samples used were from 0.5 mm distant recuts, the  $R^2$  reproducibility ranged from 0.57 to 0.72 and is considered to be very good.

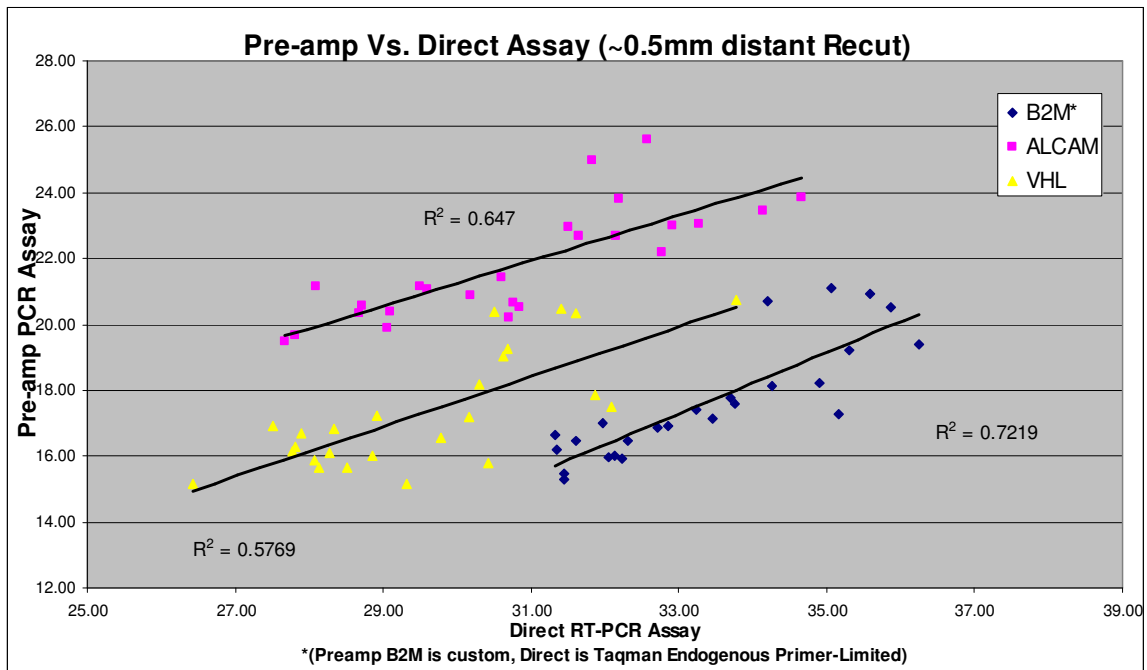


**Figure 32 – Pre-amplification and Fluidigm qPCR vs. direct one-step RT-qPCR assay on 0.5 mm distant serial recuts of the prostate TMA.**

#### 4.6.8 Primer Sets Used

**Table 19 – Custom and Taqman probe sets used**

Primer Sets (Biosearch Technologies)

<b>Target</b>	<b>Forward (5' to 3')</b>	<b>Reverse (5' to 3')</b>
Mouse Liver GYS2	GCCAGACACCTGACACTGA	TCCGTCGTTGGTGGTGATG
Mouse Kidney KCNJ1	GGCGGGAAGACTCTGGTTA	GTGCCAGGAACCAAACCTA
Mouse Control HPRT1	GCAAACCTTTGCTTCCCTGG	ACTTCGAGAGGTCTTTTCACC
<b>Target</b>	<b>Probe (5' to 3')</b>	
Mouse Liver GYS2	5'CalFluorOrange560-TTCCAGACAAATCCACCTAGAGCCC-BHQ1	
Mouse Kidney KCNJ1	5-FAM-AAGCACCGTGGCTGATCTTCCAGA-BHQ1	
Mouse Control HPRT1	5'Quasar670-CAGCCCCAAATGGTTAAGGTTGCAAG-BHQ2	

MicroRNA Primer Sets (Biosearch Technologies)

<b>Target</b>	<b>Forward (5' to 3')</b>	<b>Reverse (5' to 3')</b>
MicroRNA 191	GCCCGCTAGCTTATCAGACTGATG	GTGCAGGGTCCGAGGT
Human RNU48	ATGACCCAGGTAACCTCTGA	GAGCGCTGCGGTGAT
<b>Target</b>	<b>Probe (5' to 3')</b>	
MicroRNA 191	5'Quasar670-CTAGACTGAGCCAGCT-BHQ2	
Human RNU48	5'Quasar670-TGTGTCGCTGATGCC-BHQ2	
<b>Target</b>	<b>RT Primer (5' to 3')</b>	
MicroRNA 191	GCTCAGTCTAGTGCAGGGTCCGAGGTATTCGCACTAGACTGAGCCAGCTG	

Taqman Gene Expression Assays (20X) ordered from Applied Biosystems. B2M, Gus, ACTB, GAPDH, CYPA, AKT, ALCAM, AMACR, ANG, AR, CD69, FOLH1, GSTP1, H1F1A, HPRT, JAK1, CD10, MUC1, SOD2, STAT5B, TACSTD1, TIMP3, VEGF, VHL.

## Chapter 5: Discussion and Possible Future Work

### 5.1 Advantages of 2D-PCR

There are several advantages to 2D-PCR. Overall, the advantages described in this section demonstrate that 2D-PCR is a robust technique, as defined in the aims (section 1.4.1). 2D-PCR was found to be sensitive (detecting low-abundance mRNAs), consistent ( $R^2$  correlation above .70), not prohibitively time-consuming (requiring 4 hours), and widely applicable to different tissue types, fixation methods, and targets (see Table 20).

One advantage of 2D-PCR is that it can process many tissue samples with the low complexity of microdissection methods but allowing for high-throughput and sensitivity. Methods such as LCM and macrodissection ordinarily take days to perform an analysis of a few dozen samples<sup>18, 102</sup>. For example, as shown in Chapter 4, a traditional experimental workflow using macrodissection took 16 hours to study 24 tissue samples, while 2D-PCR took 4 hours and was more sensitive for studying the same 24 tissue samples. 2D-PCR was also able to detect low-abundance transcripts in formalin-fixed specimens more than 10 years old. Therefore 2D-PCR is sensitive and not prohibitively time-consuming.

Another advantage that is unique to 2D-PCR is the ability to lyse all the subdivided regions of tissue in as a single batch process. With LCM or macrodissection, regions

of a slide are isolated and processed in a serial process that takes hours. It is therefore possible that when the last sample is studied, so much time has passed that it is different than the first sample, for example due to rehydration of the tissue. With 2D-PCR, the lysis buffer is inverted onto all tissue subregions at the same time, reducing bias and variability. The overall variability between serial recuts of tissue was characterized in Chapter 4, and 2D-PCR between two different tissue samples on two different days was very good because it had a Pearson R correlation of 0.84. Therefore 2D-PCR is consistent.

Another advantage of 2D-PCR is that it can be applied to a variety of tissue types, tissue preservation methods, and nucleic acid targets, as summarized in Table 20. Therefore 2D-PCR is a technique that is widely applicable as specified in the aims.

<b>Preservation</b>	<b>Tissue</b>	<b>Targets</b>
Frozen	Prostate	DNA
Frozen	Breast	DNA
Frozen	Liver	mRNA
Frozen	Kidney	mRNA
Frozen	Heart	mRNA
Frozen	Brain	mRNA
Ethanol-Fixed	Prostate	mRNA, MicroRNA
Formalin-Fixed	Prostate	mRNA, MicroRNA
Formalin-Fixed	Breast	mRNA, MicroRNA
Formalin-Fixed	Liver	mRNA
Formalin-Fixed	Kidney	mRNA
Formalin-Fixed	Brain	mRNA
Formalin-Fixed	Spleen	mRNA
Formalin-Fixed	Lung	mRNA

Table 20 – Successful application of 2D-PCR to different tissues, fixation methods, and nucleic acid targets.

## 5.2 Limitations of 2D-PCR

There are some limitations to 2D-PCR. 2D-PCR shares the challenge of macrodissection in that it cannot achieve cellular-level resolution. The resolution of 2D-PCR was demonstrated at 1.6 mm for DNA and 3.7 mm for RNA. Although there is utility for mapping nucleic acids at this resolution (see section 1.3.4), there is more potential utility as the resolution decreases. However, as the size of the wells is decreased, the number of wells and pipetting steps increases by a square factor. At some point this may become prohibitive. However, the transfer step of 2D-PCR does not vary with the size of wells and can theoretically be used as-is with different wells sizes to control the size of tissue subregions.

Another disadvantage of 2DPCR is that it is unclear if the technique will work with pancreas tissue because the pancreas contains the highest amount of nucleases. The highly denaturing GITC buffer used by the method can in theory inactivate nucleases in the tissue quickly. However, the tissue transfer and sealing step requires heat-activation, which could cause the nucleases to activate.

Another disadvantage of 2DPCR is shared with the existing methods for mapping genes in tissue – the genes need to be known prior to analysis. There is therefore the following fundamental contradiction: a genetic change needs to be identified before it can be mapped, but a genetic change needs to be mapped to be identified. There are 20,000 genes, and perhaps only dozens or hundreds are relevant for a given condition. Therefore tissues need to be screened by microarray methods to narrow

the selection. The problem with microarray methods is that they require a large amount of tissue and can only characterize differential expression as significant if it is up-regulated or down-regulated by 2-fold. There is no known solution to this problem.

### **5.3 Possible future work**

There are several ways to improve or use the existing 2D-PCR method. These improvements include increasing resolution (miniaturizing the wells), improving handling time, testing new downstream methods, and aiming the technique for clinical diagnostic use.

#### **5.3.1 Miniaturization**

To miniaturize 2D-PCR further, a new method of adding and removing buffers is needed. At some point, perhaps at the level of 1 mm, it will become infeasible to pipette by hand because of the number of wells and limitations of pipette tip size. Even at the scale of 1.6 mm, hundreds of pipetting steps are required. Therefore the use of a robot to improve throughput is desired. Robots already exist that automate pipetting processes in 384-well plates. At smaller scales, non-contact pipetting robots could be used. These robots can confine a beam of fluid to about 100  $\mu\text{m}$  diameter.

#### **5.3.2 Simpler purification surface**

Some minimal care is still needed on the part of the user to ensure that the magnetic beads are not rinsed away during the wash steps of 2D-PCR. To improve the

handling of the sample purification in 384-well polypropylene plates, the plastic surface should be oxidized to produce a ChargeSwitch surface. This surface would replace the ChargeSwitch microbeads and eliminate the need to use a magnet or to wait for the microbeads to be concentrated. To prepare a charge switch surface on the surface of 384-well polypropylene plates, the plastic can be oxidized with potassium permanganate and sulphuric acid to yield a carboxylated (i.e. ChargeSwitch) surface as described in US patent 6914137<sup>53</sup>.

### 5.3.3 Other downstream methods

It is likely that 2D-PCR can be used to detect changes in methylated DNA. This may include a bisulphite modification of the purified DNA followed by qPCR (methylation specific PCR<sup>35</sup>) or an enzymatic treatment that is sensitive to methylated DNA followed by qPCR<sup>36</sup>. Another possible use of 2D-PCR would be to redesign the lysis buffer to recover proteins, carbohydrates, lipids, salts, hormones, or other biological components of interest. 2D-PCR would be used to recover the molecules while maintaining the 2D layout of a tissue sample. Traditional techniques like chromatography could be used to detect specific targets. Another possible downstream technique to use for detecting nucleic acids includes high-throughput detection systems. These include the Nanostring, Fluidigm, Biotrove, and DNA microarray platforms.

Sequencing technologies also have significant potential to increase the number of genes studied sensitively. One such technology is called deep sequencing, and allows

infrequent mutations to be detected. In the context of 2D-PCR, nucleic acids would be purified for use, amplified by PCR, and then used with deep sequencing. A second noteworthy sequencing technique in development is called real-time sequencing using single modified polymerases. This technique has the potential to replace the PCR step currently used in 2D-PCR. All other sequencing technologies are currently not fast or inexpensive enough to be practically used with 2D-PCR.

#### 5.3.4 Speculation on the application of 2D-PCR to clinical diagnostics

2D-PCR could be used in two ways in for medical diagnostics in the near future. For example, the oncoType DX test already uses macrodissection and large sample volumes as described in section 1.3.4. Therefore it is possible to use 2D-PCR to improve the processing time and handling ease of the oncoType DX test. The test costs \$4000, a price that could be reduced using 2D-PCR if labor and consumable cost are major factors. Another way 2D-PCR could improve the diagnostic test is by reducing the amount of tissue needed to run diagnostic tests. This is described in the discussion of Chapter 4.

A second way 2D-PCR could be used is to examine tumor margins after a tumor resection. Normally, the tumor margins are examined by a pathologist to ensure that there are no tumor cells left in the patient after surgery. However, it is possible that a few cells are present and the pathologist misses the tumor cells by visual inspection, or it is possible that there are cells that look normal but harbor genetic mutations that could lead to cancerous recurrence, and more tissue may need to be removed. In

order to perform such a diagnostic test, it would need to give results within an hour so it can be done conveniently during surgery. This is possible in theory as 2D-PCR is amenable to robotic automation for the sample preparation aspect, and others have demonstrated micro-scale PCR systems that can quantify nucleic acids in less than 10 minutes. The speed of 2D-PCR could therefore be improved, whereas the other method methods have no streamlined protocol that could be hastened (macrodissection, LCM) or have no potential for results in less than an hour (ISH).

#### 5.3.5 Immediate applications of 2D-PCR

2D-PCR as presented in this thesis can be applied to improve the throughput of two specific molecular biology studies. Human brain samples may be mapped by 2D-PCR to improve the voxelation method<sup>7, 18</sup>, which is based on macrodissection. 2D-PCR could also prepare mouse and rat brains RNA for “high-resolution voxelation”<sup>18</sup> by using a 1534-well plate, but the qPCR would need to be performed in another device because there are no 1534-well plate qPCR instruments. Another useful application would be to study tumor samples and compare against normal tissues using a tissue microarray format – providing a high-throughput tool for gene validation as demonstrated in Chapter 4.

Another immediate application would be to improve the throughput of LCM and macrodissection sample processing. Typically, LCM samples are placed on a cap, and processed using a serial workflow for each sample. The single-well lysis and purification protocol developed for 2D-PCR could be used to purify templates from

LCM samples in a batch process, and may improve the nucleic acid recovery because of losses in standard LCM purification columns<sup>87, 88</sup>.

## Chapter 6: Conclusion and Technical Developments

A new approach for detecting or quantifying nucleic acids in tissues called 2D-PCR has been developed. 2D-PCR preserves the 2D layout of a tissue sample by first dividing the tissue into subregions. 2D-PCR was applied to a variety of nucleic acid targets in different tissue types, which were preserved using a variety of methods, as summarized in Table 20. DNA was extracted, amplified by PCR, and detected using DNA-specific dyes. RNA was extracted, purified, and quantified using qPCR.

The new knowledge contributed by this thesis includes three 2D-PCR protocols and the technical developments that enabled each of these protocols. The protocols were: 1) detecting one DNA target in a frozen tissue section, 2) quantifying up to three mRNAs in a frozen tissue section, and 3) quantifying up to 24 mRNAs in a formalin-fixed tissue microarray section. These developments were used successfully to overcome a series of difficult issues, as described in Chapter 7.

The first 2D-PCR protocol divided a frozen tissue section at a resolution of a 1.6 mm into an aluminum multi-well plate. DNA in each well was extracted using an optimized proteinase K buffer, the extracted DNA was amplified by PCR, and the amplified DNA was detected using a DNA-specific dye. To enable this 2D-PCR protocol, it was determined that the tissue could be stained by eosin dye to visualize the tissue without inhibiting DNA extraction or PCR. The method of transferring

tissue sections onto an adhesive film for subsequent handling and sealing was developed. Also, a compression rig providing 150 psi of pressure was built to press this tissue into the multi-well plate to in one step, subdividing the entire tissue section it and loading it into the wells for subsequent processing. In order to extract the DNA without affecting the PCR step, it was determined that proteinase K could extract DNA without buffers, and that the proteinase K could be inactivated and dried using high temperature. In order to keep DNA from spreading between wells, a method of using 2% LMP agarose added to the solution in the wells was developed that immobilized the DNA, yet did not inhibit DNA extraction or PCR. In order to prevent the inhibition of PCR due to the presence of aluminum, 0.1% BSA was identified as a PCR enabling additive. In order to prevent the heat of thermocycling during PCR from evaporating the reagents, the adhesive tape was utilized as a sealing film, applied using the compression rig. A reversible sealing film was selected to allow access to the amplified DNA for staining.

The second 2D-PCR protocol divided a frozen tissue into part of a 384-well PCR plate with a well size of 3.7 mm. To enable this protocol, a novel single-well tissue lysis and nucleic acid purification protocol was developed based on the ChargeSwitch proteinase K lysis and magnetic bead purification. This single-well protocol was then modified to allow the use of GITC lysis buffer, which fully solubilizes frozen tissue samples, preventing clogging, and providing more uniform nucleic acid recovery. The single-well buffer pH was also optimized to provide maximum nucleic acid

recovery. In order to visualize tissues during the transfer without affecting qPCR, many tissue-specific stains were tested.

The third 2D-PCR protocol divided a formalin-fixed tissue microarray into part of a 384-well PCR plate with a well size of 3.7 mm. A transfer film was rigorously selected in order to section formalin-fixed tissues, dewax them, and transfer and seal the section into a 384-well plate. A reverse-crosslinking step was optimized for recovering mRNA from formalin-fixed specimens. A one-step microRNA RT-qPCR procedure was also developed, eliminating the dilution step of traditional two-step processes to allow the detection of low-abundance microRNAs sensitively. Finally, a one-step tandem RT-PCR was optimized for amplifying 24 targets in multiplex, and a matching qPCR reagent was developed for detecting the genes efficiently using the Fluidigm RT-qPCR system.

## Chapter 7: Intellectual Contributions

Many challenges or constraints were overcome in order to produce the results shown in chapters 2-4 and to prove the concept behind 2D-PCR. These intellectual contributions/technical developments are explained below.

### 7.1 Contribution 1 – Cutting tissues into subregions

Before 2D-PCR, the only methods for cutting tissues into subregions were laser cutting methods and voxelation, which uses a garlic slicer like device to cut thick tissues. No methods provided a way to subdivide thin tissue sections and maintain the layout of the sample. 2D-PCR solved this problem using a 4-step protocol. 1) tissues were sectioned and placed on a heat activated sealing film. Heat-activated sealing film was chosen after significant trial and error. 2) Once on the sealing film, the tissue was immediately dried to prevent movement or degradation of the tissue. 3) The dried tissue was aligned over a grid of wells. 4) The tissue was then forced into the grid using a compression and heating apparatus. This step cut the tissue into subregions. After much trial and error it was also discovered that the grid of wells needs to have a flat top to create a good seal.

### 7.2 Contribution 2 – Lysis of frozen tissue for DNA recovery

No methods existed before 2D-PCR for lysing DNA from frozen samples in a single-well method. It was discovered that proteinase K is a robust enough enzyme to extract nucleic acids from frozen-dried tissues without any buffers. As a result, the

proteinase K could be heat-inactivated and the buffer could be dried and resuspended with PCR reagents for a streamlined solution.

Another problem was that the PCR and proteinase K steps required high-temperature incubations that would cause the reagents to evaporate. Therefore, a sealing film and compression strategy was developed to prevent the loss of reagents due to evaporation. However, the sealing film needs to be removed to allow the dehydration of proteinase K, which allows PCR reagents to be added in a future step. Therefore sealing film was selected that could be reversibly sealed. Another problem with seal remove was that fluid would wick between wells by surface tension when the sealing film was removed. Therefore it was determined that 2% agarose could be added to prevent the diffusion of DNA. During the proteinase K step, the heat of the incubation melts and distributes the agarose throughout the well.

### **7.3 Contribution 3 – Visualization of tissue**

2D-PCR needed a method to determine where a tissue section was placed, i.e., to figure out which wells had tissue transferred into them. Two dyes (eosin and acid fuchsin red) were found to stain tissues pink so that the tissue could be visualized, and these dyes did not inhibit PCR. However, eosin is much more fluorescent than fuchsin red, so fuchsin red is better for qPCR and better overall for use with 2D-PCR.

### **7.4 Contribution 4 – Lysis and purification of RNA from frozen samples**

No methods existed before 2D-PCR for lysing frozen tissues and purifying RNA in a single-tube procedure, as described in detail in section 8.2. The major challenges

were that RNA quality will degrade if the tissue is not lysed completely, and tissue fragments that are not lysed completely will stick to and clog purification surfaces. The major breakthrough was identifying the right amount of water and acid to add to GITC-based buffers so that tissue samples could be lysed completely, but still allow mRNA purification on magnetic beads. In effect, tissues are completely liquefied by 2D-PCR, and then the RNA is purified from the lysates in a single-tube procedure, allowing the layout of a sample to be maintained. No GITC based buffers had previously been reported for use with ChargeSwitch beads.

#### **7.5 Contribution 5 – Dewax formalin-fixed tissues on adhesive films**

No methods existed before 2D-PCR for sectioning formalin-fixed and paraffin embedded tissues onto adhesive films, treating the films with xylene, and maintaining the adhesive properties of the film. Ten films were tested before one was found that was ideal for dewaxing tissues in xylene but that also retained enough tack to prevent fluid loss from the wells of a 384-well plate. It was also crucial to use flat-top PCR plates to maintain a consistent seal.

#### **7.6 Contribution 6 – Lysis of formalin-fixed tissue for RNA recovery**

Another key development for 2D-PCR of formalin-fixed samples was the optimization of a reverse crosslinking step for tissues on adhesive films. Placing the samples in a steamer for 30 minutes provided the ideal balance between RNA recovery and RNA loss. Previously published techniques that suggested placing tissue in heated amine baths did not work as consistently as the steaming method.

Without reverse cross-linking, it was impossible to recover mRNA from a formalin-fixed sample.

### **7.7 Contribution 7 – Studying microRNA without dilution**

Existing methods for microRNA amplification by PCR required two steps. The two-step procedure dilutes microRNA by a factor of 15. For low-abundance targets, this can make the difference between inconsistent and consistent detection in a qPCR reaction (see Poisson effect 1.2.3.3). Therefore a new procedure was developed to perform microRNA amplification in a one-step process so that template was not diluted. The optimal technique was experimentally determined so that microRNA could be detected without false positives.

### **7.8 Contribution 8 – Studying nucleic acids in multiplex**

In order to maximize the throughput from small volumes of sample, a multiplexing method was tested and optimized. Tandem PCR was used to pre-amplify 28 mRNA targets at the same time. This approach maintains the concentration of mRNA in a sample to reduce the variability caused by dilute templates. The tandem PCR was optimized to provide maximum recovery by extending reaction times and increasing the amount of reverse transcriptase in the reaction. After tandem PCR, a Fluidigm chip was used to study many samples and many genes in a single day. However, the PCR reagents recommended by Fluidigm demonstrated PCR inhibition due to weak efficiency. Therefore a novel PCR mixture was optimized for use with the pre-amplified samples to allow for efficient PCR.

## Chapter 8: Appendices

### 8.1 2D-PCR Publications and presentations

1. M. Armani, J. Rodriguez-Canales, J. Gillespie, M. Tangrea, H. Erickson, M. R. Emmert-Buck, B. Shapiro, and E. Smela, "2D-PCR: A method of mapping DNA in tissue sections," **Lab Chip**, 9(24), 3526 - 3534 (2009).
2. Michael Armani, Mike Emmert-Buck, Elisabeth Smela, Ben Shapiro, Mike Tangrea, Jaime Rodriguez-Canales, Rodrigo Chuaqui "Amplification Platform and Methods of Use Thereof," submitted to the **USPTO** on 1/30/10; This patent is currently undergoing licensing negotiations with 2D-BIO LLC.
3. Michael Armani - Podium Presentation, "Mapping DNA in Tissues: A Spatially Resolved Array Technique with Integrated Tissue Transfer, DNA Extraction, Amplification and Detection," **Lab-on-a-Chip World Congress**, San Francisco, USA 6th & 7th August, 2009. Chaired new technologies session.
4. Michael Armani - Podium Presentation, **NIH Graduate Partnership Program Retreat**, Flintstone, MD 16th & 17th July, 2009.
5. Michael Armani - Podium Presentation, **UMMC Hormone Responsive Cancers Program**, Baltimore, MD 3rd April, 2009
6. Michael Armani - Poster Presentation, **UMD Bioengineering Fischell Festival**, College Park, MD 21st April, 2009.
7. Michael Armani - Poster Presentation, Tenth Principal Investigator's (PI) **Innovative Molecular Analysis Technologies Program**, Bethesda MD 7<sup>th</sup> to 9<sup>th</sup> October, 2009.
8. Michael Armani - Awarded NIH technology transfer awards in 2009 and 2010.

Manuscripts drafted:

9. M. Armani, M. Tangrea, B. Shapiro, E. Smela, M. R. Emmert-Buck. "Quantifying mRNA across a Histological Section with 2D-PCR" **to be submitted to Nucleic Acids Research, Methods Online.**
10. M. Armani, M. Tangrea, B. Yang, A. Rosenberg, K. Ylaya, J. Martinez, J. Rodriguez-Canales, B. Shapiro, E. Smela, M.R. Emmert-Buck, and S. Hewitt. "Quantitative Validation of RNA Expression Profiles in Tissue Microarrays" **to be submitted to Nature Methods.**

## 8.2 Single-well lysis & purification compared to existing methods

In this section, the single-well RNA lysis and purification workflow used in 2D-PCR is compared with 4 common commercially available kit based methods. These commercial kits are based on the methods described in section 1.2.5. This section assumes all methods start with a tissue section scrape. In summary, all of the available techniques require at least 3 tubes for lysis, but the 2D-PCR lysis and purification method is a novel approach to purifying template in a single well/tube.

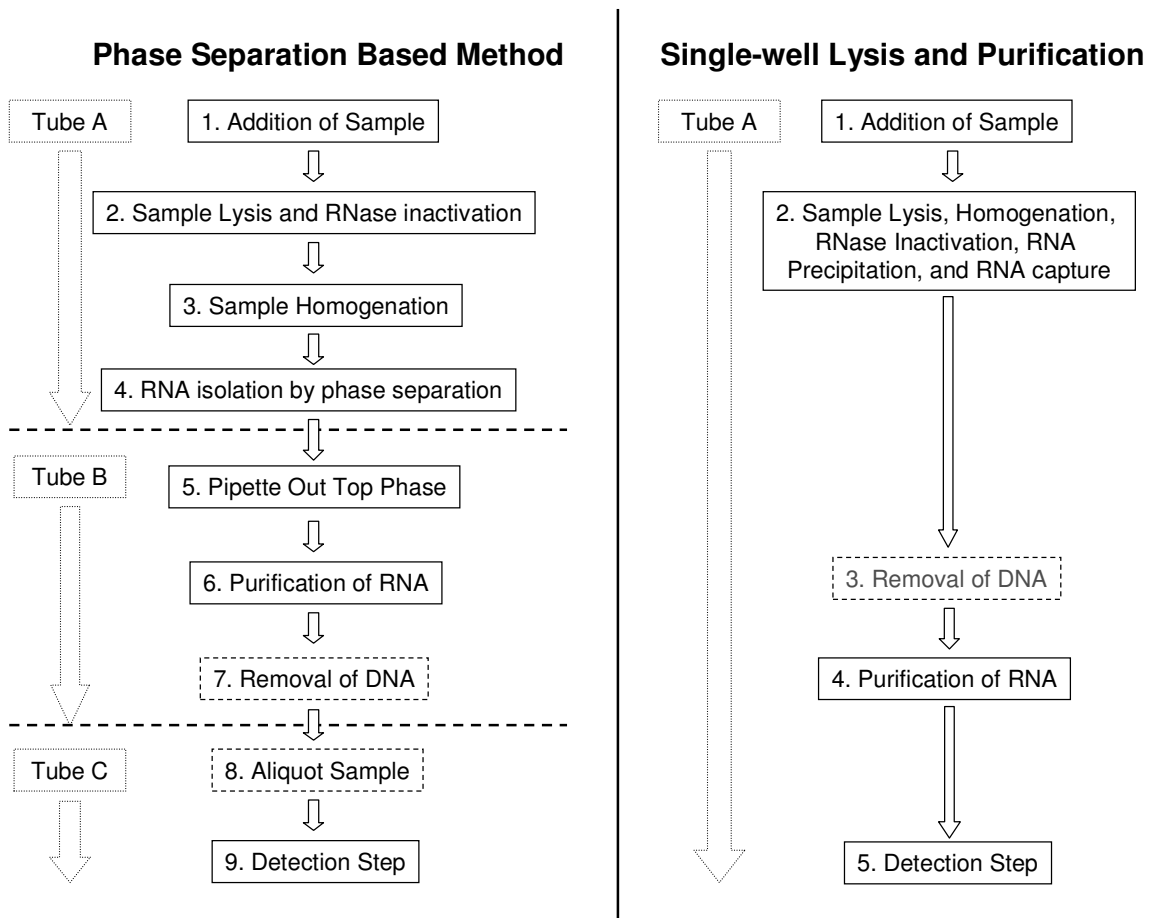


Figure 33 – Comparison between Invitrogen Trizol, based on the Chomzinski method, and 2D-PCR's single-well lysis and purification method.

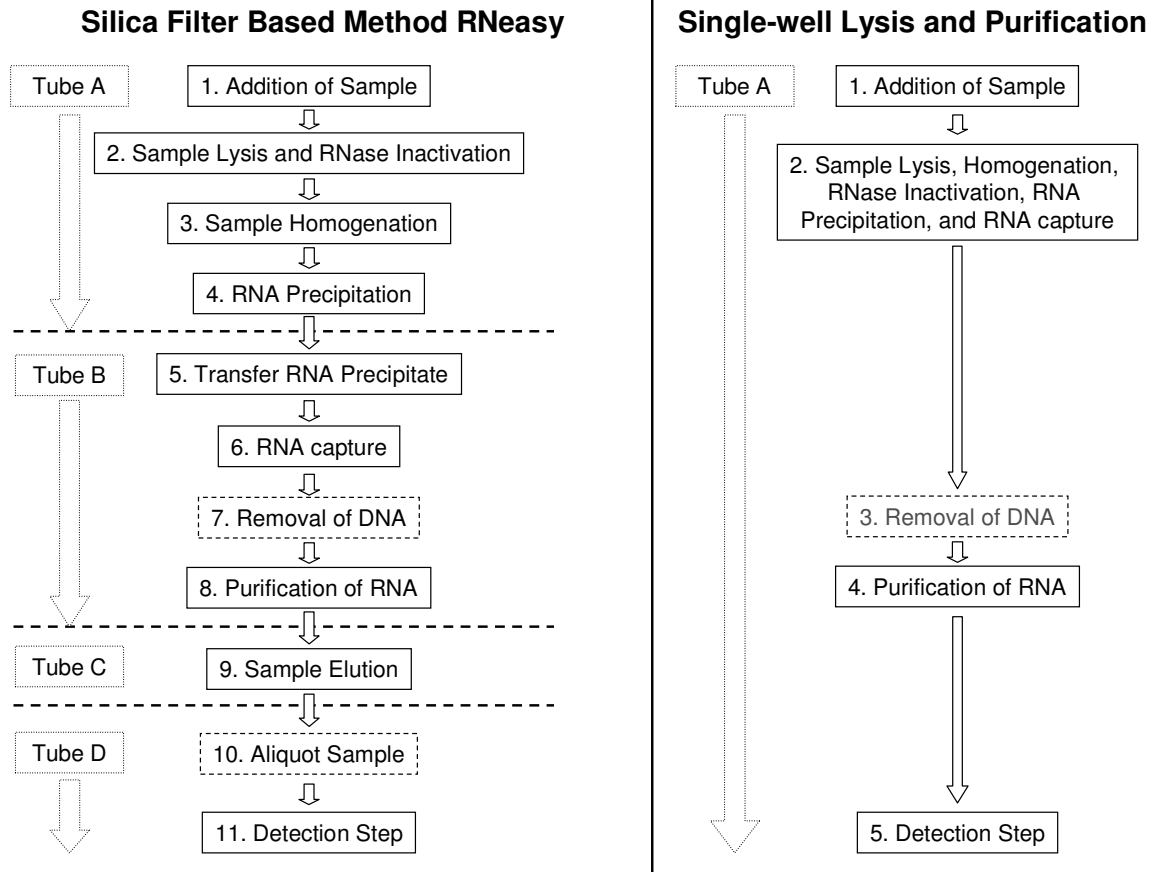


Figure 34 – Comparison between Qiagen RNeasy, based on the GITC lysis and silica column purification methods, and 2D-PCR’s single-well lysis and purification method.

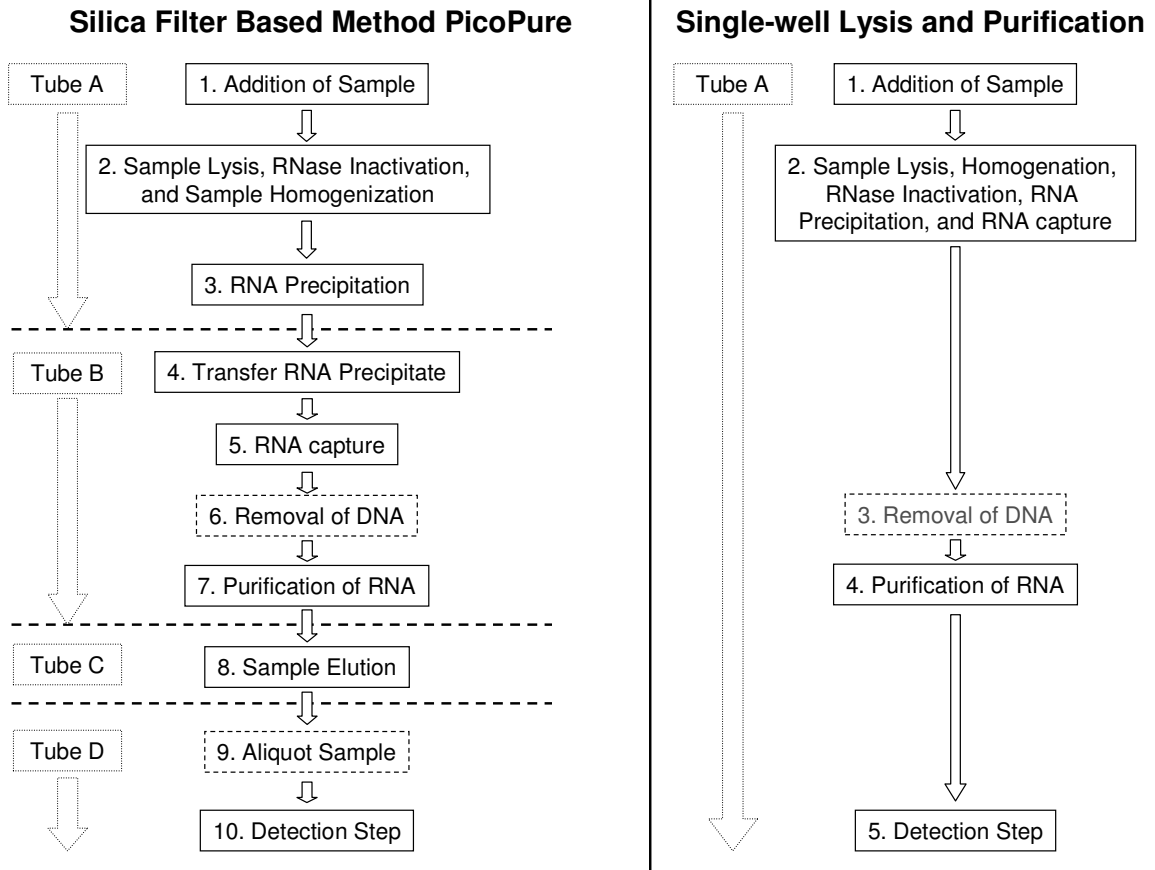


Figure 35 – Comparison between PicoPure RNA extraction kit, based on the GITC lysis and silica column purification methods, and 2D-PCR’s single-well lysis and purification method.

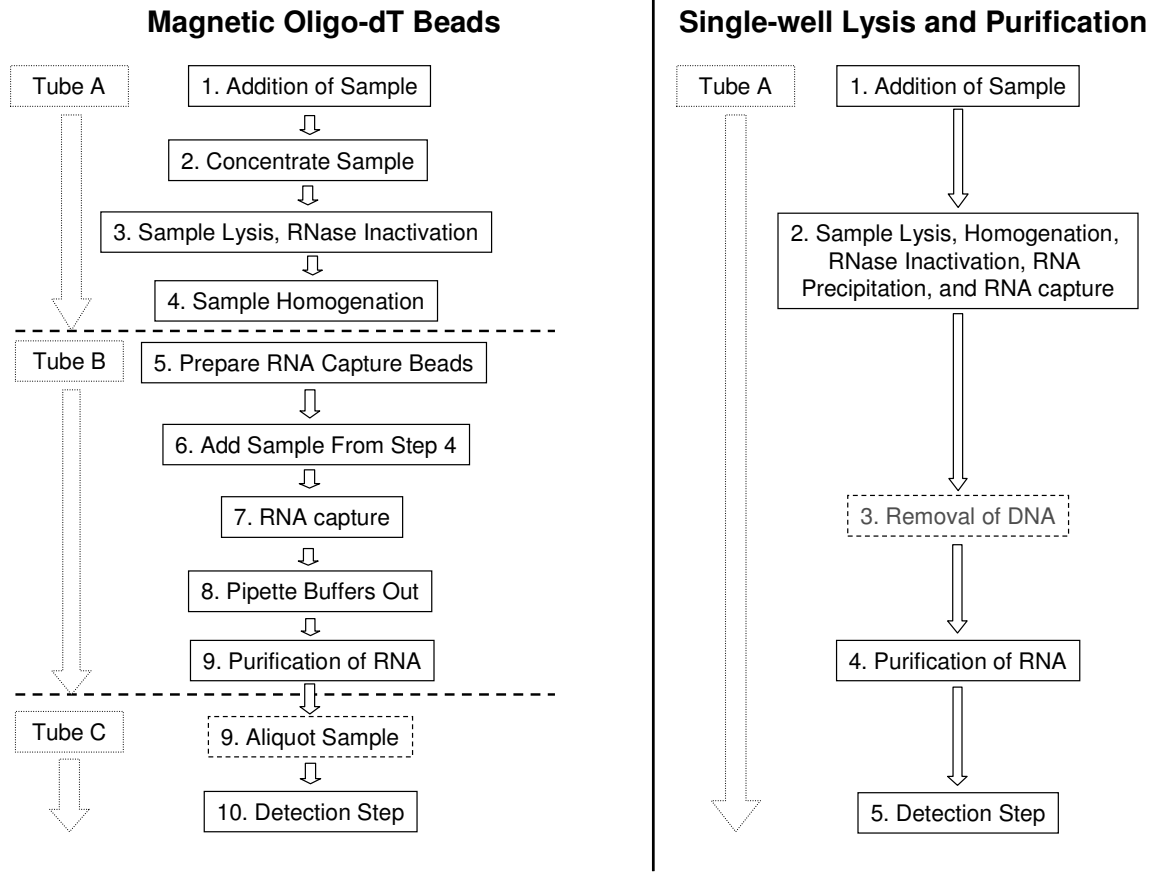


Figure 36 – Comparison between Invitrogen Dynabeads magnetic bead purification kit, based on the lithium chloride based lysis and oligo-dT magnetic bead purification methods, and 2D-PCR’s single-well lysis and purification method.

## Chapter 9: Bibliography

1. M. Clamp, B. Fry, M. Kamal, X. Xie, J. Cuff, et al., *Distinguishing protein-coding and noncoding genes in the human genome*. **P. Natl. Acad. Sci. USA**, 2007, 104, 19428-19433.
2. S. Griffiths-Jones, H. K. Saini, S. van-Dongen and A. J. Enright, *miRBase: Tools for microRNA genomics*. **Nucleic Acids Res.**, 2008, 36, D154-158.
3. M. Schena, D. Shalon, R. W. Davis and P. O. Brown, *Quantitative monitoring of gene-expression patterns with a complementary-DNA microarray*. **Science**, 1995, 270, 467-470.
4. J. R. Mora and R. C. Getts, *High-sensitivity detection methods for low-abundance RNA species: Applications for functional genomics research*. **Exp. Rev. Mol. Diagn.**, 2007, 7, 775-785.
5. C. Chuong and M. K. Richardson, *Pattern formation today*. **Int. J. Dev. Biol.**, 2009, 53, 653-658.
6. R. P. Singh and J. S. Desmond, *Genome scale mapping of brain gene expression*. **Biol. Psychiatry**, 2003, 53, 1069-1074.
7. V. M. Brown, A. Ossadtchi, A. H. Khan, S. R. Cherry, R. M. Leahy, et al., *High-throughput imaging of brain gene expression*. **Genome Res.**, 2002, 12, 244-254.
8. J. Rodriguez-Canales, J. C. Hanson, M. A. Tangrea, H. S. Erickson, P. S. Albert, et al., *Identification of a unique epigenetic sub-microenvironment in prostate cancer*. **J. Pathol.**, 2007, 211, 410-419.
9. W. P. Kloosterman, E. Wienholds, E. D. Bruijn, S. Kauppinen and R. N. H. Plasterk, *In situ detection of miRNAs in animal embryos using LNA-modified oligonucleotide probes*. **Nat. Meth.**, 2006, 3, 27-29.
10. M. Giannakis, T. S. Stappenbeck, J. C. Mills, D. G. Leip, M. Lovett, et al., *Molecular properties of adult mouse gastric and intestinal epithelial progenitors in their niches*. **J. Biol. Chem.**, 2006, 281, 11292-11300.
11. J. O. Bioshop, J. G. Morton, M. Rosbash and M. Richardson, *Three abundance classes in HeLa cell messenger RNA*. **Nature**, 1974, 250, 199-204.
12. D. J. Bertioli, U. H. Schlichter, s. M. J. Adam, P. R. Burrows, H. H. Steinbiss, et al., *An analysis of differential display shows a strong bias towards high copy number mRNAs*. **Nucleic Acids Res.**, 1995, 11, 4520-4523.
13. G. J. Nuovo, *PCR in-situ hybridization*, Methods in Molecular Biology, ed. K. H. O. Choo, Humana Press Totowa, NJ, 1994, pp. 223-241.
14. A. A. Long and P. Komminoth, *In situ PCR*, Methods In Molecular Biology, ed. J. R. Gosden, Humana Press Inc., Totowa, NJ, 1996.
15. J. J. O'Leary, R. Chetty, A. K. Graham and J. O. D. McGee, *In situ PCR: Pathologist's dream or nightmare?* **J. Pathol.**, 1996, 178, 11-20.
16. J. M. Levisky and R. H. Singer, *Fluorescence in situ hybridization: past, present and future*. **J. Cell Sci.**, 2003, 116, 2833-2838.
17. R. A. Hubbard, *Human papillomavirus testing methods*. **Arch. Pathol. Lab. Med.**, 2003, 127, 940-945.

18. R. P. Singh, V. M. Brown, A. Chaudhari, A. H. Khan, A. Ossadtchi, et al., *High-resolution voxelation mapping of human and rodent brain gene expression*. **J. Neurosci. Methods**, 2003 30, 93-101.
19. K. Mullis, F. Faloona, S. Scharf, R. Saiki, G. Horn, et al., *Specific enzymatic amplification of DNA in-vitro - The polymerase chain-reaction*. **Cold Spring Harb. Sym.**, 1986, 51, 263-273.
20. J. M. Ruijter, C. Ramakers, W. M. Hoogaars, Y. Karlen, O. Bakker, et al., *Amplification efficiency: Linking baseline and bias in the analysis of quantitative PCR data*. **Nucleic Acids Res.**, 2009, 37, e45.
21. O. Henegariu, *PCR and multiplex PCR: guide and troubleshooting*, <http://info.med.yale.edu/genetics/ward/tavi/PCR.html>, 2010.
22. O. Henegariu, N. A. Heerema, S. R. Dlouhy, G. H. Vance and P. H. Vogt, *Multiplex PCR: critical parameters and step-by-step protocol*. **BioTechniques**, 1997, 23, 504-511.
23. S. Das, S. C. Mohapatra and J. T. Hsu, *Studies on primer-dimer formation in polymerase chain reaction (PCR)*. **Biotechnol. Tech.**, 1999, 13, 643-646.
24. R. Higuchi, C. Fockler, G. Dollinger and R. Watson, *Kinetic PCR analysis - Real-time monitoring of DNA amplification reactions*. **Bio-Technol.**, 1993, 11, 1026-1030.
25. V. V. Didenko, *DNA probes using fluorescence resonance energy transfer (FRET): designs and applications*. **BioTechniques**, 2001, 31, 1106-1121.
26. A. Larionov, A. Krause and W. Miller, *A standard curve based method for relative real time PCR data processing*. **BMC Bioinformatics**, 2005, 6, 62.
27. W. Liu and D. A. Saint, *Validation of a quantitative method for real time PCR kinetics*. **Biochem. Bioph. Res. Co.**, 2002, 294, 347-353.
28. S. N. Peirson, J. N. Butler and R. G. Foster, *Experimental validation of novel and conventional approaches to quantitative real-time PCR data analysis*. **Nucleic Acids Res.**, 2003, 2003, 14.
29. R. G. Rutledge and C. Cote, *Mathematics of quantitative kinetic PCR and the application of standard curves*. **Nucleic Acids Res.**, 2003, 31, e93.
30. M. J. Wacker and M. P. Goddard, *Analysis of one-step and two-step real-time RT-PCR using SuperScript III*. **J. Biomol. Tech**, 2005, 16, 266-271.
31. A. Ståhlberg, N. Zoric, P. Aman and M. Kubista, *Quantitative real-time PCR for cancer detection: the lymphoma case*. **Exp. Rev. Mol. Diagn.**, 2005, 5, 221-230.
32. K. K. Stanley and E. Szewczuk, *Multiplexed tandem PCR: Gene profiling from small amounts of RNA using SYBR green detection*. **Nucleic Acids Res.**, 2005, 33, e180.
33. M. Cronin, M. Pho, D. Dutta, J. C. Stephans, S. Shak, et al., *Measurement of gene expression in archival paraffin-embedded tissues*. **Am. J. Pathol.**, 2004, 164, 35-42.
34. J. Li, P. Smyth, S. Cahill, K. Denning, R. Flavin, et al., *Improved RNA quality and TaqMan® pre-amplification method (PreAmp) to enhance expression analysis from formalin fixed paraffin embedded (FFPE) materials*. **BMC Biotechnol.**, 2008, 6, 10.

35. J. G. Herman, J. R. Graff, S. Myohanen, B. D. Nelkin and S. B. Baylin, *Methylation-specific PCR: A novel PCR assay for methylation status of CpG islands*. **P. Natl. Acad. Sci. USA**, 1996, 93, 9821-9826.
36. D. S. Millar, K. K. Ow, C. L. Paul, P. J. Russell, P. L. Molloy, et al., *Detailed methylation analysis of the glutathione S-transferase p (GSTP1) gene in prostate cancer*. **Oncogene**, 1999, 18, 1313-1324.
37. E. Eiseman, G. Bloom, J. Brower, N. Clancy and S. S. Olmsted, *Case study of existing human tissue repositories: "best practices" for a biospecimen resource for the genomic and proteomic era*, RAND, Santa Monica, CA, 2003.
38. J. W. Gillespie, C. J. Best, V. E. Bichsel, K. A. Cole, S. F. Greenhut, et al., *Evaluation of non-formalin tissue fixation for molecular profiling studies*. **Am. J. Pathol.** 2002, 160, 449-457.
39. C. H. Fox, F. B. Johnson, J. Whiting and P. P. Roller, *Formaldehyde fixation*. **J. Histochem. Cytochem.**, 1985, 33, 845-853.
40. M. van der Ploeg, *Cytochemical nucleic acid research during the twentieth century*. **Eur. J. Histochem.**, 2000, 44, 7-42.
41. J. Y. Chung, T. Braunschweig, R. Williams, N. Guerrero, K. M. Hoffmann, et al., *Factors in tissue handling and processing that impact RNA obtained from formalin-fixed, paraffin-embedded tissue*. **J. Histochem. Cytochem.**, 2008, 56, 1033-1042.
42. N. Masuda, T. Ohnishi, S. Kawamoto, M. Monden and K. Okubo, *Analysis of chemical modification of RNA from formalin-fixed samples and optimization of molecular biology applications for such samples*. **Nucleic Acids Res.**, 1999, 27, 4436-4443.
43. J. M. Chirgwin, A. E. Przybyla, R. J. MacDonald and W. J. Rutter, *Isolation of biologically active ribonucleic acid from sources enriched in ribonuclease*. **Biochemistry**, 1979, 18, 5294-5299.
44. S. Ahlfen, A. Missel, K. Bendrat and M. Schlumpberger, *Determinants of RNA quality from FFPE samples*. **PLOS One**, 2001, 2, e1261.
45. T. E. Godfrey, S. H. Kim, M. Chavira, D. W. Ruff, R. S. Warren, et al., *Quantitative mRNA expression analysis from formalin-fixed, paraffin-embedded tissues using 5' nuclease quantitative reverse transcription-polymerase chain reaction*. **J. Mol. Diagn.**, 2000, 2, 84-91.
46. P. Chomczynski and N. Sacchi, *Single-step method of RNA isolation by acid guanidinium thiocyanate-phenol-chloroform extraction*. **Anal. Biochem.**, 1987, 162, 156-159.
47. R. Boom, C. J. A. Sol, M. M. M. Salimans, C. L. Jansen, P. M. E. Wertheim-Van Dillen, et al., *Rapid and simple method for purification of nucleic acids*. **J. Clin. Microbiol.**, 1990, 28, 495-503.
48. Invitrogen, *TRIzol<sup>(R)</sup> Reagent Manual*. 5-12-07.
49. K. A. Melzaka, C. S. Sherwooda, R. F. B. Turnerb and C. A. Haynes, *Driving forces for DNA adsorption to silica in perchlorate solutions* **J. Colloid Int. Sci.**, 1996, 181, 635-644.
50. E. Hornes and L. Korsnes, *Magnetic DNA hybridization properties of oligonucleotide probes attached to superparamagnetic beads and their use in*

- the isolation of poly(A) mRNA from eukaryotic cells.* **GATA**, 1990, 7, 145-150.
51. K. S. Jakobsen, E. Breivoid and E. Hornes, *Purification of mRNA Directly from crude plant tissues in 15 minutes using magnetic oligo dT microspheres.* **Nucleic Acids Res.**, 1990, 18, 3669-.
  52. Invitrogen, *Handbook Dynabeads<sup>(R)</sup> mRNA DIRECT<sup>TM</sup> Micro Kit Rev. no 003.* 2007.
  53. M. J. Baker, *Isolation of nucleic acids U.S. Patent #6,914,137*, 2005, United States, DNA Research Innovations Limited.
  54. H. Hilz, U. Wieggers and P. Adamietz, *Stimulation of proteinase K action by denaturing agents : Application to the isolation of nucleic acids and the degradation of 'masked' proteins.* **Eur. J. Biochem.**, 1975, 56, 103-108.
  55. S. Bonin, F. Hlubek, J. Benhattar, C. Denkert, M. Dietel, et al., *Multicentre validation study of nucleic acids extraction from FFPE tissues.* **Virchows Arch.**, 2010, 457, 309-317.
  56. F. Lewis, N. J. Maughan, V. Smith, K. Hillan and P. Quirke, *Unlocking the archive – Gene expression in paraffin-embedded tissue.* **J. Pathol.**, 2001, 195, 66-71.
  57. T. Korbler, M. Grskovic, M. Dominis and M. Anticua, *A simple method for RNA isolation from formalin-fixed and paraffin-embedded lymphatic tissues.* **Exp. Mol. Pathol.**, 2003, 74, 336-340.
  58. S. R. Shi, R. J. Cote, L. Wu, C. Liu, R. Datar, et al., *DNA extraction from archival formalin-fixed, paraffin-embedded tissue sections based on the antigen retrieval principle: Heating under the Influence of pH.* **J. Histochem. Cytochem.**, 2002, 59, 1005-1011.
  59. S. Niranjanakumari, E. Lasda, R. Brazas and M. A. Garcia-Blanco, *Reversible cross-linking combined with immunoprecipitation to study RNA-protein interactions in-vivo.* **Methods**, 2002, 26, 182-190.
  60. I. Koch, J. Slotta-Huspenina, R. Hollweck, N. Anastasov, H. Hofler, et al., *Real-time quantitative RT-PCR shows variable, assay-dependent sensitivity to formalin fixation: implications for direct comparison of transcript levels in paraffin-embedded tissues.* **Diagn. Mol. Pathol.**, 2006, 15, 149-156.
  61. H. S. Erickson, P. S. Albert, J. W. Gillespie, B. S. Wallis, J. Rodriguez-Canales, et al., *Assessment of normalization strategies for quantitative RT-PCR using microdissected tissue samples.* **Lab. Invest.**, 2007, 87, 951-962.
  62. O. Thellin, W. Zorzi, B. Lakaye, B. De Borman, B. Coumans, et al., *Housekeeping genes as internal standards: use and limits.* **J. Biotechnol.**, 1999, 75, 291-295.
  63. A. Arvey, A. Hermann, C. C. Hsia, E. Le, Y. Freund, et al., *Minimizing off-target signals in RNA fluorescent in situ hybridization.* **Nucleic Acids Res.**, 2010, 38, e115.
  64. C. Coghlin and G. I. Murray, *Current and emerging concepts in tumour metastasis.* **J. Pathol.**, 2010, 222, 1-15.
  65. M. R. Emmert-Buck, R. F. Bonner, P. D. Smith, R. F. Chuaqui, Z. P. Zhuang, et al., *Laser capture microdissection.* **Science**, 1996, 274, 998-1001.

66. K. M. Correia and R. A. Conlon, *Whole-mount in situ hybridization to mouse embryos*. **Methods**, 2001, 23, 335-338.
67. D. A. Eastmond, M. Schuler and D. S. Rupa, *Advantages and limitations of using fluorescence in situ hybridization for the detection of aneuploidy in interphase human cells*. **Mutat. Res.**, 1995, 348, 153-162.
68. J. H. Steel, D. E. Morgan and R. Poulson, *Advantages of in situ hybridisation over direct or indirect in situ reverse transcriptase-polymerase chain reaction for localisation of galanin mrna expression in rat small intestine and pituitary*. **J. Histochem. Cytochem.**, 2001, 33, 201-211.
69. D. Pinkel, T. Straume and J. W. Gray, *Cytogenetic analysis using quantitative, high-sensitivity, fluorescence hybridization*. **P. Natl. Acad. Sci. USA**, 1986, 83, 2934-2938.
70. E. J. M. Speel, A. H. N. Hopman and P. Komminoth, *Amplification methods to increase the sensitivity of in situ hybridization: Play CARD (S)*. **J. Histochem. Cytochem.**, 1999, 47, 281.
71. K. H. Wiedorn, H. Kühn, J. Galle, J. Caselitz and E. Vollmer, *Comparison of in-situ hybridization, direct and indirect in-situ PCR as well as tyramide signal amplification for the detection of HPV*. **Histochem. Cell. Biol.**, 1999, 111, 89-95.
72. P. Komminoth and A. A. Long, *In-situ polymerase chain reaction*. **Virchows Arch. B.**, 1993, 64, 67-73.
73. J. F. Breininger and D. G. Baskin, *Fluorescence in situ hybridization of scarce leptin receptor mRNA using the enzyme-labeled fluorescent substrate method and tyramide signal amplification*. **J. Histochem. Cytochem.**, 2000, 48, 1593-1599.
74. J. T. Pena, C. Sohn-Lee, S. H. Rouhanifard, J. Ludwig, M. Hafner, et al., *miRNA In situ hybridization in formaldehyde and EDC-fixed tissues*. **Nat. Methods**, 2009, 6, 139-141.
75. T. Koji, S. Kondo, Y. Hishikawa, S. An and Y. Sato, *In situ detection of methylated DNA by histo endonuclease-linked detection of methylated DNA sites: a new principle of analysis of DNA methylation*. **Histochem. Cell. Biol.**, 2008, 131, 165.
76. M. R. Speicher and N. P. Carter, *The new cytogenetics: blurring the boundaries with molecular biology*. **Nat. Rev. Genet.**, 2005, 6, 782-792.
77. P. M. Nederlof, D. Robinson, R. Abuknesha, J. Wiegant, A. H. Hopman, et al., *Three-color fluorescence in situ hybridization for the simultaneous detection of multiple nucleic acid sequences*. **Cytometry**, 1989, 10, 20-27.
78. P. Chan, T. Yuen, F. Ruf, J. Gonzalez-Maeso and S. S.C., *Method for multiplex cellular detection of mRNAs using quantum dot fluorescent in situ hybridization* **Nucleic Acids Res.**, 2005, 33, e161.
79. A. M. McNicol and M. A. Farquharson, *In situ hybridization and its diagnostic applications in pathology*. **J. Pathol.**, 1997, 182, 250-261.
80. M. Dowsett, J. Bartlett, I. O. Ellis, J. Salter, M. Hills, et al., *Correlation between immunohistochemistry (HerceptTest) and fluorescence in situ hybridization (FISH) for HER-2 in 426 breast carcinomas from 37 centres*. **J. Pathol.**, 2003, 4, 418-423.

81. M. Mino-Kenudson, L. R. Chirieac, K. Law, J. L. Hornick, N. Lindeman, et al., *A novel, highly sensitive antibody allows for the routine detection of ALK-rearranged lung adenocarcinomas by standard immunohistochemistry*. **Clin. Cancer Res.**, 2010, 16, 1561-1571.
82. A. T. Haase, E. F. Retzel and K. A. Staskus, *Amplification and detection of lentiviral DNA inside cells*. **P. Natl. Acad. Sci. USA**, 1990, 87, 4971-4975.
83. A. C. Stamps, J. A. Terrett and P. J. Adam, *Application of in situ reverse transcriptase-polymerase chain reaction (rt-pcr) to tissue microarrays*. **J. Nanobiotechnology**, 2003, 1, 3.
84. G. R. Bicknell, J. A. Shaw, J. H. Pringle and P. N. Furness, *Amplification of specific mRNA from a single human renal glomerulus, with an approach to the separation of epithelial cell mRNA*. **J. Pathol.**, 1996, 180, 188-193.
85. B. Heng, W. K. Glenn, Y. Ye, B. Tran, W. Delprado, et al., *Human papilloma virus is associated with breast cancer*. **Brit. J. Cancer**, 2009, 101, 1345-1350.
86. Arcturus, *User guide PicoPure<sup>TM</sup> RNA isolation kit version D*. 2004.
87. S. A. Bustin, *Quantification of mRNA using real-time reverse transcription PCR (RT-PCR): trends and problems*. **J. Mol. Endocrinol.**, 2002, 29, 23-39.
88. M. D. To, S. J. Done, M. Redston and I. L. Andrulis, *Analysis of mRNA from microdissected frozen tissue sections without RNA isolation*. **ASIP**, 1998, 153, 47-51.
89. F. Kamme, J. Zhu, L. Luo, J. Yu, D. Tran, et al., *Single-cell laser-capture microdissection and RNA Amplification*, Methods in Molecular Medicine, ed. Z. D. Luo, Humana Press Inc., Totowa, NJ, 2003.
90. F. Celotti, R. C. Melcangi, P. Negri-Cesi, M. Ballabio and L. Martini, *Differential distribution of the 5-alpha-reductase in the central nervous system of the rat and the mouse: are the white matter structures of the brain target tissue for testosterone action?* **J. Steroid Biochem.**, 1987, 26, 125-129.
91. S. Paik, S. Shak, G. Tang, C. Kim, J. Baker, et al., *A multigene assay to predict recurrence of Tamoxifen-treated, node-negative breast cancer*. **New Engl. J. Med.**, 2004, 351, 2817-2826.
92. E. C. de Bruin, S. van de Pas, E. H. Lips, R. van Eijk, M. M. van der Zee, et al., *Macrodissection versus microdissection of rectal carcinoma: minor influence of stroma cells to tumor cell gene expression profiles*. **BMC Genomics**, 2005, 6, 142.
93. R. J. Klebe, G. M. Grant, A. M. Grant, M. A. Garcia, T. A. Giambernardi, et al., *RT-PCR without RNA isolation*. **BioTechniques**, 1996, 21, 1094-1100.
94. H. Tian, A. F. R. Hühmer and J. P. Landers, *Evaluation of silica resins for direct and efficient extraction of DNA from complex biological matrices in a miniaturized format*. **Anal. Biochem.**, 2000, 283, 175-191.
95. D. Greenbaum, C. Colangelo, K. Williams and M. Gerstein, *Comparing protein abundance and mRNA expression levels on a genomic scale*. **Genome Biol.**, 2003, 4, 117.
96. N. S. Goldstein, S. M. Hewitt, C. R. Taylor, H. Yaziji, D. G. Hicks, et al., *Recommendations for improved standardization of immunohistochemistry*. **Appl. Immunohisto. M. M.**, 2007, 15, 124-133.

97. D. J. Brennan, D. P. O'Connor, E. Rexhepaj, F. Ponten and W. M. Gallagher, *Antibody-based proteomics: fast-tracking molecular diagnostics in oncology*. **Nat. Rev. Cancer.**, 2010, 10, 605-617.
98. R. D. Mass, M. F. Press, S. Anderson, M. A. Cobleigh, C. L. Vogel, et al., *Evaluation of clinical outcomes according to HER2 detection by fluorescence in situ hybridization in women with metastatic breast cancer treated with Trastuzumab*. **Clin. Breast Cancer**, 2005, 6, 240-246.
99. S. Kakar, A. M. Gown, Z. D. Goodman and L. D. Ferrel, *Best practices in diagnostic immunohistochemistry*. **Arch. Pathol. Lab. Med.**, 2007, 131, 1648-1654.
100. M. Armani, J. Rodriguez-Canales, J. Gillespie, M. Tangrea, H. Erickson, et al., *2D-PCR: a method of mapping DNA in tissue sections*. **Lab Chip**, 2009, 9, 3526-3534.
101. A. M. Wang, M. V. Doyle and D. F. Mark, *Quantitation of messenger-RNA by the polymerase chain-reaction*. **P. Natl. Acad. Sci. USA**, 1989, 86, 9717-9721.
102. H. S. Erickson, P. S. Albert, J. W. Gillespie, J. Rodriguez-Canales, W. M. Linehan, et al., *Quantitative RT-PCR gene expression analysis of microdissected tissue samples*. **Nature Protocols**, 2009, 4, 902-922.
103. A. Dahl, M. Sultan, A. Jung, R. Schwartz, M. Lange, et al., *Quantitative PCR based expression analysis on a nanoliter scale using polymer nano-well chips*. **Biomed. Microdevices**, 2007, 9, 307-314.
104. L. Warren, D. Bryder, I. L. Weissman and S. R. Quake, *Transcription factor profiling in individual hematopoietic progenitors by digital RT-PCR*. **P. Natl. Acad. Sci. USA**, 2006, 103, 17807.
105. D. A. Kulesh, D. R. Clive, D. S. Zarlenga and J. J. Greene, *Identification of interferon-modulated proliferation-related cDNA sequences*. **P. Natl. Acad. Sci. USA**, 1987, 84, 8453-8457.
106. V. E. Velculescu, L. Zhang, B. Vogelstein and K. W. Kinzler, *Serial analysis of gene-expression*. **Science**, 1995, 270, 484-487.
107. A. Y. Rubina, S. V. Pan'kov, E. I. Dementieva, D. N. Pen'kov, A. V. Butygin, et al., *Hydrogel drop microchips with immobilized DNA: properties and methods for large-scale production*. **Anal. Biochem.**, 2004, 325, 92-106.
108. C. J. H. Brenan, T. Morrison, K. Stone, T. Heitner, A. Katz, et al., *Massively parallel microfluidics platform for storage and ultra-high-throughput screening*. **SPIE**, 2002, 4626, 560.
109. W. Meier-Ruge, W. Bielser, E. Remy, F. Hillenkamp, R. Nitsche, et al., *The laser in the Lowry technique for microdissection of freeze-dried tissue slices*. **Histochem J.**, 1976, 8, 387-401.
110. M. A. Tangrea, R. F. Chuaqui, J. W. Gillespie, M. Ahram, G. Gannot, et al., *Expression microdissection - Operator-independent retrieval of cells for molecular profiling*. **Diagn. Mol. Pathol.**, 2004, 13, 207-212.
111. J. A. Macdonald, N. Murugesan and J. S. Pachter, *Validation of immuno-laser capture microdissection coupled with quantitative RT-PCR to probe blood-brain barrier gene expression in situ*. **J. Neurosci. Meth.**, 2008, 174, 219-226.

112. M. N. Bobrow, T. D. Harris, K. J. Shaughnessy and G. J. Litt, *Catalyzed reporter deposition, a novel method of signal amplification. Application to immunoassays*. **J. Immunol. Methods**, 1989, 125, 279-285.
113. T. Moriyama, H. R. Murphy, B. M. Martin and A. Garciaperez, *Detection of specific messenger-RNAs in single nephron segments by use of the polymerase chain-reaction*. **Am. J. Phys.**, 1990, 258, F1470-F1474.
114. A. T. Christian, M. S. Pattee, C. M. Attix, B. E. Reed, K. J. Sorensen, et al., *Detection of DNA point mutations and mRNA expression levels by rolling circle amplification in individual cells*. **P. Natl. Acad. Sci. USA**, 2001, 98, 14238-14243.
115. M. Flagella, S. Bui, Z. Zheng, C. T. Nguyen, A. G. Zhang, et al., *A multiplex branched DNA assay for parallel quantitative gene expression profiling*. **Anal. Biochem.**, 2006, 352, 50-60.
116. M. L. Collins, B. Irvine, D. Tyner, E. Fine, C. Zayati, et al., *A branched DNA signal amplification assay for quantification of nucleic acid targets below 100 molecules/ml*. **Nucleic Acids Res.**, 1997, 25, 2979-2984.
117. G. L. E. Koch, D. R. J. Macer and M. J. Smith, *Visualization of the intact endoplasmic-reticulum by immunofluorescence with antibodies to the major ER glycoprotein, endoplasmic reticulum chaperone*. **J. Cell Sci.**, 1987, 87, 535-542.
118. K. Kubota, A. Ohashi, H. Imachi and H. Harada, *Visualization of mcr mRNA in a methanogen by fluorescence in situ hybridization with an oligonucleotide probe and two-pass tyramide signal amplification (two-pass TSA-FISH)*. **J. Microbiol. Meth.**, 2006, 66, 521-528.
119. R. Holm, F. Karlsen and J. M. Nesland, *In situ hybridization with nonisotopic probes using different detection systems*. **Mod. Pathol.**, 1992, 5, 315-319.
120. C. R. Englert, G. V. Baibakov and M. R. Emmert-Buck, *Layered expression scanning: rapid molecular profiling of tumor samples*. **AACR**, 2000, 60, 1526-1530.
121. D. Gründemann and E. Schömig, *Protection of DNA during preparative agarose gel electrophoresis against damage induced by ultraviolet light*. **BioTechniques**, 1996, 21, 898-903.
122. C. Zhang, J. Xu, W. Ma and W. Zheng, *PCR microfluidic devices for DNA amplification*. **Biotechnol. Adv.**, 2006, 24, 243-284.
123. J. G. Lee, K. H. Cheong, N. Huh, S. Kim, J. W. Choi, et al., *Microchip-based one step DNA extraction and real-time PCR in one chamber for rapid pathogen identification*. **Lab Chip**, 2006, 6, 886-895.
124. M. C. Breadmore, K. A. Wolfe, I. G. Arcibal, W. K. Leung, D. Dickson, et al., *Microchip-based purification of DNA from biological samples*. **Anal. Chem.**, 2003, 75, 1880-1886.
125. J. F. Zhong, Y. Chen, J. S. Marcus, A. Scherer, S. R. Quake, et al., *A microfluidic processor for gene expression profiling of single human embryonic stem cells*. **Lab Chip**, 2008, 8, 68-74.
126. Invitrogen, *Instruction Manual - SuperScript™ III CellsDirect cDNA Synthesis System Version B*. 4-18-05.
127. Qiagen, *RNeasy™ Mini Handbook Fourth Edition*. 2006.

128. N. Bontoux, L. Dauphinot, T. Vitalis, V. Studer, Y. Chen, et al., *Integrating whole transcriptome assays on a lab-on-a-chip for single cell gene profiling*. **Lab Chip**, 2008, 8, 443-450.
129. M. R. Andersen and C. J. Omiecinski, *Direct extraction of bacterial plasmids from food for polymerase chain reaction amplification*. **Appl. Environ. Microb.**, 1992, 58, 4080-4082.
130. K. A. Hagan, J. M. Bienvenue, C. A. Moskaluk and J. P. Landers, *Microchip-based solid-phase purification of RNA from biological samples*. **Anal. Chem.**, 2008, 80, 8453-8460.
131. R. Ilaria, D. Wines, S. Pardue, S. Jamison, S. R. Ojeda, et al., *A rapid microprocedure for isolating RNA from multiple samples of human and rat brain*. **J. Neurosci. Methods**, 1985, 15, 165-174.
132. P. A. Orlandi and K. A. Lampel, *Extraction-free, filter-based template preparation for rapid and sensitive PCR detection of pathogenic parasitic protozoa*. **J. Clin. Microbiol.**, 2000, 38, 2271-2277.
133. S. A. Leadon and P. A. Cerutti, *A rapid and mild procedure for the isolation of DNA from mammalian cells*. **Anal. Biochem.**, 1982, 120, 282-288.
134. M. Ronaghi and M. Uhlén, *DNA sequencing: A sequencing method based on real-time pyrophosphate*. **Science**, 1998, 281, 363.
135. E. T. Lagally, I. Medintz and R. A. Mathies, *Single-molecule DNA amplification and analysis in an integrated microfluidic device*. **Anal. Chem.**, 2001, 73, 565-570.
136. L. Chen, A. Manz and P. J. R. Day, *Total nucleic acid analysis integrated on microfluidic devices*. **Lab Chip**, 2007, 7, 1413-1423.
137. E. Kiss-Toth, E. E. Qvarnstrom and S. K. Dower, *Hunting for genes by functional screens*. **Cytokine Growth F. R.**, 2004, 15, 97-102.
138. S. Magdaleno, P. Jensen, C. L. Brumwell, A. Seal, K. Lehman, et al., *BGEM: An in situ hybridization database of gene expression in the embryonic and adult mouse nervous system*. **PLOS Biol.**, 2006, 4, 497.
139. M. S. Boguski and A. R. Jones, *Neurogenomics: at the intersection of neurobiology and genome sciences*. **Nature Neurosci.**, 2004, 7, 429-433.
140. A. Visel, C. Thaller and G. Eichele, *GenePaint.org: an atlas of gene expression patterns in the mouse embryo*. **Nucleic Acids Res.**, 2004, 32, D552.
141. S. Gong, C. Zheng, M. L. Doughty, K. Losos, N. Didkovsky, et al., *A gene expression atlas of the central nervous system based on bacterial artificial chromosomes*. **Nature**, 2003, 425, 917-925.
142. L. Neidhardt, S. Gasca, K. Wertz, F. Obermayr, S. Worpenberg, et al., *Large-scale screen for genes controlling mammalian embryogenesis, using high-throughput gene expression analysis in mouse embryos*. **Mech. Develop.**, 2000, 98, 77-94.
143. J. H. Christiansen, Y. Yang, S. Venkataraman, L. Richardson, P. Stevenson, et al., *EMAGE: a spatial database of gene expression patterns during mouse embryo development*. **Nucleic Acids Res.**, 2006, 34, D637 - D641.
144. S. Rozen and H. Skaletsky, *Primer3 on the WWW for general users and for biologist programmers*. **Methods Mol. Biol.**, 2000, 132, 365-386.

145. P. Rådström, R. Knutsson, P. Wolffs, M. Lövenklev and C. Löfström, *Pre-PCR processing: strategies to generate PCR-compatible samples*. **Mol. Biotechnol.**, 2004, 26, 133-146.
146. J. Thompson and D. Gillespie, *Molecular hybridization with RNA probes in concentrated solutions of guanidine thiocyanate*. **Anal. Biochem.**, 1987, 163, 281-291.
147. R. F. Chuaqui, R. F. Bonner, C. J. Best, J. W. Gillespie, M. J. Flaig, et al., *Post-analysis follow-up and validation of microarray experiments*. **Nature Genet.**, 2002, 32 509-514.
148. H. J. Peltier and G. J. Latham, *Normalization of microRNA expression levels in quantitative RT-PCR assays: Identification of suitable reference RNA targets in normal and cancerous human solid tissues*. **RNA**, 2008, 14, 844-852.
149. A. M. Glas, A. Floore, L. J. Delahaye, A. T. Witteveen, R. C. Pover, et al., *Converting a breast cancer microarray signature into a high-throughput diagnostic test*. **BMC Genomics**, 2006, 7, 278.
150. M. J. van de Vijver, Y. D. He, L. J. van't Veer, H. Dai, A. A. Hart, et al., *A gene-expression signature as a predictor of survival in breast cancer*. **New Engl. J. Med.**, 2002, 347, 1999-2009.
151. L. J. van 't Veer, H. Dai, M. J. van de Vijver, Y. D. He, A. A. Hart, et al., *Gene expression profiling predicts clinical outcome of breast cancer*. **Nature**, 2002, 415, 530-536.